CATALYST DEACTIVATION AND REGENERATION

1. Introduction

Catalyst deactivation, the loss over time of catalytic activity and/or selectivity, is a problem of great and continuing concern in the practice of industrial catalytic processes. Costs to industry for catalyst replacement and process shutdown total billions of dollars per year. Time scales for catalyst deactivation vary considerably; for example, in the case of cracking catalysts, catalyst mortality may be on the order of seconds, while in ammonia synthesis the iron catalyst may last for 5–10 years. It is inevitable, however, that all catalysts will decay.

Typically, the loss of activity in a well-controlled process occurs slowly. However, process upsets or poorly designed hardware can bring about catastrophic failure. For example, in steam reforming of methane or naphtha great care must be taken to avoid reactor operation at excessively high temperatures or at steam-to-hydrocarbon ratios below a critical value. Indeed, these conditions can cause formation of large quantities of carbon filaments that plug catalyst pores and voids, pulverize catalyst pellets, and bring about process shutdown, all within a few hours.

While catalyst deactivation is inevitable for most processes, some of its immediate, drastic consequences may be avoided, postponed, or even reversed. Thus, deactivation issues (ie, extent, rate, and reactivation) greatly impact research, development, design, and operation of commercial processes. Accordingly, there is considerable motivation to understand and treat catalyst decay. Indeed, over the past three decades, the science of catalyst deactivation has been steadily developing, while literature addressing this topic has expanded considerably to include books (1–4); comprehensive reviews (5–8); proceedings of international symposia (9–14); topical journal issues (eg, Ref. 15); and more than 7000 patents for the period of 1976–2001. (In a patent search conducted in April 2001 for the keywords catalyst and deactivation, catalyst and life, and catalyst and regeneration, 1781, 3134, and 5068 patents were found respectively.) This area of research provides a critical understanding that is the foundation for modeling deactivation processes, designing stable catalysts, and optimizing processes to prevent or slow catalyst deactivation.

2. Mechanisms of Deactivation of Heterogeneous Catalysts

There are many paths for heterogeneous catalyst decay. For example, a catalyst solid may be poisoned by any one of a dozen contaminants present in the feed. Its surface, pores, and voids may be fouled by carbon or coke produced by cracking/condensation reactions of hydrocarbon reactants, intermediates, and/or products. In the treatment of a power plant flue gas, the catalyst can be dusted or eroded by and/or plugged with fly ash. Catalytic converters used to reduce emissions from gasoline or diesel engines may be poisoned or fouled by fuel or lubricant additives and/or engine corrosion products. If the catalytic reaction is

conducted at high temperatures, thermal degradation may occur in the form of active phase crystallite growth, collapse of the carrier (support) pore structure, and/or solid-state reactions of the active phase with the carrier or promoters. In addition, the presence of oxygen or chlorine in the feed gas can lead to formation of volatile oxides or chlorides of the active phase, followed by gas-phase transport from the reactor. Similarly, changes in the oxidation state of the active catalytic phase can be induced by the presence of reactive gases in the feed.

Thus, the mechanisms of solid catalyst deactivation are many; nevertheless, they can be grouped into six intrinsic mechanisms of catalyst decay: (*1*) poisoning, (*2*) fouling, (*3*) thermal degradation, (*4*) vapor compound formation and/or leaching accompanied by transport from the catalyst surface or particle, (*5*) vapor–solid and/or solid–solid reactions, and (*6*) attrition/crushing. As mechanisms 1, 4, and 5 are chemical in nature while 2 and 5 are mechanical, the causes of deactivation are basically threefold: chemical, mechanical, and thermal. Each of the six basic mechanisms is defined briefly in Table 1. Mechanisms 4 and 5 are treated together, since 4 is a subset of 5.

2.1. Poisoning. *Poisoning* (3,16–22) is the strong chemisorption of reactants, products, or impurities on sites otherwise available for catalysis. Thus, poisoning has operational meaning; that is, whether a species acts as a poison depends upon its adsorption strength relative to the other species competing for catalytic sites. For example, oxygen can be a reactant in partial oxidation of ethylene to ethylene oxide on a silver catalyst and a poison in hydrogenation of ethylene on nickel. In addition to physically blocking adsorption sites, adsorbed poisons may induce changes in the electronic or geometric structure of the surface (17,21).

Mechanisms by which a poison may affect catalytic activity are multifold as illustrated by a conceptual two-dimensional model of sulfur poisoning of ethylene hydrogenation on a metal surface shown in Fig. 1. To begin with, a strongly adsorbed atom of sulfur physically blocks at least one three- or fourfold adsorption/reaction site (projecting into three dimensions) and three or four

Table 1. **Mechanisms of Catalyst Deactivation**

Mechanism	Type	Brief definition/description
poisoning	chemical	strong chemisorption of species on catalytic sites which block sites for catalytic reaction
fouling	mechanical	physical deposition of species from fluid phase onto the catalytic surface and in catalyst pores
thermal degradation	thermal	thermally induced loss of catalytic surface area, support area, and active phase-support reactions
vapor formation	chemical	reaction of gas with catalyst phase to produce volatile compounds
vapor–solid and solid–solid reactions	chemical	reaction of vapor, support, or promoter with catalytic phase to produce inactive phase
attrition/crushing	mechanical	loss of catalytic material due to abrasion loss of internal surface area due to mechanical-induced crushing of the catalyst particle

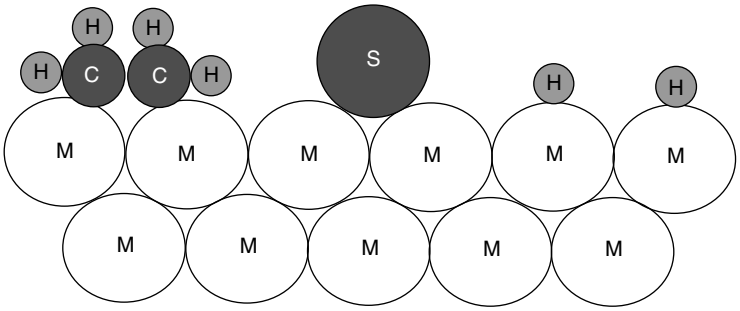

Fig. 1. Conceptual model of poisoning by sulfur atoms of a metal surface during ethylene hydrogenation.

topside sites on the metal surface. Second, by virtue of its strong chemical bond, it electronically modifies its nearest neighbor metal atoms and possibly its next-nearest neighbor atoms, thereby modifying their abilities to adsorb and/or dissociate reactant molecules (in this case H_2 and ethylene molecules), although these effects do not extend beyond about 5 atomic units (21). A third effect may be the restructuring of the surface by the strongly adsorbed poison, possibly causing dramatic changes in catalytic properties, especially for reactions sensitive to surface structure. In addition, the adsorbed poison blocks access of adsorbed reactants to each other (a fourth effect) and finally prevents or slows the surface diffusion of adsorbed reactants (effect number five).

Catalyst poisons can be classified according to their chemical makeup, selectivity for active sites, and the types of reactions poisoned. Table 2 lists four groups of catalyst poisons classified according to chemical origin and their type of interaction with metals. It should be emphasized that interactions of Group VA–VIIIA elements with catalytic metal phases depend on the oxidation state of the former, ie, how many electron pairs are available for bonding and the degree of shielding of the sulfur ion by ligands (16). Thus, the order of decreasing toxicity for poisoning of a given metal by different sulfur species is H_2S, SO_2, SO_4^{2-}, ie, in the order of increased shielding by oxygen. Toxicity also increases with increasing atomic or molecular size and electronegativity, but decreases if the poison can be gasified by O_2, H_2O, or H_2 present in the reactant stream (21); for example, adsorbed carbon can be gasified by O_2 to CO or CO_2 or by H_2 to CH_4.

Table 2. **Common Poisons Classified According to Chemical Structure**

Chemical type	Examples	Type of interaction with metals
Groups VA and VIA	N, P, As, Sb, O, S, Se, Te	through *s* and *p* orbitals; shielded structures are less toxic
Group VII A	F, Cl, Br, I	through *s* and *p* orbitals; formation of volatile halides
toxic heavy metals and ions	As, Pb, Hg, Bi, Sn, Zn, Cd, Cu, Fe	occupy *d* orbitals; may form alloys
molecules that adsorb with multiple bonds	CO, NO, HCN, benzene, acetylene, other unsaturated hydrocarbons	chemisorption through multiple bonds and back bonding

Table 3. **Poisons for Selected Catalysts in Important Representative Reactions**

Catalyst	Reaction	Poisons
silica–alumina, zeolites	cracking	organic bases, hydrocarbons heavy metals
nickel, platinum, palladium	hydrogenation/ dehydrogenation	compounds of S, P, As, Zn, Hg, halides, Pb, NH_3, C_2H_2
nickel	steam reforming of methane, naphtha	H_2S, As
iron, ruthenium	ammonia synthesis	O_2, H_2O, CO, S, C_2H_2, H_2O
cobalt, iron	Fischer–Tropsch synthesis	H_2S, COS, As, NH_3, metal carbonyls
noble metals on zeolites	hydrocracking	NH_3, S, Se, Te, P
silver	ethylene oxidation to ethylene oxide	C_2H_2
vanadium oxide	oxidation/selective catalytic reduction	As/Fe, K, Na from fly ash
platinum, palladium	oxidation of CO and hydrocarbons	Pb, P, Zn, SO_2, Fe
cobalt and molybdenum sulfides	hydrotreating of residues	asphaltenes; N, Ni, V compounds

Table 3 lists a number of common poisons for selected catalysts in important representative reactions. It is apparent that organic bases (eg, amines) and ammonia are common poisons for acidic solids such as silica–aluminas and zeolites in cracking and hydrocracking reactions, while sulfur- and arsenic-containing compounds are typical poisons for metals in hydrogenation, dehydrogenation, and steam reforming reactions. Metal compounds (eg, of Ni, Pb, V, and Zn) are poisons in automotive emissions control, catalytic cracking, and hydrotreating. Acetylene is a poison for ethylene oxidation, while asphaltenes are poisons in hydrotreating of petroleum residues.

"Selective" poisoning involves preferential adsorption of the poison on the most active sites at low concentrations. If sites of lesser activity are blocked initially, the poisoning is "antiselective." If the activity loss is proportional to the concentration of adsorbed poison, the poisoning is "nonselective." An example of selective poisoning is the deactivation of platinum by CO for the para-H_2 conversion (23) while Pb poisoning of CO oxidation on platinum is apparently antiselective (24), and arsenic poisoning of cyclopropane hydrogenation on Pt is nonselective (25). For nonselective poisoning the linear decrease in activity with poison concentration or susceptibility (σ) is defined by the slope of the activity versus poison concentration curve. Several other important terms associated with poisoning are defined in Table 4. Poison tolerance, the activity at saturation coverage of the poison, and resistance (the inverse of deactivation rate) are important concepts that are often encountered in discussions of poisoning including those defined in Table 4.

Activity versus poison concentration patterns are based on the assumption of uniform poisoning of the catalyst surface and surface reaction rate controlling, ie, negligible pore-diffusional resistance. These assumptions, however, are rarely

Table 4. **Important Poisoning Parameters**

Parameter	Definition
activity (a)	reaction rate at time t relative to that at $t = 0$
susceptibility (σ)	negative slope of the activity versus poison concentration curve [$\sigma = (a-1)/C\ (t)$]. Measure of a catalyst's sensitivity to a given poison
toxicity	susceptibility of a given catalyst for a poison relative to that for another poison
resistance	inverse of the deactivation rate, property that determines how rapidly a catalyst deactivates
tolerance ($a(C_{sat})$)	activity of the catalyst at saturation coverage (some catalysts may have negligible activity at saturation coverage)

met in typical industrial processes because the severe reaction conditions of high temperature and high pressure bring about a high pore-diffusional resistance for either the main or poisoning reaction or both. In physical terms, this means that the reaction may occur preferentially in the outer shell of the catalyst particle, or that poison is preferentially adsorbed in the outer shell of the catalyst particle, or both. The nonuniformly distributed reaction and/or poison leads to nonlinear activity versus poison concentration curves, but do not represent truly selective or antiselective poisoning. For example, if the main reaction is limited to an outer shell in a pellet where poison is concentrated, the drop in activity with concentration will be precipitous.

As sulfur poisoning is a difficult problem in many important catalytic processes (eg, hydrogenation, methanation, Fischer–Tropsch synthesis, steam reforming, and fuel cell power production), it merits separate discussion as an example of catalyst poisoning phenomena. Studies of sulfur poisoning in hydrogenation and CO hydrogenation reactions have been thoroughly reviewed (8,21,26–30). Much of the previous work focused on poisoning of nickel metal catalysts by H_2S, the primary sulfur poison in many important catalytic processes, and thus provides some useful case studies of poisoning.

Previous adsorption studies (27–29) indicate that H_2S adsorbs strongly and dissociatively on nickel metal surfaces. Extrapolation of high temperature data to zero coverage using a Tempkin isotherm (28) yields an enthalpy of adsorption of −250 kJ/mol; in other words, at low sulfur coverages, surface nickel–sulfur bonds are a factor of 3 more stable than bulk nickel–sulfur bonds. The absolute heat of adsorption increases with decreasing coverage and the equilibrium partial pressure of H_2S increases with increasing temperature and increasing coverage. It is expected that H_2S (and other sulfur impurities) will adsorb essentially irreversibly to high coverage in most catalytic processes involving metal catalysts.

Two important keys to reaching a deeper understanding of poisoning phenomena include (*1*) determining surface structures of poisons adsorbed on metal surfaces and (*2*) understanding how surface structure and hence adsorption stoichiometry change with increasing coverage of the poison. Studies of structures of adsorbed sulfur on single crystal metals (especially Ni) (3,27,31–34) provide such information. They reveal, for example, that sulfur adsorbs on Ni(100) in an ordered P(2×2) overlayer, bonded to four Ni atoms at $S/Ni_s < 0.25$ and in a

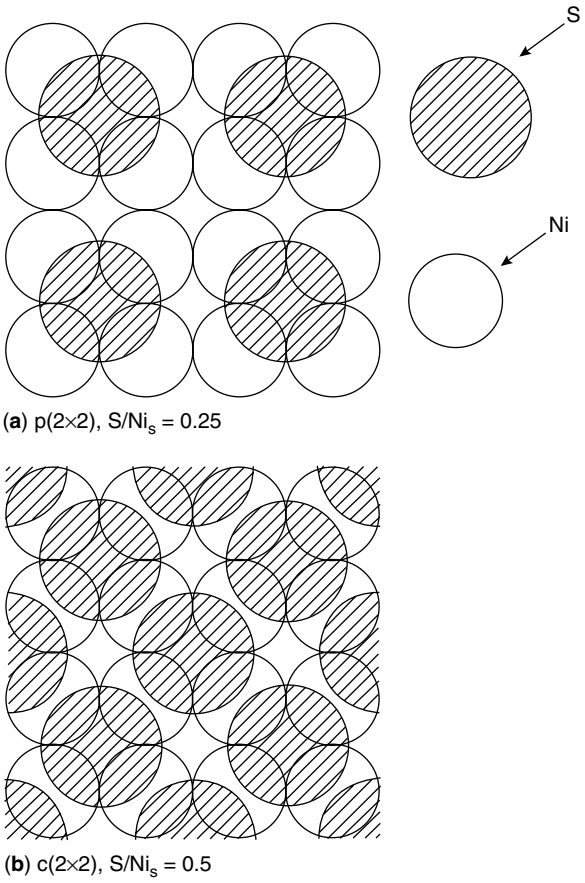

Fig. 2. Schematic view of sulfur adsorbed on a Ni(100) surface at a (**a**) $S/Ni_s = 0.25$ in a $p(2 \times 2)$ structure and (**b**) $S/Ni_s = 0.50$ in a $c(2 \times 2)$ structure.

$C(2 \times 2)$ overlayer to two Ni atoms for $S/Ni_s = 0.25-0.50$ (see Fig. 2; Ni_s denotes a surface atom of Ni); saturation coverage of sulfur on Ni(100) occurs at $S/Ni_s = 0.5$. Adsorption of sulfur on Ni(110), Ni(111), and higher index planes of Ni is more complicated; while the same $P(2 \times 2)$ structure is observed at low coverage, complex overlayers appear at higher coverages—for example on Ni(111) in two additional stages (structures) up to saturation at $S/Ni_s = 0.5$. In more open surface structures such as Ni(110) and Ni(210), saturation coverage occurs at $S/Ni_s = 0.74$ and 1.09 respectively; indeed, there is a trend of increasing S/Ni_s with decreasing planar density for Ni while the saturation sulfur concentration remains constant at 44 ng/cm^2 Ni (see Table 5).

Reported saturation stoichiometries for sulfur adsorption on polycrystalline and supported Ni catalysts (S/Ni_s) vary from 0.25 to 1.3 (27). The values of saturation coverage greater than $S/Ni_s = 0.5$ may be explained by (*1*) a higher fractional coverage of sites of lower coordination number, ie, involving more open planes or intersections of planes (Table 5); (*2*) enhanced adsorption capacity at higher gas phase concentrations of H_2S in line with the observed trend of

Table 5. **Sulfur Adsorption Densities on Various Crystal Faces of Nickel**[a]

Crystal face	Sulfur conc. at saturation, ng·S/cm^2	Number of S atoms/cm^2 ($\times 10^{15}$)	Number of Ni atoms/cm^2 ($\times 10^{15}$)	S atoms per surface Ni atoms
(111)	47 ± 1	0.86	1.8	0.48
(100)	43 ± 1	0.80	1.6	0.50
(110)	44.5 ± 1	0.82	1.1	0.74
(210)	42 ± 1	0.78	0.72	1.09
polycrystalline	44.5 ± 1	0.82	—	—

[a]Data from Ref. 31.

increasing saturation coverage with increasing H_2S concentration; and/or (*3*) reconstruction of the surface by adsorbed sulfur at higher adsorption temperatures.

The first effect would be favored, and in fact is observed, for supported catalysts of higher dispersion (27). The second effect may explain the typically lower observed values of S/Ni_s for single crystal Ni, which are measured at extremely low pressures (high vacuum) relative to the higher values of S/Ni_s for polycrystalline and supported Ni, typically measured at orders of magnitude higher pressure; in the case of the single crystal work the surface is not in equilibrium with gas phase H_2S/H_2. The third effect, reconstruction of nickel surfaces by adsorbed sulfur, has been reported by a number of workers (27); for example, McCarroll and co-workers (33,34) found that sulfur adsorbed at near saturation coverage on a Ni(111) face was initially in a hexagonal pattern but upon heating above 700 K reoriented to a distorted $C(2 \times 2)$ structure on a Ni(100) layer. In another study (32), sulfur adsorbed on a Ni(810) caused decomposition to (100) and (410) facets. On the basis of their review of the reconstruction studies, Bartholomew and co-workers (27) concluded that at high temperatures and near saturation coverages, restructuring by sulfur of different facets of Ni to the more stable Ni(100) is probably a general phenomenon. If so, the S/Ni_s ratio at saturation would in principle be 0.5 for the reconstructed surface. In the first example above, restructuring would not affect the S/Ni_s ratio at saturation, since it is 0.5 for both (100) and (111) planes; however, in the second example, the S/Ni_s ratio at saturation would probably decrease, as rough planes transform to smoother ones. Nevertheless, the possibility of increases in the S/Ni_s ratio at saturation due to reconstruction cannot be ruled out.

The nature of reconstruction of a surface by a poison may depend on its pretreatment. For example, in a scanning tunneling microscopy (STM) study of room temperature H_2S adsorption on Ni(110), Ruan and co-workers (35) found that the S/Ni structure at saturation varied with the initial state of the surface, ie, whether clean or oxygen covered (see Fig. 3). This study showed that no reconstruction occurs by direct exposure to H_2S at room temperature, rather only in the presence of O_2 (or air). This emphasizes the complexities inherent in predicting the structure and stability of a given poison adsorbed on a given catalyst during a specified reaction as a function of different pretreatments or process disruptions, eg, exposure to air.

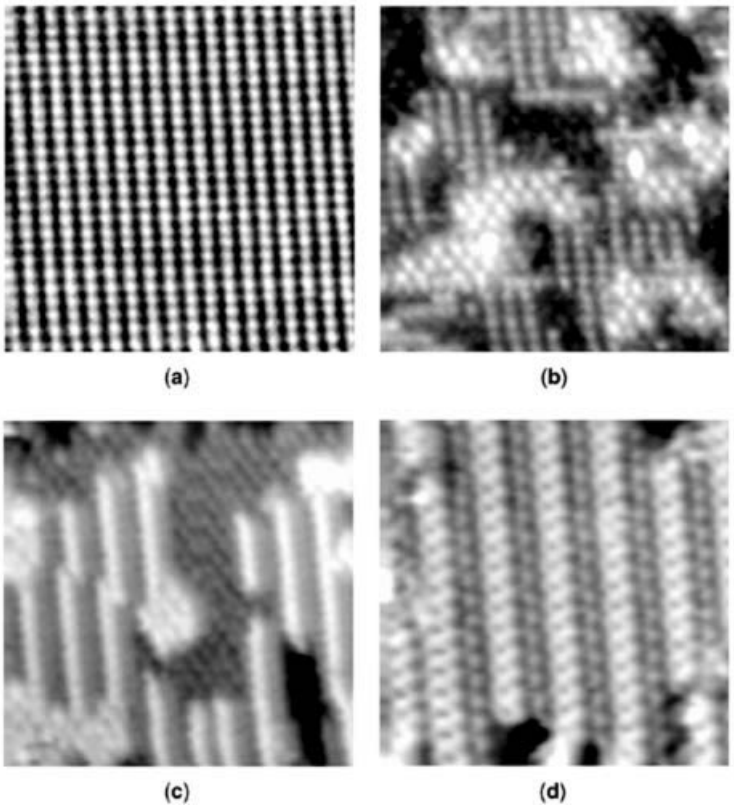

Fig. 3. A series of *in situ* STM images recorded after exposure of Ni(110) to oxygen and then progressively higher exposures of H_2S: (**a**) (2×1)O overlayer; (**b**) white islands and black troughs with a $C(2 \times 2)$S structure after exposure to 3 and 8 L of H_2S; (**c**) 25 L, islands transform to low-coordinated rows in the [001] direction; and (**d**) 50 L, stable, well-ordered (4×1)S (35).

It is evident that structure and stoichiometry of sulfur adsorbed on nickel are complex functions of temperature, H_2S concentration, sulfur coverage, and pretreatment, phenomena that account at least in part for the complex nature of nickel poisoning by sulfur (27,36). Could one expect similar complexities in the poisoning of other metals? Probably, since poisoning of nickel is prototypical, ie, similar principles operate and similar poisoning behaviors are observed in other poison/metal systems, although none have been studied to the same depth as sulfur/nickel.

Since one of the necessary steps in a catalytic reaction is the adsorption of one or more reactants, investigation of the effects of adsorbed sulfur on the adsorption of other molecules can provide useful insights into the poisoning process (21,27). Previous investigations (27,37–43) indicate that both H_2 and CO adsorptions on nickel are poisoned by adsorbed sulfur. Sulfur poisoning can affect reaction selectivity as well as activity (27).

Because sulfur adsorbs so strongly on metals and prevents or modifies the further adsorption of reactant molecules, its presence on a catalyst surface

usually effects substantial or complete loss of activity in many important reactions. The steady-state methanation activities of Ni, Co, Fe, and Ru are relative to the fresh, unpoisoned surface activity as a function of gas phase H_2S concentration. Data indicate that Ni, Co, Fe, and Ru all suffer 3–4 orders of magnitude loss in activity at 15–100 ppb of H_2S, ie, their sulfur tolerances are extremely low. Moreover, the sharp drop in activity with increasing H_2S concentration suggests highly selective poisoning. Nevertheless, the rate of sulfur poisoning and hence sulfur resistance varies from catalyst to catalyst and is apparently a function of catalyst composition (27) and reaction conditions (44). Indeed, it is possible to significantly improve sulfur resistance of Ni, Co, and Fe with catalyst additives such as Mo and B that selectively adsorb sulfur. Because the adsorption of sulfur compounds is generally rapid and irreversible, surface sulfur concentrations in catalyst particles and beds are nonuniform, eg, H_2S adsorbs selectively at the entrance to a packed bed and on the outer surface of catalyst particles, making the experimental study and modeling of sulfur poisoning extremely difficult.

There are other complications in the study of sulfur poisoning. For example, the adsorption stoichiometry of sulfur in CO hydrogenation on Ni is apparently a function of the temperature, H_2/CO ratio, and water partial pressure (44). Moreover, at high CO partial pressures sulfur may be removed from the surface as COS, which is not as strongly adsorbed as H_2S. At low temperature conditions, eg, those representative of Fischer–Tropsch synthesis or liquid phase hydrogenations, the gas phase concentration of H_2S in poisoning studies must be kept very low, ie, below 0.1–5 ppm, to avoid formation of bulk metal sulfides — a phenomenon that seriously compromises the validity of the results. Thus, the importance of studying poisoning phenomena *in situ* under realistic reaction conditions, at low process-relevant poison concentrations, and over a process-representative range of temperature and concentration conditions is emphasized.

There are a number of industrial processes in which one intentionally poisons the catalyst in order to improve its selectivity. For example, to minimize unwanted cracking reactions, to improve isomerization selectivity, to minimize coking, etc.

2.2. Fouling, Coking, and Carbon Deposition. *Fouling* is the physical (mechanical) deposition of species from the fluid phase onto the catalyst surface, which results in activity loss due to blockage of sites and/or pores. In its advanced stages it may result in disintegration of catalyst particles and plugging of the reactor voids. Important examples include mechanical deposits of carbon and coke in porous catalysts, although carbon- and coke-forming processes also involve chemisorption of different kinds of carbons or condensed hydrocarbons that may act as catalyst poisons. The definitions of carbon and coke are somewhat arbitrary and by convention related to their origin. Carbon is typically a product of CO disproportionation while coke is produced by decomposition or condensation of hydrocarbons on catalyst surfaces and typically consists of polymerized heavy hydrocarbons. Nevertheless, coke forms may vary from high molecular weight hydrocarbons to primarily carbons such as graphite, depending upon the conditions under which the coke was formed and aged. A number of books and reviews treat the formation of carbons and coke on catalysts and the attendant deactivation of the catalysts (1,4,45–50).

The chemical structures of cokes or carbons formed in catalytic processes vary with reaction type, catalyst type, and reaction conditions. Menon (50) suggested that catalytic reactions accompanied by carbon or coke formation can be broadly classified as either coke-sensitive or coke-insensitive, analogous to Boudart's more general classification of structure-sensitive and structure-insensitive catalytic reactions. In coke-sensitive reactions, unreactive coke is deposited on active sites, leading to activity decline, while in coke-insensitive reactions, relatively reactive coke precursors formed on active sites are readily removed by hydrogen (or other gasifying agents). Examples of coke-sensitive reactions include catalytic cracking and hydrogenolysis; on the other hand, Fischer–Tropsch synthesis, catalytic reforming, and methanol synthesis are examples of coke-insensitive reactions. On the basis of this classification Menon (50) reasoned that the structure and location of a coke are more important than its quantity in affecting catalytic activity.

Consistent with Menon's classification, it is also generally observed that not only structure and location of coke vary but also its mechanism of formation varies with catalyst type, eg, whether it is a metal or metal oxide (or sulfide, sulfides being similar to oxides).

Carbon and Coke Formation on Supported Metal Catalysts. Possible effects of fouling by carbon (or coke) on the functioning of a supported metal catalyst are as follows. Carbon may (*1*) chemisorb strongly as a monolayer or physically adsorb in multilayers and in either case block access of reactants to metal surface sites, (*2*) totally encapsulate a metal particle and thereby completely deactivate that particle, and (*3*) plug micro- and mesopores such that access of reactants is denied to many crystallites inside these pores. Finally, in extreme cases, strong carbon filaments may build up in pores to the extent that they stress and fracture the support material, ultimately causing the disintegration of catalyst pellets and plugging of reactor voids.

Mechanisms of carbon deposition and coke formation on metal catalysts from carbon monoxide and hydrocarbons (4,45–49) are illustrated in Figs. 4

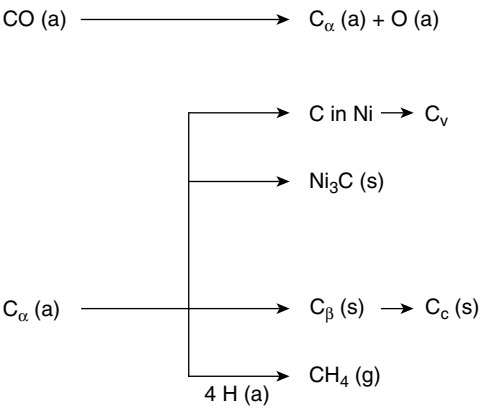

Fig. 4. Formation, transformation, and gasification of carbon on nickel (a, g, s refer to adsorbed, gaseous, and solid states respectively) (48).

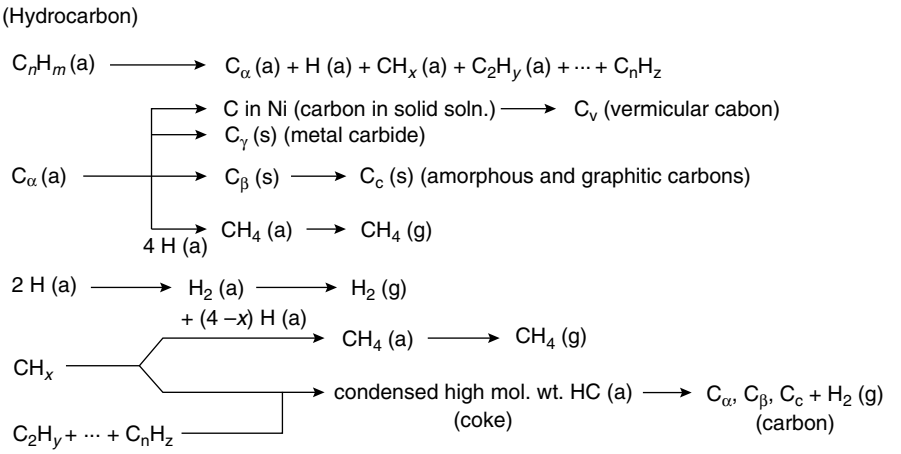

Fig. 5. Formation and transformation of coke on metal surfaces (a, g, s refer to adsorbed, gaseous, and solid states respectively); gas phase reactions are not considered (48).

and 5. Different kinds of carbon and coke that vary in morphology and reactivity are formed in these reactions. For example, CO dissociates on metals to form C_a, an adsorbed atomic carbon; C_a can react to C_b, a polymeric carbon film. The more reactive, amorphous forms of carbon formed at low temperatures (eg, C_a and C_b) are converted at high temperatures over a period of time to less reactive, graphitic forms (48).

It should also be emphasized that some forms of carbon result in loss of catalytic activity and some do not. For example, at low temperatures ($<300-375^\circ$C) condensed polymer or β-carbon films and at high temperatures ($>650^\circ$C) graphitic carbon films encapsulate the metal surfaces of methanation and steam reforming catalysts (48). Deactivation of steam reforming catalysts at high reaction temperatures ($500-900^\circ$C) may be caused by precipitation of atomic (carbidic) carbon dissolved in the Ni surface layers to a depth of more than 50–70 nm (50,51). If it accumulates on the metal surface (at high or low temperatures), adsorbed atomic carbon can deactivate metal sites for adsorption and/or reaction. For example, Durer and co-workers (52) demonstrated that carbon atoms residing in the fourfold hollow sites of Rh(100) block the adsorption of hydrogen (and hence could block sites for hydrogenation). In the intermediate temperature range of $375-650^\circ$C, carbon filaments are formed by precipitation of dissolved carbon at the rear side of metal crystallites, causing the metal particles to grow away from the support (45). Filament growth ceases when sufficient carbon accumulates on the free surface to cause encapsulation by a carbon layer; however, encapsulation of the metal particles does not occur if H_2/CO or H_2O/hydrocarbon ratios are sufficiently high. Thus, carbon filaments sometimes formed in CO hydrogenation or steam reforming of hydrocarbons would not necessarily cause a loss of intrinsic catalyst activity unless they are formed in sufficient quantities to cause plugging of the pores (48) or loss of metal occurs as the carbon fibers are removed during regeneration (53,54). However, in practice, regions of carbon forming potential in steam reforming must be carefully avoided, since once initiated, the rates of filamentous carbon formation are sufficiently high

to cause catastrophic pore plugging and catalyst failure within a few hours to days.

The rate at which deactivation occurs for a given catalyst and reaction depends greatly on reaction conditions—especially temperature and reactant composition. A fundamental principle for coke-insensitive reactions on metals (eg, methanation, Fischer–Tropsch synthesis, steam reforming, catalytic reforming, and methanol synthesis) is that deactivation rate depends greatly on the difference in rates of formation and gasification of carbon/coke precursors, ie, $r_d = r_f - r_g$. If the rate of gasification r_g is equal to or greater than that of formation r_f, carbon/coke is not deposited. Rates of carbon/coke precursor formation and gasification both increase exponentially with temperature, although the difference between them varies a great deal with temperature because of differences in preexponential factors and activation energies. Thus, carbon/coke formation is avoided in regions of temperature in which precursor gasification rate exceeds deposition rate. A similar principle operates in steam reforming, ie, at a sufficiently low reaction temperature, the rate of hydrocarbon adsorption exceeds the rate of hydrocracking and a deactivating polymer film is formed (55); accordingly, it is necessary to operate above this temperature to avoid deactivation.

In steam reforming filamentous carbon formation rate is a strong function of hydrocarbon structure; for example, it decreases in the order acetylenes, olefins, paraffins, ie, in order of decreasing reactivity, although activation energies for nickel are in the same range (125–139 kJ) independent of hydrocarbon structure and about the same as those observed for formation of filamentous carbon from decomposition of CO (48). This latter observation suggests that the reactions of CO and different hydrocarbons to filamentous carbon proceed by a common mechanism and rate-determining step—probably the diffusion of carbon through the metal crystallites (48).

The rate at which a carbon or coke is accumulated in a given reaction under given conditions can vary significantly with catalyst structure, including metal type, metal crystallite size, promoter, and catalyst support. For example, supported Co, Fe, and Ni are active above 350–400°C for filamentous carbon formation from CO and hydrocarbons; the order of decreasing activity is reportedly Fe, Co, Ni (48). Pt, Ru, and Rh catalysts, on the other hand, while equally or more active than Ni, Co, or Fe in steam reforming produce little or no coke or carbon. This is attributed to reduced mobility and/or solubility of carbon in the noble metals, thus retarding the nucleation process. Thus, it is not surprising that addition of noble metals to base metals retards carbon formation; for example, addition of Pt in Ni lowers carbon deposition rate during methanation, while addition of Cu or Au to Ni substantially lowers carbon formation in steam reforming (48,56). In contrast to the moderating effects of noble metal additives, addition of 0.5% Sn to cobalt substantially increases the rate of carbon filament formation from ethylene (57), an effect desirable in the commercial production of carbon filament fibers.

Since carbon formation and gasification rates are influenced differently by modifications in metal crystallite surface chemistry, which are in turn a function of catalyst structure, oxide additives or oxide supports may be used to moderate the rate of undesirable carbon or coke accumulation. For example, Bartholomew and Strasburg (58) found the specific rate (turnover frequency) of filamentous

carbon deposition on nickel during methanation at 350°C to decrease in the order Ni/TiO_2, $NiAl_2O_3$, Ni/SiO_2, while Vance and Bartholomew (59) observed C_α hydrogenation rates at 170°C to decrease in this same order (the same as for methanation at 225°C). This behavior was explained in terms of promotional or inhibiting effects due to decoration of metal crystallites by the support, for example silica, inhibiting both CO dissociation and carbon hydrogenation. This hypothesis is consistent with observations (60,61) that silica evaporated on metal surfaces and supported metals inhibits formation of filamentous carbon. Similarly Bitter and co-workers (62) observed rates of carbon formation in CO_2/CH_4 reforming to decrease in the order $Pt/g\text{-}Al_2O_3 \rightarrow Pt/TiO_2 > Pt/ZrO_2$; while 90% of the carbon deposited on the support, the authors linked deactivation to carbon accumulated on the metal owing to an imbalance between carbon formed by methane dissociation and oxidation by chemisorbed CO_2. The rate of formation of coke in steam reforming is delayed and occurs at lower rates in nickel catalysts promoted with alkali or supported on basic MgO (63).

Since formation of coke, graphite, or filamentous carbon involves the formation of C−C bonds on multiple atoms sites, one might expect that coke or carbon formation on metals is structure-sensitive, ie, sensitive to surface structure and metal crystallite size. Indeed, Bitter and co-workers (62) found that catalysts containing larger Pt crystallites deactivate more rapidly than those containing small crystallites. Moreover, a crystallite size effect, observed in steam reforming of methane on nickel (48,63), appears to operate in the same direction, ie, formation of filamentous carbon occurs at lower rates in catalysts containing smaller metal crystallites.

In summary, deactivation of supported metals by carbon or coke may occur chemically owing to chemisorption or carbide formation or physically and mechanically owing to blocking of surface sites, metal crystallite encapsulation, plugging of pores, and destruction of catalyst pellets by carbon filaments. Blocking of catalytic sites by chemisorbed hydrocarbons, surface carbides, or relatively reactive films is generally reversible in hydrogen, steam, CO_2, or oxygen. Further details of the thermodynamics, kinetics, and mechanisms of carbon and coke formation in methanation and steam reforming reactions are available in reviews by Bartholomew (48) and Rostrup-Nielsen (55,63).

Coke Formation on Metal Oxide and Sulfide Catalysts. In reactions involving hydrocarbons, coke may be formed in the gas phase and on both noncatalytic and catalytic surfaces. Nevertheless, formation of coke on oxides and sulfides is principally a result of cracking reactions involving coke precursors (typically olefins or aromatics) catalyzed by acid sites (64,65). Dehydrogenation and cyclization reactions of carbocation intermediates formed on acid sites lead to aromatics, which react further to higher molecular weight polynuclear aromatics and condense as coke.

Olefins, benzene and benzene derivatives, and polynuclear aromatics are precursors to coke formation. However, the order of reactivity for coke formation is clearly structure dependent, ie, decreases in the order polynuclear aromatics > aromatics > olefins > branched alkanes > normal alkanes. For example, the weight percent coke formed on silica–alumina at 500°C is 0.06, 3.8, 12.5, and 23% for benzene, naphthalene, fluoranthene, and anthracene respectively (66).

Coking reactions in processes involving heavy hydrocarbons are very complex; different kinds of coke may be formed and they may range in composition from CH to C and have a wide range of reactivities with oxygen and hydrogen depending upon the time on stream and temperature to which they are exposed. For example, coke deposits occurring in hydrodesulfurization of residues have been classified into three types (67):

1. Type I deposits are reversibly adsorbed normal aromatics deposited during the first part of the cycle at low temperature.
2. Type II deposits are reversibly adsorbed asphaltenes deposited early in the coking process.
3. Type III deposits result from condensation of aromatic concentrates into clusters and then crystals that constitute a "mesophase." This crystalline phase is formed after long reaction times at high temperature. This hardened coke causes severe deactivation of the catalyst (67).

In addition to hydrocarbon structure and reaction conditions, extent and rate of coke formation are also a function of the acidity and pore structure of the catalyst. Generally, the rate and extent of coke formation increase with increasing acid strength and concentration. Coke yield decreases with decreasing pore size (for a fixed acid strength and concentration); this is especially true in zeolites where shape selectivity plays an important role in coke formation. However, in pores of molecular diameter, a relatively small quantity of coke can cause substantial loss of activity. It should be emphasized that coke yield can vary considerably into the interior pores of a catalyst particle or along a catalyst bed, depending upon the extent to which the main and deactivation reactions are affected by film mass transport and pore diffusional resistance.

The mechanisms by which coke deactivates oxide and sulfide catalysts are, as in the case of supported metals, both chemical and physical. However, some aspects of the chemistry are quite different. The principal chemical loss of activity in oxides and sulfides is due to the strong adsorption of coke molecules on acidic sites. But as discussed earlier, strong acid sites also play an important role in the formation of coke precursors, which subsequently undergo condensation reactions to produce large polynuclear aromatic molecules that physically coat catalytic surfaces. Physical loss of activity also occurs as coke accumulates, ultimately partially or completely blocking catalyst pores as in supported metal catalysts. For example, in isomerization of *cis*-butene on SiO_2/Al_2O_3 (68) catalyst deactivation occurs by rapid, selective poisoning of strong acid sites; coke evolved early in the reaction is soluble in dichloromethane and pyridine and is slightly aromatic. Apparently, the blocking of active sites does not significantly affect porosity or catalyst surface area, as SiO_2/Al_2O_3 contains relatively large mesopores.

In the case of supported bifunctional metal/metal oxide catalysts, different kinds of coke are formed on the metal and the acidic oxide support, eg, soft coke (high H/C ratio) on Pt or Pt–Re metals and hard coke (low H/C ratio) on the alumina support in catalytic reforming (69). In this case coke precursors may be formed on the metal via hydrogenolysis, following which they migrate to the support and undergo polymerization and cyclization reactions, after which the larger

molecules are dehydrogenated on the metal and finally accumulate on the support, causing loss of isomerization activity. Mild sulfiding of these catalysts (especially Pt–Re/alumina) substantially reduces the rate of hydrogenolysis and the overall formation of coke on both metal and support; it especially reduces the hard coke, which is mainly responsible for deactivation.

Several studies (65,70–80) have focused on coke formation during hydrocarbon reactions in zeolites including (*1*) the detailed chemistry of coke precursors and coke molecules formed in zeolite pores and pore intersections (or supercages) and (*2*) the relative importance of adsorption on acid sites versus pore blockage. The principal conclusions from these studies can be summarized as follows: (*1*) the formation of coke and the manner in which it deactivates a zeolite catalyst are shape-selective processes, (*2*) deactivation is mainly due to the formation and retention of heavy aromatic clusters in pores and pore intersections, and (*3*) while both acid-site poisoning and pore blockage participate in the deactivation, the former dominates at low coking rates, low coke coverages (eg, in Y-zeolite below 2 wt%), and high temperatures, while the latter process dominates at high reaction rates, low temperatures, and high coke coverages. Thus, pore size and pore structure are probably more important than acid strength and density under typical commercial process conditions. Indeed, deactivation is typically more rapid in zeolites having small pores or apertures and/or a monodimensional structure (78). Fig. 6 illustrates four possible modes of deactivation of HZSM-5 by carbonaceous deposits with increasing severity of coking (78).

These conclusions (in the previous paragraph) are borne out, for example, in the study by Cerqueira and co-workers (80) of USHY zeolite deactivation during methylcyclohexane transformation at 450°C, showing the following:

1. Coke is probably mainly formed by rapid transformation of styrenic C_7 carbenium ions with lesser contributions from reactions of cyclopentadiene, C_3–C_6 olefins, and aromatics.

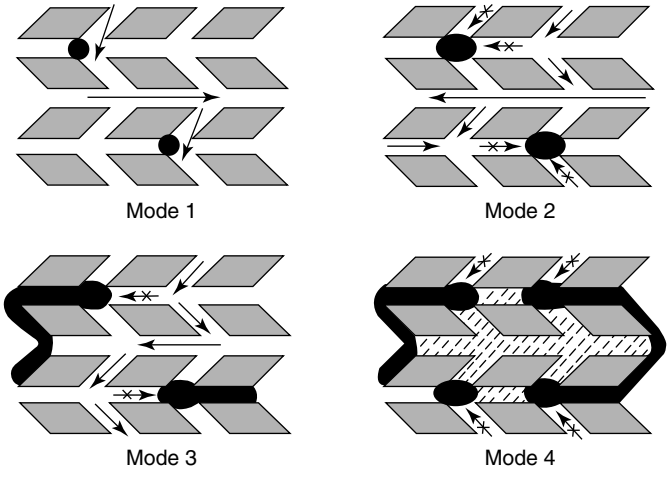

Fig. 6. Schematic of the four possible modes of deactivation by carbonaceous deposits in HZSM-5: (*1*) reversible adsorption on acid sites, (*2*) irreversible adsorption on sites with partial blocking of pore intersections, (*3*) partial steric blocking of pores, and (*4*) extensive steric blocking of pores by exterior deposits (78).

2. Soluble coke consists of polynuclear aromatic clusters containing three to seven five- and six-membered rings having typical compositions of $C_{30}H_{40}$ to $C_{40}H_{44}$ and having dimensions of 0.9×1.1 nm to 1.1×1.5 nm, ie, sizes that would cause them to be trapped in the supercages of Y-zeolite.
3. At short contact times, coking is relatively slow and deactivation is mainly due to acid-site poisoning, while at long contact times, coking is much faster because of the high concentrations of coke precursors; under these latter conditions coke is preferentially deposited at the outer pore openings of zeolite crystallites and deactivation is dominated by pore-mouth blockage.

That coke formed at large contact times not only blocks pores and/or pore intersections inside the zeolite but also migrates to the outside of zeolite crystallites where it blocks pore entrances has been observed in several studies (74,76,77,80). However, the amount, structure, and location of coke in ZSM-5 depends strongly on the coke precursor, eg, coke formed from mesitylene is deposited on the external zeolite surface whereas coking with isobutene leads to largely paraffinic deposits inside pores; coke from toluene, on the other hand, is polyaromatic and is deposited both on external and internal zeolite surfaces (74).

2.3. Thermal Degradation and Sintering. *Background.* Thermally induced deactivation of catalysts results from (*1*) loss of catalytic surface area due to crystallite growth of the catalytic phase, (*2*) loss of support area due to support collapse and of catalytic surface area due to pore collapse on crystallites of the active phase, and/or (*3*) chemical transformations of catalytic phases to noncatalytic phases. The first two processes are typically referred to as "sintering." Sintering processes generally take place at high reaction temperatures (eg, $>500^{\circ}C$) and are generally accelerated by the presence of water vapor.

Most of the previous sintering and redispersion work has focused on supported metals. Experimental and theoretical studies of sintering and redispersion of supported metals published before 1997 have been reviewed fairly extensively (8,81–90). Three principal mechanisms of metal crystallite growth have been advanced: (*1*) crystallite migration, (*2*) atomic migration, and (*3*) (at very high temperatures) vapor transport. Crystallite migration involves the migration of entire crystallites over the support surface, followed by collision and coalescence. Atomic migration involves detachment of metal atoms or molecular metal clusters from crystallites, migration of these atoms over the support surface, and ultimately, capture by larger crystallites. Redispersion, the reverse of crystallite growth in the presence of O_2 and/or Cl_2, may involve (*1*) formation of volatile metal oxide or metal chloride complexes that attach to the support and are subsequently decomposed to small crystallites upon reduction and/or (*2*) formation of oxide particles or films that break into small crystallites during subsequent reduction.

There is controversy in the literature regarding which mechanism of sintering (or redispersion) operates at a given set of conditions. Logically, atomic migration would be favored at lower temperatures than crystallite migration, since the higher diffusivities of atoms or small clusters would facilitate their migration, whereas the thermal energy necessary to induce motion of larger

crystallites would only be available at higher temperatures. Moreover, migration of small crystallites might be favorable early in the sintering process but unfavorable as crystallites become larger. However, fixing on only one of the three sintering mechanisms (and two dispersion mechanisms) is a simplification that ignores the possibility that all mechanisms may occur simultaneously and may be coupled with each other through complex physicochemical processes including the following: (*1*) dissociation and emission of metal atoms or metal-containing molecules from metal crystallites, (*2*) adsorption and trapping of metal atoms or metal-containing molecules on the support surface, (*3*) diffusion of metal atoms, metal-containing molecules and/or metal crystallites across support surfaces, (*4*) metal or metal oxide particle spreading, (*5*) support surface wetting by metal particles, (*6*) metal particle nucleation, (*7*) coalescence of, or bridging between, two metal particles, (*8*) capture of atoms or molecules by metal particles, (*9*) liquid formation, (*10*) metal volatilization through volatile compound formation, (*11*) splitting of crystallites in O_2 atmosphere owing to formation of oxides of a different specific volume, and (*12*) metal atom vaporization. Depending upon reaction or redispersion conditions, a few or all of these processes may be important; thus, the complexity of sintering/redispersion processes is emphasized.

In general, sintering processes are kinetically slow (at moderate reaction temperatures) and irreversible or difficult to reverse. Thus, sintering is more easily prevented than cured.

Factors Affecting Metal Particle Growth and Redispersion in Supported Metals. Temperature, atmosphere, metal type, metal dispersion, promoters/impurities and support surface area, texture, and porosity are the principal parameters affecting rates of sintering and redispersion (see Table 6) (8,86–90). Sintering rates increase exponentially with temperature. Metals sinter relatively

Table 6. **Effects of Important Reaction and Catalyst Variables on Sintering Rates of Supported Metals Based on GPLE Data**[a]

Variable	Effect
temperature	sintering rates are exponentially dependent on T; E_{act} varies from 30 to 150 kJ/mol. E_{act} decreases with increasing metal loading; it increases in the following order with atmosphere: NO, O_2, H_2, N_2
atmosphere	sintering rates are much higher for noble metals in O_2 than in H_2 and higher for noble and base metals in H_2 relative to N_2; sintering rate decreases for supported Pt in atmospheres in the following order: NO, O_2, H_2, N_2
metal	observed order of decreasing thermal stability in H_2 is Ru > Ir ≅ Rh > Pt; thermal stability in O_2 is a function of (*1*) volatility of metal oxide and (*2*) strength of metal oxide–support interaction
support	metal–support interactions are weak (bond strengths of 5–15 kJ/mol); with a few exceptions, thermal stability for a given metal decreases with support in the following order: Al_2O_3 > SiO_2 > carbon
promoters	some additives decrease atom mobility, eg, C, O, CaO, BaO, CeO_2, GeO_2; others increase atom mobility, eg, Pb, Bi, Cl, F, or S; oxides of Ba, Ca, or Sr are "trapping agents" that decrease sintering rate
pore size	sintering rates are lower for porous versus nonporous supports; they decrease as crystallite diameters approach those of the pores

[a]Refs. 8 and 86–90.

rapidly in oxygen and relatively slowly in hydrogen, although depending upon the support, metal redispersion can be facilitated by exposure at high temperature (eg, 500–550°C for Pt/Al_2O_3) to oxygen and chlorine, followed by reduction. Water vapor also increases the sintering rate of supported metals.

Normalized dispersion (percentage of metal exposed at any time divided by the initial percentage exposed) versus time data show that at temperatures of 650°C or higher, rates of metal surface area loss (measured by hydrogen chemisorption) due to sintering of Ni/silica in hydrogen atmosphere are significant, causing 70% loss of the original metal surface area within 50 h at 750°C. In reducing atmosphere, metal crystallite stability generally decreases with decreasing metal melting temperature, ie, in the order Ru > Ir > Rh > Pt > Pd > Ni > Cu > Ag, although this order may be affected by relatively stronger metal–support interactions, eg, the observed order of decreasing stability of supported platinum in vacuum is $Pt/Al_2O_3 > Pt/SiO_2 > Pt/C$. In oxidizing atmospheres, metal crystallite stability depends on the volatility of metal oxides and the strength of the metal–oxide–support interaction. For noble metals, metal stability in air decreases in the order Rh > Pt > Ir > Ru; formation of volatile RuO_4 accounts for the relative instability of ruthenium (91).

The effect of temperature on sintering of metals and oxides can be understood physically in terms of the driving forces for dissociation and diffusion of surface atoms, which are both proportional to the fractional approach to the absolute melting point temperature (T_{mp}). Thus, as temperature increases, the mean lattice vibration of surface atoms increases; when the Hüttig temperature ($0.3T_{mp}$) is reached less strongly bound surface atoms at defect sites (eg, edges and corner sites) dissociate and diffuse readily over the surface, while at the Tamman temperature ($0.5T_{mp}$) atoms in the bulk become mobile. Accordingly, sintering rates of a metal or metal oxide are significant above the Hüttig temperature and very high near the Tamman temperature; thus, the relative thermal stability of metals or metal oxides can be correlated in terms of the Hüttig or Tamman temperatures (92). For example, sintering of copper catalysts for methanol synthesis is promoted by traces of chlorine in the feed, which react at about 225°C (500 K) with the active metal/metal oxide surface to produce a highly mobile copper chloride phase having a Tamman temperature of only 79–174°C (352–447 K) relative to 405–527°C (678–800 K) for copper metal or metal oxides (93).

Promoters or impurities affect sintering and redispersion by either increasing (eg, chlorine and sulfur) or decreasing (eg, oxygen, calcium, cesium) metal atom mobility on the support; in the latter case this is due to their high resistance to dissociation and migration due to high melting points as well as their hindering dissociation and surface diffusion of other atoms. Similarly, support surface defects or pores impede surface migration of metal particles — especially micropores and mesopores with pore diameters about the same size as the metal crystallites.

Historically, sintering rate data were fitted to a simple power-law expression (SPLE) of the form

$$-d(D/D_0)/dt = k_s(D/D_0)^n \quad (1)$$

where k_s is the sintering rate constant, D_0 the initial dispersion, and n the sintering order, which for typical catalyst systems may vary from 3 to 15; unfortunately, the SPLE is in general not valid for sintering processes because it assumes that surface area or dispersion ultimately reaches zero, given sufficient time, when in fact, for a given temperature and atmosphere, a nonzero or limiting dispersion is observed after long sintering times. Moreover, the use of the SPLE is further questionable because variations in sintering order are observed as a function of time and temperature for a given catalyst in a fixed atmosphere (88–90); thus, data obtained for different samples and different reaction conditions cannot be quantitatively compared. Nevertheless, it has been shown by Fuentes (94) and Bartholomew (87–89) that the effects of temperature, atmosphere, metal, promoter, and support can be quantitatively determined by fitting sintering kinetic data to the general power-law expression (GPLE)

$$-d(D/D_0)/dt = k_s(D/D_0 - D_{eq}/D_0)^m \quad (2)$$

which adds a term $-D_{eq}/D_0$ to account for the observed asymptotic approach of the typical dispersion versus time curve to a limiting dispersion D_{eq} at infinite time; m, the order of sintering, is found to be either 1 or 2. A recently compiled, comprehensive quantitative treatment of previous sintering rate data based on the GPLE with an order m of 2 (87–89) quantitatively addresses the effects of catalyst properties and reaction conditions on sintering rate (91,95–97).

Sintering studies of supported metals are generally of two types: (*1*) studies of commercially relevant supported metal catalysts and (*2*) studies of model metal–support systems. The former type provides useful rate data that can be used to predict sintering rates, while the latter type provides insights into the mechanisms of metal particle migration and sintering, although the results cannot be quantitatively extrapolated to predict behavior of commercial catalysts. There is direct evidence from the previous studies of model-supported catalysts (87,90) for the occurrence of crystallite migration (mainly in well-dispersed systems early in the sintering process), atomic migration (mainly at longer sintering times), and spreading of metal crystallites (mainly in oxygen atmosphere). There is also evidence that under reaction conditions, the surface is dynamic, ie, adsorbates and other adatoms rapidly restructure the surface and slowly bring about faceting; moreover, thermal treatments cause gradual changes in the distribution of coordination sites to minimize surface energy. There is a trend in increasing sophistication of spectroscopic tools used to study sintering and redispersion. Additional insights into atomic and molecular processes during reaction at the atomic scale using STM, analytical HRTEM, and other such powerful surface science tools are expected during the next decade.

Sintering of Catalyst Carriers. Sintering of carriers has been reviewed by Baker and co-workers (86) and Trimm (98). Single-phase oxide carriers sinter by one or more of the following processes: (*1*) surface diffusion, (*2*) solid-state diffusion, (*3*) evaporation/condensation of volatile atoms or molecules, (*4*) grain boundary diffusion, and (*5*) phase transformations. In oxidizing atmospheres, γ-alumina and silica are the most thermally stable carriers; in reducing atmospheres, carbons are the most thermally stable carriers. Additives and impurities

affect the thermal properties of carriers by occupying defect sites or forming new phases. Alkali metals, for example, accelerate sintering, while calcium, barium, nickel, and lanthanum oxides form thermally stable spinel phases with alumina. Steam accelerates support sintering by forming mobile surface hydroxyl groups that are subsequently volatilized at higher temperatures. Chlorine also promotes sintering and grain growth in magnesia and titania during high temperature calcination (99). By contrast, sulfuric acid treatment of hydrated alumina (gibbsite) followed by two-step calcination results in a very stable transitional alumina with needle-like particle morphology (98). Dispersed metals in supported metal catalysts can also accelerate support sintering; for example, dispersed nickel accelerates the loss of Al_2O_3 surface area in Ni/Al_2O_3 catalysts.

Effects of Sintering on Catalyst Activity. Baker and co-workers (86) have reviewed the effects of sintering on catalytic activity. Specific activity (based on catalytic surface area) can either increase or decrease with increasing metal crystallite size during sintering if the reaction is structure-sensitive, or it can be independent of changes in metal crystallite size if the reaction is structure-insensitive. Thus, for a structure-sensitive reaction, the impact of sintering may be either magnified or moderated; while for a structure insensitive-reaction, sintering has in principle no effect on specific activity (per unit surface area). In the latter case, the decrease in mass-based activity is proportional to the decrease in metal surface area. Ethane hydrogenolysis and ethane steam reforming are examples of structure-sensitive reactions, while CO hydrogenation on supported cobalt, nickel, iron, and ruthenium is structure-insensitive.

2.4. Gas/Vapor–Solid and Solid-State Reactions. In addition to poisoning, there are a number of chemical routes leading to catalyst deactivation: (*1*) reactions of the vapor phase with the catalyst surface to produce (a) inactive bulk and surface phases (rather than strongly adsorbed species) or (b) volatile compounds that exit the catalyst and reactor in the vapor phase; (*2*) catalytic solid-support or catalytic solid-promoter reactions, and (*3*) solid-state transformations of the catalytic phases during reaction.

Gas/Vapor–Solid Reactions. Reactions of Gas/Vapor with Solid to Produce Inactive Phases. Dispersed metals, metal oxides, metal sulfides, and metal carbides are typical catalytic phases, the surfaces of which are similar in composition to the bulk phases. For a given reaction, one of these catalyst types is generally substantially more active than the others, eg, only Fe and Ru metals are active for ammonia synthesis, while the oxides, sulfides, and carbides are inactive. If, therefore, one of these metal catalysts is oxidized, sulfided, or carbided, it will lose essentially all of its activity. While these chemical modifications are closely related to poisoning, the distinction here is that rather than losing activity owing to the presence of an adsorbed species, the loss of activity is due to the formation of a new phase altogether.

Examples of vapor-induced chemical transformations of catalysts to inactive phases are listed in Table 7.

Reactions of Gas/Vapor with Solid to Produce Volatile Compounds. Metal loss through direct vaporization is generally an insignificant route to catalyst deactivation. By contrast, metal loss through formation of volatile compounds, eg, metal carbonyls, oxides, sulfides, and halides in CO, O_2, H_2S, and halogen-containing environments, can be significant over a wide range of

Table 7. **Examples of Reactions of Gases/Vapors with Catalytic Solids to Produce Inactive Phases**

Catalytic process	Gas/vapor composition	Catalytic solid	Deactivating chemical reaction	Ref.
auto emissions control	N_2, O_2, HCs, CO, NO, H_2O, SO_2	Pt–Rh/Al_2O_3	$2\ Rh_2O_3 + \gamma\text{-}Al_2O_3 \rightarrow RhAl_2O_4 + 0.5\ O_2$	100,101
ammonia synthesis and regeneration	H_2, N_2	Fe/K/Al_2O_3	$Fe \rightarrow FeO$ at >50 ppm O_2	8
	Traces O_2, H_2O		$Fe \rightarrow FeO$ at >0.16 ppm H_2O/H_2	
catalytic cracking	HCs, H_2, H_2O	La-Y-zeolite	H_2O induced Al migration from zeolite framework causing zeolite destruction	8
CO oxidation, gas turbine exhaust	N_2, O_2, 400 ppm CO, 100–400 ppm SO_2	Pt/Al_2O_3	$2\ SO_3 + \gamma\text{-}Al_2O_3 \rightarrow Al_2(SO_4)_3$ which blocks catalyst pores	8
diesel HC/soot emissions control	N_2, O_2, HCs (gas and liquid), CO, NO, H_2O, soot, SO_2	Pt/Al_2O_3 and β-zeolite; oxides of CaCuFeVK on TiO_2	formation of $Al_2(SO_4)_3$ or sulfates of Ca, Cu, Fe, or V which block catalysts pores and lower activity for oxidation; Al_2O_3 stabilized by BaO	102–104
Fischer–Tropsch	CO, H_2, H_2O, CO_2, HCs	Fe/K/Cu/SiO_2	$Fe_5C_2 \rightarrow Fe_3O_4$ due to oxidation at high X_{CO} by-product H_2O, CO_2	105
Fischer–Tropsch	CO, H_2, H_2O, HCs	Co/SiO_2	$Co + SiO_2 \rightarrow CoO \cdot SiO_2$ and collapse of SiO_2 by-product H_2O	106
selective catalytic reduction (SCR), stationary	N_2, O_2, NO, PM,[a] H_2O, SO_2	$V_2O_5/WO_3/TiO_2$	formation of $Al_2(SO_4)_3$ if Al_2O_3 is used	107
steam reforming and regeneration in H_2O	CH_4, H_2O, CO, H_2, CO_2	Ni/Al_2O_3	$Ni + Al_2O_3 \rightarrow Ni_2Al_2O_4$	8

[a]Particulate matter.

Table 8. **Types and Examples of Volatile Compounds Formed in Catalytic Reactions**

Gaseous environment	Compound type	Example of compound
CO, NO	carbonyls and nitrosyl carbonyls	$Ni(CO)_4$, $Fe(CO)_5$ (0–300°C)[a]
O_2	oxides	RuO_3 (25°C), PbO (> 850°C), PtO_2 (>700°C)
H_2S	sulfides	MoS_2 (>550°C)
halogens	halides	$PdBr_2$, $PtCl_4$, PtF_6, $CuCl_2$, Cu_2Cl_2

[a]Temperatures of vapor formation are listed in parentheses.

conditions, including relatively mild conditions. Classes and examples of volatile compounds are listed in Table 8.

While the chemical properties of volatile metal carbonyls, oxides, and halides are well known, there is surprisingly little information available on their rates of formation during catalytic reactions. There have been no reviews on this subject and relatively few reported studies to define the effects of metal loss on catalytic activity (27,108–121). Most of the previous work has focused on volatilization of Ru in automotive converters (108–111); nickel carbonyl formation in nickel catalysts during methanation of CO (113,119) or during CO chemisorption at 25°C (27,115); formation of Ru carbonyls during Fischer–Tropsch synthesis (116,117); volatilization of Pt during ammonia oxidation on Pt–Rh gauze catalysts (120,121); and volatilization of Cu from methanol synthesis and diesel soot oxidation catalysts, leading to sintering in the former and better catalyst–soot contact but also metal loss in the latter case (92).

Results of selected studies are summarized in Table 9.

Loss of nickel metal during CO chemisorption on nickel catalysts at temperatures above 0°C is also a serious problem; moreover, this loss is catalyzed by sulfur poisoning (27). In view of the toxicity of nickel tetracarbonyl, the rapid loss of nickel metal, and the ill-defined adsorption stoichiometries, researchers are advised to avoid using CO chemisorption for measuring nickel surface areas; instead, hydrogen chemisorption, an accepted ASTM method with a well-defined adsorption stoichiometry, is recommended (124).

Decomposition of volatile platinum oxide species formed during high temperature reaction may (125–127) lead to formation of large Pt crystallites and/or substantial restructuring of the metal surface. For example, Wu and Phillips (125–127) observed surface etching, enhanced sintering, and dramatic surface restructuring of Pt thin films to faceted particles during ethylene oxidation over a relatively narrow temperature range (500–700°C). The substantially higher rate of sintering and restructuring in O_2/C_2H_4 relative to that in nonreactive atmospheres was attributed to the interaction of free radicals such as HO_2, formed homogeneously in the gas phase, with the metal surface to form metastable mobile intermediates. Etching of Pt–Rh gauze in a H_2/O_2 mixture under the same conditions as Pt surfaces (600°C, $N_2/O_2/H_2 = 90/7.5/2.5$) has also been reported (123). A significant weight loss was observed in a laminar flow reactor with little change in surface roughness, while in an impinging jet reactor, there was little weight loss, but substantial restructuring of the surface to particle-like structures, 1–10 μm in diameter; these particles were found to have the same

Table 9. **Documented Examples of Reactions of Vapor with Solid to Produce Volatile Compounds**

Catalytic process	Catalytic solid	Vapor formed	Comments on deactivation process	Ref.
automotive converter	$Pd–Ru/Al_2O_3$	RuO_4	50% loss of Ru during 100-h test in reducing automotive exhaust	111
methanation of CO	Ni/Al_2O_3	$Ni(CO)_4$	$P_{CO} > 20$ kPa and $T < 425°C$ due to $Ni(CO)_4$ formation, diffusion and decomposition on the support as large crystallites	113
CO chemisorption	Ni catalysts	$Ni(CO)_4$	$P_{CO} > 0.4$ kPa and $T > 0°C$ due to $Ni(CO)_4$ formation; catalyzed by sulfur compounds	114
Fischer–Tropsch synthesis (FTS)	Ru/NaY zeolite Ru/Al_2O_3, Ru/TiO_2	$Ru(CO)_5$, $Ru_3(CO)_{12}$	loss of Ru during FTS ($H_2/CO = 1$, 200–250°C, 1 atm) on Ru/NaY zeolite and Ru/Al_2O_3; up to 40% loss while flowing CO at 175–275°C over Ru/Al_2O_3; for 24 h, rate of Ru loss less on titania-supported Ru and for catalysts containing large metal crystallites (3 nm) relative to small metal crystallites (1.3 nm); surface carbon lowers loss	116,117
ammonia oxidation	Pt–Rh gauze	PtO_2	loss: 0.05–0.3 g Pt/ton HNO_3; recovered with Pd gauze; loss of Pt leads to surface enrichment with inactive Rh	8,120,122
HCN synthesis	Pt–Rh gauze	PtO_2	extensive restructuring and loss of mechanical strength	8,123
methanol synthesis	CuZnO	$CuCl_2$, Cu_2Cl_2	mobile copper chloride phase leads to sintering at reaction temperature (225°C)	92
diesel soot oxidation	oxides of K, Cu, Mo, and trace Cl	$CuCl_2$, Cu_2Cl_2	mobile copper chloride improves catalyst–soot contact; catalyst evaporation observed	92

Pt–Rh composition as the original gauze. The nodular structures of about 10-μm diameter formed in these experiments are strikingly similar to those observed on Pt–Rh gauze after use in production of HCN at 1100°C in 15% NH_3, 13% CH_4, and 72% air. Moreover, because of the high space velocities during HCN production, turbulent rather than laminar flow would be expected as in the impinging jet reactor. While little Pt is volatilized from the Pt–Rh gauze catalyst during HCN synthesis, the extensive restructuring leads to mechanical weakening of the gauze (8).

Other examples of catalyst deactivation due to volatile compound formation include (*1*) loss of the phosphorus promoter from the VPO catalyst used in the fluidized-bed production of maleic anhydride with an attendant loss of catalyst selectivity (8), (*2*) vapor-phase loss of the potassium promoter from steam-reforming catalysts in the high temperature, steam-containing environment (8), and (*3*) loss of Mo from a 12-Mo-V-heteropolyacid due to formation of a volatile Mo species during oxydehydrogenation of isobutyric acid to methacrylic acid (118).

While relatively few definitive studies of deactivation by volatile compound formation have been reported, the previous work does provide the basis for enumerating some general principles. A generalized mechanism of deactivation by formation of volatile metal compounds can be postulated (see Fig. 7). In addition, the roles of kinetics and thermodynamics can be stated in general terms:

1. At low temperatures and partial pressures of the volatilization agent (VA), the overall rate of the process is limited by the rate of volatile compound formation.
2. At intermediate temperatures and partial pressures of the VA, the rate of formation of the volatile compound exceeds the rate of decomposition. Thus, the rate of vaporization is high, the vapor is stable, and metal loss is high.
3. At high temperatures and partial pressures of the VA, the rate of formation equals the rate of decomposition, ie, equilibrium is achieved. However, the volatile compound may be too unstable to form or may decompose before there is an opportunity to be transported from the system. From the previous work, it is also evident that besides temperature and gas phase composition, catalyst properties (crystallite size and support) can play an important role in determining the rate of metal loss.

Solid-State Reactions. Catalyst deactivation by solid-state diffusion and reaction appears to be an important mechanism for degradation of complex multi-

Generalized Mechanism:

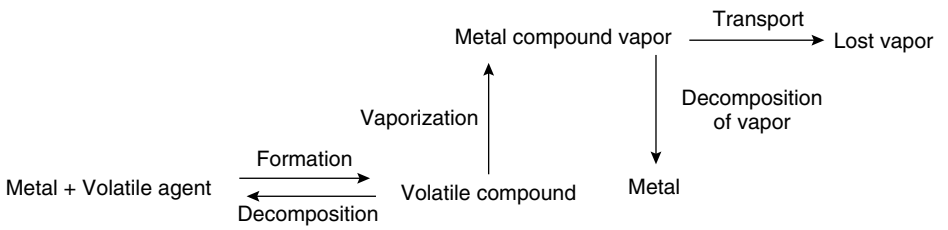

Generalized Kinetics:

(a) rate of volatile compound formation = rate of formation – rate of decomposition

(b) rate of metal loss = rate of vaporizaion – rate of vapor decomposition

Fig. 7. Generalized mechanisms and kinetics for deactivation by metal loss (8).

component catalysts in dehydrogenation, synthesis, partial oxidation, and total oxidation reactions (8,128–139). However, it is difficult in most of these reactions to know the extent to which the solid-state processes such as diffusion and solid-state reaction are affected by surface reactions. For example, the rate of diffusion of Al_2O_3 to the surface to form an aluminate may be enhanced by the presence of gas-phase oxygen or water or the nucleation of a different phase may be induced by either reducing or oxidizing conditions. Recognizing this inherent limitation, the focus here is nevertheless on processes in which formation of a new bulk phase (and presumably the attendant surface phase) leads to substantially lower activity. There is probably some overlap with some of the examples given under Gas/Vapor–Solid Reactions involving reactions of gas/vapor with solid to produce inactive phases.

Examples from the literature of solid-state transformations leading to catalyst deactivation are summarized in Table 10.

There are basic principles underlying most solid-state reactions in working catalysts that have been enumerated by Delmon (135): (*1*) the active catalytic phase is generally a high-surface-area defect structure of high surface energy and as such a precursor to more stable, but less active phases and (*2*) the basic reaction processes may themselves trigger the solid-state conversion of the active

Table 10. **Examples of Solid-State Transformations Leading to Catalyst Deactivation**

Catalytic process	Catalytic solid	Deactivating chemical reaction	Ref.
ammonia synthesis	$Fe/K/Al_2O_3$	formation of $KAlO_2$ at catalyst surface	138
catalytic combustion	PdO/Al_2O_3, PdO/ZrO_2	$PdO \rightarrow Pd$ at $T > 800^\circ C$	131
catalytic combustion	Co/K on MgO, CeO_2, or La_2O_3	formation of CoO–MgO solid soln., $LaCoO_3$, or K_2O film on CeO_2	139
dehydrogenation of styrene to ethyl benzene	$Fe_2O_3/Cr_2O_3/K_2O$	K migration to center of pellet caused by thermal gradient	8
Fischer–Tropsch	Fe/K, Fe/K/CuO	transformation of active carbides to inactive carbides	136,137
oxidation of SO_2 to SO_3	$V_2O_5/K_2O/Na_2O$/ kieselguhr	formation of inactive V(IV) compounds at $T < 420$–$430^\circ C$	134
partial oxidation of benzene to maleic anhydride	V_2O_5–MoO_3	decreased selectivity due to loss of MoO_3 and formation of inactive vanadium compounds	128
partial oxidation of methanol to formaldehyde	$Fe_2(MoO_4)_3$ plus MoO_3	structural reorganization to β-$FeMoO_4$; reduction of MoO_3	129,135
partial oxidation of propene to acrolein	$Fe_2(MoO_4)_3$	reductive transformation of $Mo_{18}O_{52}$ to Mo_4O_{11}	132,135
partial oxidation of isobutene to methacrolein	$Fe_2(MoO_4)_3$	reduction to $FeMoO_4$ and MoO_{3-x}	130,133

phase to an inactive phase; for example, it may involve a redox process, part of which nucleates the inactive phase.

A well-documented example of these principles occurs in the partial oxidation of propene to acrolein on a $Fe_2(MoO_4)_3$ catalyst (132,135). This oxidation occurs by the *"Mars van Krevelen" mechanism*, ie, a redox mechanism in which lattice oxygen reacts with the adsorbed hydrocarbon to produce the partially oxygenated product; the reduced catalyst is restored to its oxidized state through reaction with gaseous oxygen. In propene oxidation, two atoms of oxygen from the catalyst are used, one for removing two hydrogen atoms from the olefin and the other one in forming the unsaturated aldehyde. The fresh, calcined catalyst MoO_3 consists of corner-sharing MoO_6 octahedra (with Mo at the center and six oxygen atoms at the corners), but upon reduction to MoO_2, octahedra share edges. However, it has been reported (132,135) that only slightly reduced (relative to MoO_3), open structures such as $Mo_{18}O_{52}$ and Mo_8O_{23} are the most active, selective phases; more complete reduction of either of these structures leads to formation of Mo_4O_{11} having substantially lower selectivity. Delmon and co-workers (133,135) have shown that addition of an oxygen donor such as Sb_2O_4 facilitates spillover of oxygen and thereby prevents overreduction and deactivation of the catalyst.

2.5. Mechanical Failure of Catalysts. *Forms and Mechanisms of Failure.* Mechanical failure of catalysts is observed in several different forms, including (*1*) crushing of granular, pellet, or monolithic catalyst forms due to a load; (*2*) attrition, the size reduction, and/or breakup of catalyst granules or pellets to produce fines, especially in fluid or slurry beds; and (*3*) erosion of catalyst particles or monolith coatings at high fluid velocities. Attrition is evident by a reduction in the particle size or a rounding or smoothing of the catalyst particle easily observed under an optical or electron microscope. Washcoat loss is observed by scanning a cross section of the honeycomb channel with either an optical or an electron microscope. Large increases in pressure drop in a catalytic process are often indicative of fouling, masking, or the fracturing and accumulation of attritted catalyst in the reactor bed.

Commercial catalysts are vulnerable to mechanical failure in large part because of the manner in which they are formed; that is, catalyst granules, spheres, extrudates, and pellets ranging in diameter from 50 μm to several millimeters are in general prepared by agglomeration of 0.02–2 μm aggregates of much smaller primary particles having diameters of 10–100 nm by means of precipitation or gel formation followed by spray drying, extrusion, or compaction. These agglomerates have in general considerably lower strengths than the primary particles and aggregates of particles from which they are formed.

Two principal mechanisms are involved in mechanical failure of catalyst agglomerates: (*1*) fracture of agglomerates into smaller agglomerates of approximately $0.2d_0$–$0.8d_0$ and (*2*) erosion (or abrasion) of aggregates of primary particles having diameters ranging from 0.1 to 10 μm from the surface of the agglomerate (140). While erosion is caused by mechanical stresses, fracture may be due to mechanical, thermal, and/or chemical stresses. Mechanical stresses leading to fracture or erosion in fluidized or slurry beds may result from (*1*) collisions of particles with each other or with reactor walls or (*2*) shear forces created by turbulent eddies or collapsing bubbles (cavitation) at high fluid velocities. Thermal

stresses occur as catalyst particles are heated and/or cooled rapidly; they are magnified by temperature gradients across particles and by differences in thermal expansion coefficients at the interface of two different materials, eg, catalyst coating/monolith interfaces; in the latter case the heating or cooling process can lead to fracture and separation of the catalyst coating. Chemical stresses occur as phases of different density are formed within a catalyst particle via chemical reaction; for example, carbiding of primary iron oxide particles increases their specific volume and micromorphology leading to stresses that break up these particles (141).

Role of Properties of Ceramic Agglomerates in Determining Strength and Attrition Resistance. Factors Affecting the Magnitude of Stress Required for Agglomerate Breakage and the Mechanisms by Which it Occurs. The extent to which a mechanism, ie, fracture or erosion, participates in agglomerate size reduction depends upon several factors: (*1*) the magnitude of a stress, (*2*) the strength and fracture toughness of the agglomerate, (*3*) agglomerate size and surface area, and (*4*) crack size and radius. Erosion (abrasion) occurs when the stress (eg, force per area due to collision or cavitation pressure) exceeds the agglomerate strength, ie, the strength of bonding between primary particles. Erosion rate is reportedly (140) proportional to the external surface area of the catalyst; thus, erosion rate increases with decreasing agglomerate size.

Most heterogeneous catalysts are complex, multiphase materials that consist in large part of porous ceramic materials, ie, are typically oxides, sulfides, or metals on an oxide carrier or support. When a tensile stress of a magnitude close to the yield point is applied, ceramics almost always undergo brittle fracture before plastic deformation can occur. Brittle fracture occurs through formation and propagation of cracks through the cross section of a material in a direction perpendicular to the applied stress. Agglomerate fracture due to a tensile stress occurs by propagation of internal and surface flaws; these flaws created by external stresses or inherent defects are stress multipliers, ie, the stress is multiplied by $2(a/r)^{0.5}$, where a is the crack length and r is the radius of curvature of the crack tip; since a/r can vary from 2 to 1000, the effective stress at the tip of a crack can be 4–60 times the applied stress. Tensile stress multipliers may be microcracks, internal pores, and grain corners.

The ability of a material to resist fracture is termed fracture toughness. The plain strain fracture toughness K_{Ic} is defined as

$$K_{Ic} = Y\sigma(\pi a)^{0.5} \tag{3}$$

where Y is a dimensionless parameter (often close to 1.0–2.0), the magnitude of which depends upon both specimen and crack geometries, σ is the applied stress, and a is the length of a surface crack or half the length of an internal crack. Crack propagation and fracture are likely if the right hand side of equation 3 exceeds the experimental value of plain strain fracture toughness (left-hand side of eq. 3). Plane strain fracture toughness values for ceramic materials are significantly smaller than for metals and typically below 10 $MPa(m)^{0.5}$; reported values for nonporous, crystalline alumina (99.9%), fused silica, and zirconia (3 mol% Y_2O_3) are 4–6, 0.8, and 7–12 $MPa(m)^{0.5}$ respectively; flexural strengths

(analogous to yield strengths for metals) for the same materials are 280–550, 100, and 800–1500 MPa (142). Thus, on the basis of both fracture toughness and flexural strength, nonporous, crystalline zirconia is much stronger toward fracture than alumina, which in turn is much stronger than fused silica.

The introduction of porosity to crystalline or polycrystalline ceramic materials will, on the basis of stress amplification, significantly decrease elastic modulus and flexural strength for materials in tension.

Thus far the discussion has focused mainly on tensile strength, the extent of which is greatly reduced by the presence of cracks or pores. However, for ceramic materials in compression, there is no stress amplification due to flaws or pores; thus ceramic materials (including catalytic materials) in compression are much stronger (approximately a factor of 10) than in tension. In addition, the strength of ceramic materials can be dramatically enhanced by imposing a residual compressive stress at the surface through thermal or chemical tempering. Moreover, introduction of binders such as graphite enables agglomerates of ceramic powders to undergo significant plastic deformation before fracture.

Tensile Strengths and Attrition Resistance of Catalyst Supports and Catalysts. The strengths cited above for nonporous, annealed crystalline or polycrystalline materials do not necessarily apply to porous catalyst agglomerates even under compression; rather, agglomerate strength is dependent upon the strengths of chemical and physical bonds including the cohesive energy between primary particles. Agglomerate strength would depend greatly on the preparation of the compact. Representative data for catalyst agglomerates (see Table 11) suggest they are generally substantially weaker than polycrystalline ceramic materials prepared by high temperature sintering, such as alumina (140,142,144–148).

From the data in Table 11 it is evident that even subtle differences in preparation and pretreatment also affect agglomerate strength. For example, spheres of γ-Al_2O_3 prepared by sol–gel granulation are substantially (17 times) stronger than commercial γ-Al_2O_3 spheres (143). Moreover, 30- and 90-μm diameter particles of TiO_2 prepared by thermal hydrolysis or basic precipitation are 30 and 15 times stronger than commercially available 4-mm extrudates (146).

Catalyst attrition is a difficult problem in the operation of moving-bed, slurry-bed, or fluidized-bed reactors. Generally, stronger materials have greater attrition resistance; this conclusion is supported by representative data in Table 11 for γ-Al_2O_3, showing that the strength of the alumina prepared by sol–gel granulation is 17 times higher, while its attrition rate is 5 times lower.

The mechanism by which attrition occurs (erosion or fracture) can vary with catalyst or support preparation, crush strength, and with reactor environment; it can also vary with the mechanical test method. There is some evidence in the attrition literature supporting the hypothesis that in the presence of a large stress, weaker oxide materials are prone to failure by fracture, while stronger materials tend to erode (149). However, there is also contrary evidence (145), showing that fracture may be the preferred mechanism for strong TiO_2 agglomerates, while abrasion is favored for weaker agglomerates. Supporting a third trend, data (140) show that attrition mechanism and rate are independent of agglomerate strength but depend instead on the type of material. 100-μm-diameter agglomerates of precipitated Fe/Cu/K Fischer–Tropsch catalyst

Table 11. **Mechanical Strengths and Attrition Rates of Catalyst Supports Compared to Those of Sintered Ceramic Agglomerates**

Catalyst support or ceramic	Preparation/pretreatment/ properties	Strength, MPa	Attrition index, wt%/h	Ref.
	High surface area catalyst supports			
γ-Al_2O_3, 1.2–4.25-mm spheres	sol–gel granulation/dried 10 h at 40°C, calcined 3 h at 450°C/ 389 m^2/g, $d_{pore} = 3.5$ nm	11.6 ± 1.9	0.033	144
γ-Al_2O_3, 4.25-mm spheres	Alcoa LD-350	0.7	0.177	144
g-Al_2O_3, 100 μm	VISTA-B-965-500C	6.2 ± 1.3	140	
TiO_2 (anatase), 30 μm	thermal hydrolysis/dried 110°C, calcined 2 h at 500°C/92 m^2/g, <10-nm primary crystallites	28[a]	145	
TiO_2 (anatase), 90 μm	basic precipitation/dried 110°C, calcined 2 h at 500°C/81 m^2/g, 10–14-nm primary crystallites	15[a]	145	
TiO_2 (75% anatase, 25% rutile)	Degussa P25, fumed/4-mm extrudates/48 m^2/g, $V_{pore} = 0.34$ cm^3/g, $d_{pore} = 21$ nm	0.9	146	
TiO_2 (anatase)	Rhone-Poulenc DT51, ppt./4 mm extrudates/92 m^2/g, $V_{pore} = 0.40$ cm^3/g, $d_{pore} = 8, 65$ nm	0.9	146	
	Low surface area ceramics			
Al_2O_3	spray dried with organic binder; plastic deformation observed	2.3	147	
Al_2O_3	heat treated (sintered), 99.9%	282–551	142	
TiO_2 (Rutile)	partially sintered	194	147	
ZrO_2 (yttria additive)	commercial samples from three companies, spray-dried	0.035–0.43	148	
ZrO_2 (3% Y_2O_3)	heat treated (sintered)	800–1500	142	

[a]Rough estimates from break points on relative density versus log[applied pressure] curves; data are consistent with mass distribution versus pressure curves from ultrasonic tests.

[prepared by United Catalyst (UCI)] and having nearly the same strength shown in Table 11 for Vista-B Al_2O_3 (6.3 vs. 6.2 MPa), were found to undergo substantial fracture to 5–30-μm fragments (an increase from 45 to 85%) as well as substantial erosion to 1 μm or less fragments (increase from 2 to 50%). Under the same treatment conditions, 90-μm-diameter agglomerates of Vista-B Al_2O_3 underwent by comparison much less attrition, mainly by erosion (20% increase in 0.1–5-μm fragments). The very low attrition resistance of the Fe/Cu/K UCI catalyst is further emphasized by the unsatisfactory outcome of a test of this catalyst by the U.S. Department of Energy (DOE) in a pilot-scale slurry-phase bubble-column reactor in LaPorte, Tex.; following one day of operation, the filter system was plugged with catalyst fines, preventing catalyst–wax separation and forcing shutdown of the plant (150).

Thus, based on these three representative examples, it follows that which of the two attrition mechanisms predominates depends much more on material

composition and type than on agglomerate strength. However, irrespective of mechanism the rate of attrition is usually greater for the weaker material.

The catalyst preparation method can have a large effect on the attrition resistance of an Fe/Cu Fischer–Tropsch catalyst (151). This catalyst, prepared by precipitation, undergoes severe attrition during a 25-min treatment with ultrasonic radiation; indeed the mass fraction finer than 0.1–5 μm increases from 0 to 65%. However, after a spray drying treatment of the same catalyst, less than a 10% increase in the same fractions is evident.

In their review of attrition and attrition test methods, Bemrose and Bridgewater (152) discuss how attrition varies with reactor type, eg, involves mainly particle–wall impacts in moving pellet bed reactors and particle–particle impacts in fluidized-bed reactors of high fluid velocity. In fact, jet attrition of catalyst particles in a gas fluidized bed involving principally abrasion due to collision of high-velocity particles has been modeled in some detail (149,153). Thus, given such important differences in attrition mechanism, realistic attrition test methods should attempt to model reactor operation as closely as possible. In addition, the ideal test would require only a small catalyst sample, a simple, inexpensive apparatus, and a few minutes to complete the test. Relatively quick, inexpensive single-particle crushing tests have been devised (152); however, properties of a single particle are rarely representative of those for the bed; moreover, it is difficult to relate the results of this crushing test to the actual abrasion process. Realistic tests have been devised for two reactor types involving a moving catalyst, ie, an air-jet test for fluidized-bed catalysts (154,155), and a rotating drum apparatus for moving-bed catalysts (156); however, the air-jet test requires a large quantity (eg, 50 g) of catalyst, an expensive apparatus, and about 20 h to run. In the past decade a new jet-cup test has been developed for testing of fluidized-bed catalysts (154,155), which requires only a 5-g sample and about 1 h to complete; comparisons of results for the jet-cup and air-jet tests indicate that the two tests give comparable results (154,155). Nevertheless, the mechanisms for the two tests are different, ie, the air-jet (fluid-bed) test is abrasion- (erosion-) dominant, while the jet-cup test includes both abrasion and fracture mechanisms (155). A 30-min, 10-g ultrasonic attrition test based on cavitation has also been developed in the past decade (145,151,157); while it likewise involves both abrasion and fracture mechanisms, the results appear to correlate with other methods. For example, particle size distributions for the same Co/silica catalyst after ultrasonic, jet-cup, and laboratory-scale, slurry-bed column reactor (SBCR) tests are very similar, indicating that both fracture and abrasion mechanisms operate in the small-scale SBCR. Moreover, the good agreement among the three methods suggests that both the jet-cup and ultrasonic tests may provide data representative of the attrition process in laboratory-scale SBCR reactors. It is evident that these two small-scale methods are especially useful for screening of a series of catalysts to determine relative strength.

Nevertheless, the more realistic large-scale tests are probably needed for accurately determining design attrition rates of a commercial catalyst to be used in a full-scale process. The observation that attrition of a fluid catalytic cracking (FCC) catalyst initially involves fracture of weak agglomerates followed by abrasion of strong agglomerates emphasizes the need to collect and analyze the particle size distribution of attrited fines as a function of time in order to

define which mechanism (or mechanisms) operates at startup as well as in the steady-state process. Because the mechanism may be time dependent, rapid, small-scale tests may produce misleading results.

While realistic laboratory-scale tests have been developed for simulating attrition in large moving-bed and fluidized-bed reactors, no such laboratory test has been developed and demonstrated yet for simulation of large-scale SBCR reactors, although recent research has focused on the development of such tests. For example, in laboratory-scale, SBCR tests of supported cobalt catalysts over several days (157), it was observed that the attrition resistance decreases in the order Co/Al_2O_3, Co/SiO_2, Co/TiO_2 (especially the anatase form underwent attrition at a high rate); attrition resistance was observed to increase with increasing cobalt loading from 10 to 40 wt%.

Implications of Mechanistic Knowledge of Attrition for Catalyst Design. The understanding of mechanisms important in attrition of catalyst supports and catalysts, the relationship between strength and attrition rate for a given material, and test data can be used to great advantage in the design of attrition resistant catalysts. Several alternatives follow from the previous discussion for increasing attrition resistance: (*1*) increasing aggregate/agglomerate strength by means of advanced preparation methods, eg, sol–gel granulation, spray drying, and carefully controlled precipitation methods (see Table 11 for examples), (*2*) adding binders to improve strength and toughness, eg, the addition of a polyvinylpyrrolidone binder to agglomerates of quartz sand increases agglomerate strength from 0.1 to 3 MPa (158), (*3*) coating aggregates with a porous but very strong material such as ZrO_2, eg, embedding a fluidized-bed catalyst for partial oxidation of *n*-butane to maleic anhydride in a strong, amorphous matrix of zirconium hydrogen phosphate significantly improves its attrition resistance (159), and (*4*) chemical or thermal tempering of agglomerates to introduce compressive stresses that increase strength and attrition resistance, eg, heating and cooling particles rapidly by passing them through a low-residence-time, high-temperature furnace to harden the agglomerate exterior, while preventing significant sintering of or phase changes in the porous interior. The subject of preventing mechanical degradation and other forms of catalyst deactivation is addressed in greater detail under Prevention of Catalyst Decay.

2.6. Summary of Deactivation Mechanisms for Solid Catalysts. Causes of solid (heterogeneous) catalyst deactivation are basically threefold: (*1*) chemical, (*2*) mechanical, and (*3*) thermal. Mechanisms of heterogeneous catalyst deactivation can be classified into five general areas: (*1*) chemical degradation including volatilization and leaching, (*2*) fouling, (*3*) mechanical degradation, (*4*) poisoning, and (*5*) thermal degradation. Poisoning and thermal degradation are generally slow processes, while fouling and some forms of chemical and mechanical degradation can lead to rapid, catastrophic catalyst failure. Some forms of poisoning and many forms of fouling are reversible; hence, reversibly poisoned or fouled catalysts are relatively easily regenerated. On the other hand, chemical, mechanical, and thermal forms of catalyst degradation are rarely reversible.

It is often easier to prevent rather than cure catalyst deactivation. Many poisons and foulants can be removed from feeds using guard beds, scrubbers, and/or filters. Fouling, thermal degradation, and chemical degradation can be

minimized through careful control of process conditions, eg, lowering temperature to lower sintering rate or adding steam, oxygen, or hydrogen to the feed to gasify carbon or coke-forming precursors. Mechanical degradation can be minimized by careful choice of carrier materials, coatings, and/or catalyst particle forming methods.

While treating or preventing catalyst deactivation is facilitated by an understanding of the mechanisms, additional perspectives are provided by examining the route by which each of the mechanisms causes loss of catalytic activity, ie, how it influences reaction rate (92). Thus, catalytic activity can be defined in terms of the observed site-based rate constant k_{obs}, which is equal to the product of the active site density σ (number of sites per area of surface), the site-based intrinsic rate constant k_{intr}, and the effectiveness factor η, ie,

$$k_{obs} = \sigma k_{intr} \eta \tag{4}$$

Loss of catalytic activity may be due to a decrease in any of the three factors in equation 4, whose product leads to k_{obs}. Thus, catalyst deactivation can be caused by (*1*) a decrease in the site density σ, (*2*) a decrease in intrinsic activity (ie, decrease in k_{intr}), and/or (*3*) lowered access of reactants to active sites (decrease in η). Poisoning, for example, leads to a loss of active sites, ie, $\sigma = \sigma_0(1-\alpha)$, where α is the fraction of sites poisoned; sintering causes loss of active sites through crystallite growth and reduction of active surface area. Fouling can cause both loss of active sites due to blocking of surface sites as well as plugging of pores causing a decrease in the effectiveness η. Moreover, poisoning, as discussed earlier, can also lead to a decrease in intrinsic activity by influencing the electronic

Table 12. **How Deactivation Mechanisms Affect the Rate of a Catalyzed Reaction and the Rapidity and Reversibility of Deactivation Process**

	Effects on reaction rate		Deactivation process		
Deactivation mechanism	Decrease in number of active sites	Decrease in intrinisic activity (k_{intr})	Decrease in effectiveness factor (η)	Fast or slow[a]	Reversible
chemical degradation	×	×	×[b,c]	varies	no
fouling	×		×	fast	yes
mechanical degradation	×			varies	no
poisoning	×	×[b,d]		slow	usually
sintering	×		×[b,e]	slow	sometimes
vaporization/ leaching	×		×[b,f]	fast	sometimes

[a]Generally.
[b]In some cases.
[c]Chemical degradation can cause breakdown of support, pore plugging, and loss of porosity.
[d]If the reaction is structure-sensitive, sintering could either increase or decrease intrinsic activity.
[e]Sintering of the support may cause support collapse and loss of porosity; it may also increase average pore diameter.
[f]Leaching of aluminum or other cations from zeolites can cause buildup of aluminum or other oxides in zeolite pores.

structure of neighboring atoms. Thus, each of the deactivation mechanisms affects one or more of the factors comprising observed activity (see Table 12); all of the mechanisms, however, can effect a decrease in the number of catalytic sites.

3. Homogeneous Catalysts and Enzymes

3.1. Homogeneous Catalysts. The discussion of the deactivation of homogeneous catalysts has received less attention relative to that of heterogeneous catalysts (160,161). Indeed, the first comprehensive review of homogeneous catalyst deactivation appeared just recently (160). Nevertheless, the vast literature of homogeneous catalysis provides numerous anecdotal accounts of problems with catalyst decomposition and references to homogeneous catalysts having a limited number of turnovers, all testifying to the importance of these phenomena.

Homogeneous catalysts may undergo degradation by routes similar to those of heterogeneous catalysts, eg, by chemical modification, poisoning, and thermal degradation. However, the specific details of these mechanistic routes are generally somewhat different, since the catalyst is a molecule rather than a solid; that is, an organometallic complex is quite different from a metal surface in terms of structure and scale. For example, reaction of impurities with homogeneous catalytic complexes is analogous to poisoning of a heterogeneous catalyst by impurities, although the former is essentially a chemical reaction of two species of similar dimensions while the latter involves adsorption of a molecule on the surface of a crystallite containing hundreds to thousands of atoms.

Homogeneous catalysts are generally metal–ligand complexes. The metal center functions as the active site, while the ligands serve to influence site chemistry through electronic modifications of the metal that influence activity/selectivity and through geometric constraints that enhance selectivity. Hence activity and selectivity properties of homogeneous catalysts can be significantly influenced by processes that change the chemistry either of the metal center or the ligands or both.

Mechanisms (or causes) of homogeneous catalyst degradation can be classified as (*1*) metal deposition reactions, eg, decarbonylation of carbonyl complexes, loss of protons from cationic species, or reductive elimination of C-, N-, or O-donor fragments; (*2*) decomposition of ligands attached to a catalytic complex; (*3*) reactions of metal–carbon and metal–hydride bonds with polar species (eg, water, oxygen, acids, alcohols, olefins, and halides); and (*4*) poisoning of active sites by impurities, reactants, or products or by dimerization of the catalyst.

Principal features of these mechanisms and examples thereof are summarized in Table 13. It is noteworthy that mechanisms 1 and 2 lead mainly to deactivation by either loss or modification of ligands, while mechanisms 3 and 4 cause deactivation largely by either modifying or poisoning the metal, although ligands are also clearly modified by type 3 mechanisms. Of the four mechanisms, deactivation by metal formation and deposition is the most common, although all are important.

Table 13. **Deactivation Mechanisms for Homogeneous Catalysts**[a]

Deactivation mechanism	Comments	Examples
1. *Metals deposition reactions*	most common decomposition mechanism	
ligand loss	decarbonylation is most common	2 $HCo(CO)_4 \rightarrow CO_2(CO)_8 \rightarrow CO_4(CO)_{12} \rightarrow$ Co metal
loss of protons from cationic species	reductive elimination as HX; pH dependent; basic media lead to zero-valent metals	in Wacker reaction elimination of HCl from PdHCl leads to Pd(0); in Heck reaction Pd(0) is an intermediate
reductive elimination of C-, N-, O-donor fragments	occurs in cross-coupling reactions to form C-C, C-N, C-O bonds	oxidative addition of aryl halides
2. *Ligand decompositions*	ligands greatly influence activity and selectivity of homogeneous catalysts	
oxidation	phosphorus or sulfur-based ligands are readily oxidized by O_2, H_2O, CO_2, peroxides; nitrogen-based ligands are more stable	$PR_3 + H_2O \rightarrow H_2 + O$ "PR_3; $PR_3 + 1/2\ O_2 \rightarrow O$ "PR_3
oxidative addition	breaking of C-P bond with insertion of a metal	decomposition of Rh and Co hydroformylation catalysts (161)
nucleophilic attack	internal or external attack causing insertion of metal in C-P bond or displacement of metal with Ar	decomposition of triphenylphosphines (TPPs) in Pd catalyst by acetate ion
thermal decomposition	depends on temperature and gas composition	decomposition of $RhH(CO)(PPh_3)$ hydroformylation catalysts to stable cluster containing μ_2-PPh_2 fragments in absence of H_2 and CO
reactions with water alcohols; rearrangements	hydrolysis, alcoholysis, and transesterification of phosphites, imines, and pyridines	hydrolysis of diphosphites in Rh-catalyzed hydroformylation of alkenes
3. *Reactions of metal–carbon and metal–hydride bonds*		
with water, oxygen, acids, and alcohols	decomposition of reactive metal alkyls with water or oxygen	deactivation of Ziegler catalysts containing alkyl complexes of Ti, Zr, and V
with olefins, halides, and aluminoxanes	formation of metallated transition metal ion complex deactivates polymerization catalysts	reaction of propene with zirconium alkyl catalyst forms an alkane and a π-allyl zirconium species
4. *Poisoning of active sites*		
by dienes and alkynes	forms a stable π-allylic complex; these poisons must be removed in polyolefin manufacture	methoxycarbonylation of propyne using Pd-2-pyridyl-DPP is poisoned by butadiene and 1,2-propadiene

Table 13 (*Continued*)

Deactivation mechanism	Comments	Examples
by polar impurities	such as basic amines	enantioselective isomerization of the allylamine to the asymmetric enamine (in menthol synthesis) is poisoned by a stronger basic amine isomer
by dimer formation	active monomeric catalyst species form dimers	Rh–TPP hydroformylation catalyst dimerizes; Pd(I) dimers in carbonylation catalysts

[a]Data from 160.

Mechanisms 1 and 4 are reversible to some extent. Mechanisms 2 and 3, involving breaking of active site bonds and formation of stable products, are largely irreversible. Products of ligand oxidation are generally more stable than the complexes from which they were formed.

3.2. Enzymes. *Structural and Catalytic Properties of Enzymes.* Enzymes are globular macromolecular polypeptide proteins (molecular weights of $10^4 - 10^6$) synthesized by living organisms (8,162). Each enzyme has a unique three-dimensional structure with a binding site or pocket that is chemically and geometrically compatible with a single reactant molecule (substrate) or group of chemically related reactants; in other words enzymes have molecular-recognition capability. Enzymes are unique in their ability to catalyze biochemical reactions with high selectivity (essentially 100%) at extraordinarily high rates, ie, 10–10,000 molecules/(enzymes) compared to typical values of 1–10 or less for conventional catalysts. These activities enable enzymes to be effective catalysts at extremely low concentrations, eg, $10^{-5} - 10^{-10}$ mol/L, at substrate (reactant) concentrations of greater than 10^{-6} mol/L.

The high activity of enzymes has been illustrated for urease and catalase (163,164). The stereochemical specificity of enzymes is unmatched and absolute, ie, their sites can distinguish between optical and geometrical isomers, almost always catalyzing only the reaction of one isomer of an enantiomeric pair (162). Nevertheless, some enzymes catalyze reactions of chemically unrelated species; for example, nitrogenase reduces N_2 to NH_3 as well as hydrogenating acetylene to ethylene (165).

In 1976 there were 1800 known enzymes, and new enzymes were being discovered at the rate of about 60 per year (166); accordingly, there were an estimated 3000 known enzymes in 1996. It is estimated that an average cell contains 3000 different enzymes (165), and it is speculated that as many as 25,000 different enzymes exist (167).

While they are synthesized *in vitro* and are only active within a limited range of pH and temperature, enzymes otherwise have properties similar to synthetic homogeneous and polymer-supported catalysts. Moreover, they can be extracted from their biological source, purified, crystallized, and used in laboratory studies or industrial processes. Further, they can be attached to glass or

ceramic supports and used as heterogeneous catalysts. And their application in industrial processes is rapidly increasing.

Enzymes are formed in living systems by condensation/dehydration of amino acids to produce peptide (C-N) bonds that constitute the backbone of long protein chains. The active conformation of an enzyme is produced by folding of the protein chain into secondary (helical), tertiary (folded), and quaternary (combined tertiary) structures. The folded layers are held in place by hydrogen bonding and disulfide linkages. There are 20 naturally occurring amino acids, each having the composition H_2N-CHR-COOH, the R group (side chain) having different molecular functions, eg, proton donation, proton removal, and bridge formation; for example, amino acids include glycine, alanine, and serine with side chains of H, CH_3, and CH_2OH respectively. Upon folding, side chains become the functional groups of the active site or ligands for binding of metals ions, which then become functional groups at the active site. Naturally occurring metal ions in enzymes include Mg^{2+}, Zn^{2+}, Ca^{2+}, Ni^{2+}, Fe^{2+}, Fe^{3+}, Co^{3+}, and Mo^{2+}.

Distinctive catalytic characteristics of enzymes (162) include (*1*) their flexible structure, which facilitates an "induced fit" of the substrate, the making and breaking of bonds, and the departure of products, and (*2*) their sensitivity to reaction *effectors* (inhibitors or activators), which function similarly to promoters of heterogeneous catalysts. Some enzymes require a *cofactor* that combines with the enzyme to form a catalytic site; metal ions are examples of cofactors. Enzymatic reactions may also require a *coenzyme* that reacts with the reactant to produce an enzyme-compatible substrate. Living organisms control and optimize biological processes using a variety of tools: (*1*) enzyme effectors, (*2*) regulation of enzyme growth or activation rates, (*3*) compartmentalization of enzymes within organs or organelles, and (*4*) destruction (editing) of undesired intermediates or products (162).

Deactivation of Enzymes. Enzymes generally function only under mild conditions of temperature and pH observed in living organisms. Under typical commercial reaction conditions (40–60°C, 1 atm) enzymes otherwise stable in solution may lose activity rapidly as a result of only slight changes in their environment such as temperature, pressure, pH, and ionic strength that induce small free energy changes from native to denatured states (168); moreover, their separation from the product is generally difficult and may cause further denaturation and loss of catalytic activity. The modest, largely reversible losses of activity resulting from small changes in reaction environment are largely due to modest changes in conformation of the active site. More severe changes in reaction conditions (eg, a 10°C increase in temperature) typically bring about the dissociation and unfolding of the quaternary and tertiary structures, respectively, into primary chains that subsequently order into fibrous protein bundles; in the process active sites are irreversibly destroyed. If further exposed to severe conditions of temperature and pH, the principal chain structure of the protein may undergo loss or modification of functional groups or amino acid residues.

The activity of a typical enzyme increases exponentially with temperature in accordance with the Arrhenius law up to about 50–60°C, passes through a maximum and declines precipitously above about 60–70°C. Thus, catalyst life may be on the order of days to weeks at around 50°C; however, the deactivation

rate is extremely high at only slightly higher temperatures, eg, 50% loss of activity in 5 min at 65–70°C is typical. Nevertheless, a few enzymes are active and stable at temperatures exceeding 100°C; for example, α-amylase catalyzes starch liquifaction at 105–115°C. Because their deactivation rates are highly temperature-dependent, enzymes are generally shipped and stored under refrigeration (0–4°C); at these low temperatures they are generally stable for months.

Causes of deactivation can be classified (as in the case of heterogeneous catalysts) as chemical, mechanical, and thermal. However, for enzymes these causes are closely linked, since mechanically and thermally induced routes almost always effect chemical changes. Thermally induced chemical change (at elevated temperature) is the most likely scenario for enzyme deactivation.

Chemical deactivation mechanisms include (*1*) changes in stereo configuration by protons or hydroxyl ions at or near active sites (169,170), (*2*) structural modifications in aqueous or nonaqueous solvents (171–173), (*3*) poisoning of active sites by inhibitors (162,174), including "Trojan-horse inhibitors" that are activated by the target enzyme (162), (*4*) aggregation (175), (*5*) unfolding (*6*) fragmentation due to solvolysis, hydrolysis in water, or self-hydrolysis (autolysis) of proteases, eg, trypsin (176), and (*7*) oxidation in air (177,178). Mechanisms 1–5 may be reversible, while mechanisms 6 and 7 are generally irreversible. Mechanical deactivation may be caused by hydrodynamic shear forces, eg, by stirring or gas sparging, sometimes leading to fragmentation and/or aggregation (175,178).

Thermal inactivation of enzymes is a well-studied phenomenon (179–185); it may be either reversible or irreversible (180). Potentially reversible changes (due to small, short excursions in temperature near the characteristic unfolding temperature) include light aggregation, conformational changes, folding without further chemical change, disulfide exchange, and/or breaking of hydrogen bonds. Irreversible denaturation (due to prolonged, severe thermal treatment) may be caused by cleavage of disulfide bonds and/or cystinyl cross-links; unfolding followed by chemical change; chemical changes of the primary structure and/or active site, eg, cleavage of the polypeptide chain by hydrolysis or destruction of individual amino acid residues; strong aggregation of inactive unfolded forms; and formation of rubbery, tough fibrous structures due to alignment and bundling of unfolded primary chains (similar to that observed during the boiling of an egg). Chemical bonding of unfolded primary chains to form fibers is thermodynamically favorable because chemical bonding of hydrophobic functions exposed by unfolding lowers the entropy and hence free energy of the system.

Table 14 summarizes representative examples of enzyme deactivation by the various mechanisms.

Methods of enhancing enzyme stability have received considerable attention (168,173,178,180,183,185–187). Strategies to improve both chemical and thermal stability include (*1*) use of soluble additives, (*2*) immobilization, (*3*) protein engineering, and (*4*) chemical modification. Chemical modification (183, 185–187) and immobilization (164,165,172,188–191) are probably the most successful and widely used methods. As examples of the first kind, modification of protein surfaces by chemical binding with polysaccharides can improve thermostability, while polyol binding increases enzyme solubility in organic solvents with little loss of activity (171,176,183). Enzyme stability can be greatly enhanced and recovery problems obviated by immobilizing (heterogenizing)

Table 14. **Representative Examples of Deactivation Mechanisms for Enzymes**

Deactivation mechanism	Cause(s)/reversibility	Examples	Ref.
1. *Chemical*	generally involve formation or breaking of bonds in enzyme structure		
modest changes in active site configuration	caused by (a) introduction of H^+ or OH^- near active site, (b) small changes in pH or solvent environment/ largely reversible	model of effects of pH on phytases: enzyme is in equilibrium with protonated and hydroxylated forms which are less active or inactive	184
poisoning of active site	adsorption of inhibitor on active site/ sometimes reversible	mechanistic study of the inhibition of crotonase by (methylenecyclopropyl)-formyl-CoA; MCP ring trapping of an active site nucleophile is suggested	174
aggregation	caused by changes in pH or solvent environment with partial unfolding/ sometimes reversible	dimers and trimers of lysozyme are formed and activity is lost in a stirred reactor; mechanism may involve collision-induced conversion of enzyme to inactive state, followed by formation of disulfide bridges	175
unfolding, fragmentation, bundling of primary chains into fibers	cleavage of enzyme bonds due to interaction with solvent, H^+, or OH^- due to medium to large changes in pH/ irreversible	deactivation of peroxidase in organic solvents including DMSO; solvent may strip water from enzyme, leading to reduced conformational mobility and unfolding	168,172,173
2. *Mechanical*	caused by hydrodynamic shear forces, eg, stirring or gas sparging, which can break bonds and cause aggregation of enzymes/usually irreversible	lysozyme is aggregated and irreversibly inactivated in a stirred reactor; the deactivation rate constant is proportional to the impeller power	175
3. *Thermal*			
modest changes in active site configuration and reversible unfolding	caused by small, short excursions in temperature near the transition temperature[a]/ reversible	equilibrium measurements of the temperature-induced unfolding of bovine ribonuclease; repeated measurements after cooling fall on the same plot of fraction unfolded versus T	179,180

Table 14 (*Continued*)

Deactivation mechanism	Cause(s)/reversibility	Examples	Ref.
irreversible unfolding, fragmentation, bundling of primary chains into fibers	cleavage of enzyme bonds due to interaction with solvent, H^+, or OH^- due to medium to large changes in pH/ irreversible	irreversible thermoinactivation of hen egg white lysozyme at 100°C and pH 4, 6, 8; inactivation is due to monomolecular changes in coordination, eg, hydrolysis of the Asp-X peptide bonds, deamidation of Asn residues, destruction of cystine residues, and formation of incorrect structures	180

[a]Characteristic temperature for a specific enzyme above which unfolding occurs and below which refolding occurs.

enzymes (164,165,172,188–191) through (*1*) covalent binding to a support, (*2*) cross-linking of enzymes using a bifunctional agent, (*3*) adsorption on a solid surface, (*4*) entrapment in a gel, or (*5*) containment in a membrane. Moreover, immobilization enables the catalytic process to be run continuously using a reactor of substantially lower volume, thereby substantially reducing capital and operating costs. These important advantages have stimulated the development of a significant number of commercial immobilized enzyme systems.

4. Prevention of Catalyst Decay

4.1. General Principles of Prevention. The age-old adage that says "an ounce of prevention is worth a pound of cure" applies well to the deactivation of catalysts in many industrial processes. The catalyst inventory for a large plant may entail a capital investment of tens of millions of dollars. In such large-scale processes, the economic return on this investment may depend on the catalyst remaining effective over a period of up to 3–5 years. This is particularly true of those processes involving irreversible or only partially reversible deactivation (eg, sulfur poisoning or sintering). Some typical industrial catalysts, approximate catalyst lifetimes, and factors that determine their life are listed as examples in Table 15. It is evident that in many processes more than one mechanism limits catalyst life. Moreover, there is a wide variation in catalyst lifetimes among different processes, ie, from 10^{-6} to 15 years. While there is clearly greater interest in extending catalyst lifetimes in processes where life is short, it should be emphasized that great care must be exercised in protecting the catalyst in any process from process upsets (eg, temperature runaway, short-term exposure to impure feeds, or changes in reactant composition) that might reduce typical catalyst life by orders of magnitude, eg, from years to hours.

While complete elimination of catalyst deactivation is not possible, the rate of damage can be minimized in many cases through understanding of the

Table 15. **Typical Lifetimes and Factors Determining the Life of Some Important Industrial Catalysts**[a]

Reaction	Operating conditions	Catalyst	Typical life (years)	Process affecting life of catalyst charge	Catalyst property affected
Ammonia synthesis $N_2 + 3\,H_2 \rightarrow 2\,NH_3$	450–470°C, 200–300 atm	Fe with promoters (K_2O) and stabilizer (Al_2O_3)	10–15	slow sintering	activity
methanation (ammonia and hydrogen plants) $CO/CO_2 + H_2 \rightarrow CH_4 + H_2O$	250–350°C, 30 atm	supported nickel	5–10	slow poisoning by S, As, K_2CO_3 from plant upsets	activity and pore blockage
acetylene hydrogenation ("front end") $C_2H_2 + H_2 \rightarrow C_2H_4$	30–150°C, 20–30 atm	supported palladium	5–10	slow sintering	activity/selectivity and temperature
sulfuric acid manufacturing $2\,SO_2 + O_2 \rightarrow 2\,SO_3$	420–600°C, 1 atm	vanadium and potassium sulfates on silica	5–10	inactive compound formation; pellet fracture; plugging by dust	activity, pressure drop, and mass transfer
methanol synthesis $CO + 2\,H_2 \rightarrow CH_3OH$	200–300°C, 50–100 atm	copper on zinc and aluminum oxides	2–5	slow sintering; poisoning by S, Cl, and carbonyls	activity
low temperature CO shift $CO + H_2O \rightarrow CO_2 + H_2$	200–250°C, 10–30 atm	copper on zinc and aluminum oxides	2–4	slow poisoning and accelerated sintering by poisons	activity
hydrocarbon hydrode sulfurization $R_2S + 2\,H_2 \rightarrow H_2S + R_2$	300–400°C, 30 atm	cobalt and molybdenum sulfides on aluminum oxide	1–10	slow coking, poisoning by metal deposits in residues	activity, mass transfer, and pressure drop
high temperature CO shift $CO + H_2O \rightarrow H_2 + CO_2$	350–500°C, 20–30 atm	Fe_3O_4 on chromia	1–4	slow sintering, pellet breakage due to steam	activity and pressure drop
steam reforming, natural gas $CH_4 + H_2O \rightarrow CO + 3\,H_2$	500–850°C, 30 atm	nickel on calcium aluminate or α-alumina	1–3	sintering, sulfur-poisoning, carbon formation, and pellet breakage due to plant upsets	activity and pressure drop
ethylene partial oxidation $2\,C_2H_4 + O_2 \rightarrow 2\,C_2H_4O$	200–270°C, 10–20 atm	silver on α-alumina with alkali metal promoters	1–3	slow sintering, poisoning by Cl, S	activity and selectivity

butane oxidation to maleic anhydride $C_4H_{10} + 3.5\ O_2 \rightarrow C_4H_2O_3 + 4\ H_2O$	400–520°C, 1–3 atm	vanadium phosphorus oxide with transition metal additives	1–2	loss of P; attrition or pellet breakage; S, Cl poisoning	activity and selectivity
reduction of aldehydes to alcohols $RCHO + H_2 \rightarrow RCH_2OH$	220–270°C, 100–300 atm	copper on zinc oxide	0.5–1	slow sintering, pellet breakage (depends on feedstock)	activity or pressure drop
ammonia oxidation $2\ NH_3 + 5/2\ O_2 \rightarrow 2\ NO + 3\ H_2O$	800–900°C, 1–10 atm	Pt–Rh alloy gauze	0.1–0.5	surface roughness, loss of platinum, fouling by Fe	selectivity
oxychlorination of ethylene to ethylene dichloride $2\ C_2H_4 + 4\ HCl + O_2 \rightarrow 2\ C_2H_4Cl_2 + 2\ H_2O$	230–270°C, 1–10 atm	copper chlorides on alumina (fluidized bed)	0.2–0.5	loss by attrition and other causes resulting from plant upsets	fluidized state and activity
catalytic hydrocarbon reforming	460–525°C, 8–50 atm	platinum alloys on treated alumina	0.01–0.5	coking, frequent regeneration	activity and mass transfer
catalytic cracking of oils	500–560°C, 2–3 atm (fluidized bed)	synthetic zeolites	0.000002	very rapid coking (continuous regeneration)	activity and mass transfer

[a]Adapted from Ref. 9.

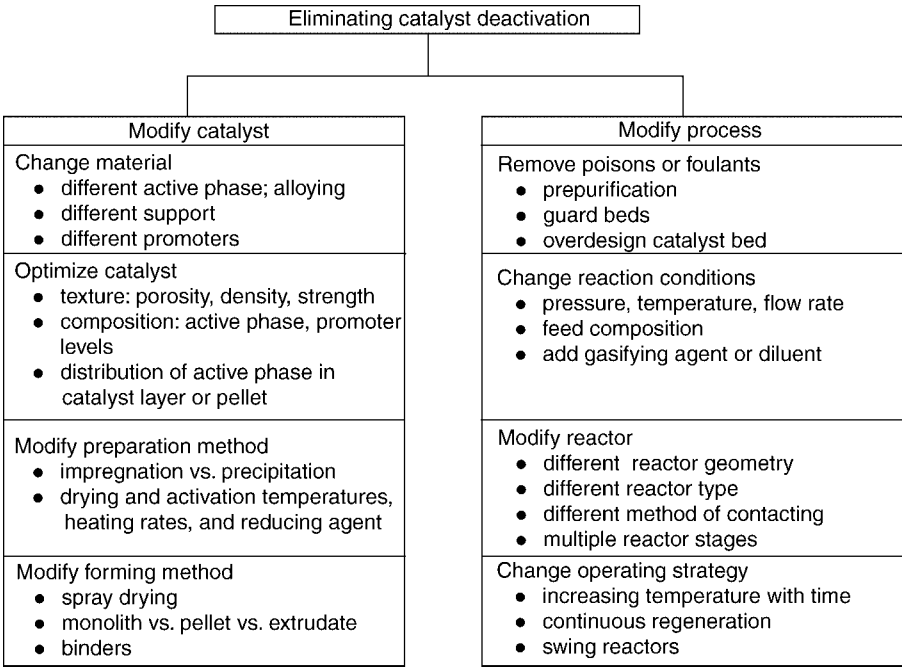

Fig. 8. Approaches to eliminating catalyst deactivation.

mechanisms, thereby enabling control of the deactivation process, ie, prevention is possible through control of catalyst properties, process conditions (ie, temperatures, pressures), feedstock impurities, methods of contacting, and process design. Figure 8 illustrates general approaches to eliminating or moderating deactivation through modifications in catalyst and/or process. Examples of how deactivation can be prevented are discussed below in connection with the most important causes of deactivation: chemical degradation, fouling by coke and carbon, poisoning, sintering, and mechanical degradation. Principles for preventing deactivation by these mechanisms are summarized in Table 16. Representative results from studies focusing on prevention or minimization of catalyst deactivation are found in Refs. 18,48,55,56,192–245.

4.2. Prevention of Chemical Degradation (by Vapor–Solid and Solid–Solid Reactions). The most serious problems-oxidation of metal catalysts, overreduction of oxide catalysts, and reaction of the active catalytic phase with carrier or promoter-can be minimized or prevented by careful catalyst and process design (as enumerated in Table 16). For example, the loss of Rh due to solid-state reaction with alumina in the automotive three-way catalyst can be prevented by supporting Rh on ZrO_2 in a separate layer from Pt and/or Pd on alumina. In Fischer–Tropsch synthesis, the oxidation of the active cobalt phase in supported cobalt catalysts to inactive oxides, aluminates, and silicates can be minimized by employing a two- or three-stage process in which product steam is moderated in the first stage by limiting conversion and in subsequent stages by interstage removal of water. It can also be moderated by addition of noble metal promoters that facilitate and maintain high reducibility of the cobalt

Table 16. **Methods for Preventing Catalyst Decay**

Basic mechanism	Problem	Cause	Methods of minimization
chemical degradation	oxidation of metal catalysts to inactive oxides	oxidation of metal by contaminant O_2 or reactant/ product water	(*1*) purify feed of oxidants; (*2*) minimize reactant/product water by recycle/separation, staged reactors, and otherwise limiting conversion; (*3*) incorporate additives that facilitate resistance to oxidation
	transformation of active phase to stable, inactive phase	solid-state reaction of active phase with support or promoters	(*1*) avoid conditions (eg, oxidizing condition, high steam pressures, and high temperatures) that favor solid-state reactions and (*2*) select combinations of active phase and promoters/supports that are noninteracting
		overreduction of active oxide phases	(*1*) stabilize oxidation state using promoters that induce resistance to reduction or that serve as oxygen donors and (*2*) add steam to the reactants to prevent overreduction
fouling by coke or carbon	loss of catalytic surface sites due to formation of carbon or coke films	free-radical reactions in gas phase	(*1*) avoid formation of free radicals, lower temp.; (*2*) minimize free space; (*3*) free radical traps, diluents; (*4*) add gasifying agents (eg, H_2, H_2O)
		free-radical reactions at reactor walls	(*1*) coat reactor with inert material
		formation and growth on metal surfaces	(*1*) avoid accumulation of coke precursors (eg, atomic carbon, olefins) through careful choice of reactant conditions or membranes; (*2*) add gasifying agents (eg, H_2, H_2O), diluents; (*3*) incorporate catalyst additives to increase rate of gasification or to change ensemble size; (*4*) passivate metal surfaces with sulfur; (*5*) decrease dispersion; and (*6*) recycle inerts to flush surface of heavy oligomers and to moderate temperature
		formation and growth on metal oxides, sulfides	(*1*) utilize measures 1, 2, 3, and 6 for metal surfaces; (*2*) design catalyst for optimum pore structure and acidity; and (*3*) use shape-selective, coke-resistant molecular sieves
	loss of catalyst effectiveness; plugging of pores; destruction of catalyst	formation of gas phase coke, vermicular carbons, and liquid or solid cokes in massive quantities	(*1*) minimize formation of free radicals or coke precursors as above; (*2*) use gasifying agents; (*3*) incorporate catalyst additives that lower solubility of carbon in metal or that change ensemble size; (*4*) use supports with large pores, large pellets

Table 16 (*Continued*)

Basic mechanism	Problem	Cause	Methods of minimization
		hot spots in pellet or bed	(*1*) use wash coat or small pellets; (*2*) use slurry- or fluid-bed reactor, gas diluents
mechanical failure	crushing of granules, pellets, or monoliths in a fixed bed	brittle fracture due to a mechanical load	(*1*) minimize porosity of pellets or monoliths; (*2*) improve bonding of primary particles in agglomerates that make up pellets or monoliths using advanced forming methods, eg, spray drying and controlled thermal treatments; (*3*) add binders such as carbon to the support material, which facilitate plastic deformation and thus protect against brittle fracture; and (*4*) chemically or thermally temper agglomerates
	attrition and/or erosion in fixed or moving beds	abrasion of catalyst coatings or particles due to mechanical, thermal, or chemical stresses	(*1*) avoid highly turbulent shear flows and/or cavitation, leading to high erosion rates; (*2*) avoid thermal stresses in the preparation and use of catalysts that lead to fracture or separation of coatings; and (*3*) avoid formation of chemical phases of substantially different densities or growth of carbon filaments that cause fracture of primary particles and agglomerates. Choose supports, support additives, and coating materials such as titanates, zirconia, and zirconates, having high fracture toughness
poisoning	loss of catalytic surface sites	blockage of sites by strong adsorption of impurity	(*1*) purify feed and/or use guard bed to adsorb poison; (*2*) employ additives that selectively adsorb poison; (*3*) choose reaction conditions that lower adsorption strength; (*4*) optimize pore structure and choose mass transfer regimes that minimize adsorption of poison on active sites; and (*5*) apply coating that serves as diffusion barrier to poison
thermal degradation, sintering	loss of metal area	metal particle or subparticle migration at high temperatures	(*1*) lower or limit reaction temperature while facilitating heat transfer; (*2*) add thermal stabilizers to catalyst; and (*3*) avoid water
	loss of support area	crystallization and/or structural modification or collapse	same as for avoiding loss of metal area

and by coating the alumina or silica support with materials such as ZrO_2 that are less likely to react with cobalt to form inactive phases.

4.3. Prevention of Fouling by Coke and Carbon. Rostrup-Nielsen and Trimm (45), Trimm (47), and Bartholomew (48) have discussed principles and methods for avoiding coke and carbon formation. General methods of preventing coke or carbon formation are summarized in Table 16. Most of these are based on one important fundamental principle, namely that *carbon or coke results from a balance between the reactions that produce atomic carbon or coke precursors and the reactions of these species with* H_2, H_2O, *or* O_2 *that remove them from the surface*. If the conditions favor formation over gasification, these species accumulate on the surface and react further to less active forms of carbon or coke, which either coat the surface with an inactive film or plug the pores, causing loss of catalyst effectiveness, pore plugging, or even destruction of the carrier matrix.

Methods to lower rates of formation of carbon or coke precursors relative to their rates of gasification vary with the mechanism of formation (ie, gas, surface, or bulk phase) and the nature of the active catalytic phase (eg, metal or oxide). For example, gas phase formation can be minimized by choosing reaction conditions that minimize the formation of free radicals, by using free-radical traps, by introducing gasifying agents (eg, H_2, H_2O) or gas diluents, and by minimizing the void space available for homogeneous reaction. Similarly, the formation and growth of carbon or coke species on metal surfaces is minimized by choosing reaction conditions that minimize the formation of atomic carbon or coke precursors and by introducing gasifying agents. Selective membranes or supercritical conditions can also be used to lower the gas-phase and surface concentrations of coke precursors. Since carbon or coke formation on metals apparently requires a critical ensemble of surface metal atoms and/or dissolution of carbon into the bulk metal, introduction of modifiers that change ensemble sizes (eg, Cu or S in Ni or Ru) or that lower the solubility of carbon (eg, Pt in Ni) can be effective in minimizing these forms of deactivation.

Coke deposition on oxide or sulfide catalysts occurs mainly on strongly acidic sites; accordingly the rate of coking can be lowered by decreasing the acidity of the support. For example, silanation of HY and HZSM-5 zeolites decreases their activities but improves catalyst life (245). In steam reforming, certain catalyst additives, eg, MgO, K_2O, or U_3O_8, facilitate H_2O or CO_2 adsorption and dissociation to oxygen atoms, which in turn gasify coke precursors (8,48,55).

As in the case of poisoning (see below), there are certain reactor bed or catalyst geometries that minimize the effects of coking on the reaction. For example, specific film-mass transport or pore diffusion regimes favor coke or carbon deposition on either the outside or inside of the catalyst pellet (246,247). Choosing supports with relatively large pores minimizes pore plugging; choice of large-diameter, mechanically-strong pellets avoids or delays reactor plugging. But in view of the rapidity at which coke and carbon can deposit on, plug, and even destroy catalyst particles, the importance of preventing the onset of such formation cannot be overemphasized.

Reforming of naphtha provides an interesting case study of catalyst and process designs to avoid deactivation by coking (8,206,208,248). The classical

Pt/Al_2O_3 catalyst is bifunctional; that is, the metal catalyzes dehydrogenation while the acid sites of the Al_2O_3 catalyze isomerization and hydrocracking. Together the two functions catalyze dehydrocylization and aromatization. Addition of Re, Sn, or Ge to Pt and sulfiding of the Pt–Re catalyst substantially reduce coke formation by diluting large Pt ensembles that would otherwise produce large amounts of coke, while addition of Sn and Ir improves selectivity for dehydrogenation relative to hydrogenolysis, the latter of which leads to coke formation. Naphtha reforming processes are designed for (*1*) high enough H_2 pressure to favor gasification of coke precursors while minimizing hydrocracking, (*2*) maintenance of Cl and S contents throughout the bed to ensure optimum acidity and coke levels, and (*3*) low enough overall pressure to thermodynamically and kinetically favor dehydrogenation and dehydrocylization. Accordingly, optimal process conditions are a compromise between case 1 and case 3. The above-mentioned improvements in catalyst technologies, especially resistance to coking, have enabled important process improvements such as optimal operation at lower pressure; thus, processes have evolved over the past two to three decades from conventional fixed-bed reactors at high pressure (35 bar) using nonregenerative Pt catalysts to low pressure (3.5 bar), slowly moving-bed, continuously regenerated units with highly selective Pt/Sn catalysts, resulting in substantial economic benefits (248).

4.4. Prevention of Poisoning. Since poisoning is generally due to strong adsorption of feed impurities and since poisoned catalysts are generally difficult or impossible to regenerate, it is best prevented by removal of impurities from the feed to levels that will enable the catalyst to operate at its optimal lifetime. For example, it is necessary to lower the feed concentration of sulfur compounds in conventional methanation and Fischer–Tropsch processes involving base metal catalysts to less than 0.1 ppm in order to ensure a catalyst lifetime of 1–2 years. This is typically accomplished using a guard bed of porous ZnO at about 200°C. In cracking or hydrocracking reactions on oxide catalysts, it is important to remove strongly basic compounds such as ammonia, amines, and pyridines from the feed; ammonia in some feedstocks, for example, can be removed by aqueous scrubbing. The poisoning of catalysts by metal impurities can be moderated by selective poisoning of the unwanted metal. For example, in catalytic cracking of nickel-containing petroleum feedstocks, nickel sites, which would otherwise produce copious amounts of coke, are selectively poisoned by antimony (249). The poisoning of hydrotreating catalysts by nickel and vanadium metals can be minimized by (*1*) using a guard bed of inexpensive Mo catalyst or a graded catalyst bed with inexpensive, low-activity Mo at the top (bed entrance) and expensive, high-activity catalyst at the bottom (see Fig. 9) and (*2*) depositing coke prior to the metals since these metal deposits can be physically removed from the catalyst during regeneration (250).

It may be possible to lower the rate of poisoning through careful choice of reaction conditions that lower the strength of poison adsorption (48) or by choosing mass-transfer-limiting regimes that limit deposits to the outer shell of the catalyst pellet, while the main reaction occurs uninterrupted on the interior of the pellet (246). The manner in which the active catalytic material is deposited on a pellet (eg, uniformly or in an eggshell or egg yolk pattern) can significantly influence the life of the catalyst (17,251).

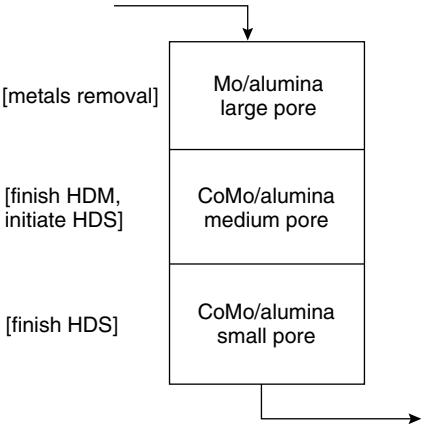

Fig. 9. Staged reactor system with decreasing pore size strategy for HDM/HDS of residues (224).

An example of reducing catalyst poisoning (and oxidation) through process design has been reported in a process patent for staged hydrocarbon synthesis via the Fischer–Tropsch reaction (252). While cobalt catalysts are favored because of their high activities and while it is desirable to achieve high conversions of CO in the process, the one-pass conversion for cobalt is limited by (*1*) its tendency to be oxidized at high partial pressures of product water observed at high CO conversions and (*2*) its tendency to form under these conditions the oxygenated products (eg, alcohols and aldehydes) that poison or suppress its synthesis activity. One alternative is to separate products and recycle the unused CO and H_2, but this requires costly recompression and separation of the oxygenates. Costly separation and/or poisoning can be prevented by operating a first-stage reactor containing a cobalt catalyst to a moderately high conversion followed by reacting the remaining CO and H_2 in a second stage to above 95% conversion on an iron catalyst, which is not sensitive to the oxygenates and which shifts some of the product water to H_2 and CO_2, thus minimizing its hydrothermal degradation.

An example of reducing catalyst poisoning through catalyst design occurs in abatement of emissions for automotive and motorcycle engines (18,222). Application of an alumina or zeolite coating or alternatively preparing the active phase in a sublayer provides a diffusion barrier that prevents or slows the access of poisons from the fuel or oil (eg, phosphorus and/or zinc from lubricating oil or corrosion products) to the catalyst surface. The principle is to optimize the pore size distribution of the diffusion barrier to provide access to the catalytic phase of relatively small hydrocarbon, CO, NO, and O_2 molecules while preventing access of larger molecules such as from lubricating oil and/or particulates.

4.5. Prevention of Sintering. Since most sintering processes are irreversible or are reversed only with great difficulty, it is important to choose reaction conditions and catalyst properties that avoid such problems. Metal growth is a highly activated process; thus by choosing reaction temperatures lower than 0.3–0.5 times the melting point of the metal, rates of metal sintering can be greatly minimized. The same principle holds true in avoiding recrystallization

of metal oxides, sulfides, and supports. Of course, one approach to lowering reaction temperature is to maximize activity and surface area of the active catalytic phase.

Although temperature is the most important variable in the sintering process, differences in reaction atmosphere can also influence the rate of sintering. Water vapor in particular accelerates the crystallization and structural modification of oxide supports. Accordingly, it is vital to minimize the concentration of water vapor in high temperature reactions on catalysts containing high surface area supports.

Besides lowering temperature and minimizing water vapor, it is possible to lower sintering rates through addition of thermal stabilizers to the catalyst. For example, the addition of higher melting noble metals (such as rhodium or ruthenium) to a base metal (such as nickel) increases the thermal stability of the base metal (253). Addition of Ba, Zn, La, Si, and Mn oxide promoters improves the thermal stability of alumina (254).

Designing thermally stable catalysts is a particular challenge in high temperature reactions such as automotive emissions control, ammonia oxidation, steam reforming, and catalytic combustion. The development of thermally stable automotive catalysts has received considerable attention, thus providing a wealth of scientific and technological information on catalyst design (eg, Refs. 8 and 225–232). The basic design principles are relatively simple: (*1*) utilize thermally and hydrothermally stable supports, eg, high-temperature δ- or θ-aluminas or alkaline-earth or rare-earth oxides that form ultrastable spinels with γ-alumina; (*2*) use PdO rather than Pt or Pt–Rh for high temperature converters, since PdO is considerably more thermally stable in an oxidizing atmosphere because of its strong interaction with oxide supports; and (*3*) use multilayer strategies and/or diffusion barriers to prevent thermally induced solid-state reactions (eg, formation of Rh aluminate) and to moderate the rate of highly exothermic CO and hydrocarbon oxidations. For example, a typical three-way automotive catalyst may contain alkaline-earth metal oxides (eg, BaO) and rare-earth oxides (eg, La_2O_3 and CeO_2) for stabilizing Pt and/or PdO on alumina and ZrO_2 as a thermal stabilizer for the CeO_2, an oxygen storage material, and as a noninteracting support for Rh in a separate layer or in a separate phase in a composite layer.

4.6. Prevention of Mechanical Degradation. While relatively few studies have focused on this topic, there are nevertheless principles that guide the design of processes and catalysts in preventing or minimizing mechanical degradation. In terms of catalyst design it is important to (*1*) choose supports, support additives, and coatings that have high fracture toughness, (*2*) use preparation methods that favor strong bonding of primary particles and agglomerates in pellets and monolith coatings, (*3*) minimize (or rather optimize) porosity (thus maximizing density), and (*4*) use binders such as carbon to facilitate plastic deformation and thus protect against brittle fracture. Processes (and to some extent preparation procedures) should be designed to minimize (*1*) highly turbulent shear flows or cavitation that lead to fracture of particles or separation of coatings, (*2*) large thermal gradients or thermal cycling leading to thermal stresses, and (*3*) formation of chemical phases of substantially different densities or formation of carbon filaments leading to fracture of primary particles and

agglomerates. Nevertheless, thermal or chemical tempering can be used in a controlled fashion to strengthen catalyst particles or agglomerates.

Examples of catalyst design to minimize attrition can be found in the recent scientific (239,240) and patent (241–244) literature focusing on the Fischer–Tropsch synthesis in slurry reactors. These studies indicate that (*1*) spray drying of particles improves their density and attrition resistance; (*2*) addition of silica and/or alumina into titania improves its attrition resistance, while addition of only 2000–3000 ppm of titania to γ-alumina improves alumina's attrition resistance; and (*3*) preformed alumina spheres promoted with La_2O_3 provide greater attrition resistance relative to silica. Increasing attrition resistance is apparently correlated with increasing density (239,240,244). According to Singleton and coworkers (244), attrition resistance of Co/Al_2O_3 is improved when the γ-alumina support is (*1*) formed from synthetic boehmite having a crystallite diameter of 4–5 nm and (*2*) pretreated in acidic solution having a pH of 1–3; moreover, attrition resistance decreases in the order Co/Al_2O_3, Co/SiO_2, Co/TiO_2 and is greater for catalyst prepared by aqueous versus nonaqueous impregnation.

5. Regeneration of Deactivated Catalysts

Despite our best efforts to prevent it, the loss of catalytic activity in most processes is inevitable. When the activity has declined to a critical level, a choice must be made among four alternatives: (*1*) restore the activity of the catalyst, (*2*) use it for another application, (*3*) reclaim and recycle the important and/or expensive catalytic components, or (*4*) discard the catalyst. The first alternative (regeneration and reuse) is almost always preferred; catalyst disposal is usually the last resort especially in view of environmental considerations.

The ability to reactivate a catalyst depends upon the reversibility of the deactivation process. For example, carbon and coke formation is relatively easily reversed through gasification with hydrogen, water, or oxygen. Sintering on the other hand is generally irreversible, although metal redispersion is possible under certain conditions in selected noble metal systems. Some poisons or foulants can be selectively removed by chemical washing, mechanical treatments, heat treatments, or oxidation (255,256); others cannot be removed without further deactivating or destroying the catalyst.

The decision to regenerate/recycle or discard the entire catalyst depends largely on the rate of deactivation. If deactivation is very rapid, as in the coking of cracking catalysts, repeated or continuous regeneration becomes an economic necessity. Precious metals are almost always reclaimed where regeneration is not possible. Disposal of catalysts containing nonnoble heavy metals (eg, Cr, Pb, or Sn) is environmentally problematic and should be a last resort; if disposal is necessary, it must be done with great care, probably at great cost. Accordingly, a choice to discard depends upon a combination of economic and legal factors (256). Indeed, because of the scarcity of landfill space and an explosion of environmental legislation, both of which combine to make waste-disposal prohibitively expensive, there is a growing trend to regenerate or recycle spent catalysts (257,258). A sizeable catalyst regeneration industry benefits petroleum refiners by helping to control catalyst costs and limiting liabilities (259,260); it provides

for *ex situ* regeneration of catalyst and recovery/recycling of metals, eg, of cobalt, molybdenum, nickel, and vanadium from hydroprocessing catalysts (257).

Consistent with its importance the scientific literature treating catalyst regeneration is significant and growing (includes several hundred journal articles since 1990), (eg. refs. 256,261–263).

The patent literature treating catalyst regeneration/reactivation is enormous (more than 2000 patents); the largest fraction of this literature describes processes for regeneration of catalysts in three important petroleum refining processes, FCC, catalytic hydrocarbon reforming, and alkylation. However, a significant number of patents also claim methods for regenerating absorbents and catalysts used in aromatization, oligomerization, catalytic combustion, SCR of NO, hydrocracking, hydrotreating, halogenation, hydrogenation, isomerization, partial oxidation of hydrocarbons, carbonylations, hydroformylation, dehydrogenation, dewaxing, Fisher–Tropsch synthesis, steam reforming, and polymerization.

Conventional methods for regenerating (largely *in situ*) coked, fouled, poisoned, and/or sintered catalysts in some of these processes and representative examples thereof (264–296) are summarized in Table 17, while the basic principles and limitations involved in regeneration of coked, poisoned, and sintered catalysts are briefly treated in the subsections that follow.

5.1. Regeneration of Catalyst Deactivated by Coke or Carbon. Carbonaceous deposits can be removed by gasification with O_2, H_2O, CO_2, and H_2. The temperature required to gasify these deposits at a reasonable rate varies with the type of gas, the structure and reactivity of the carbon or coke, and the activity of the catalyst. Walker and co-workers (305) reported the following order for rates of uncatalyzed gasification at 10 kN/m^3 and 800°C (relative rates in parenthesis): O_2 (105) > H_2O (3) > CO_2 (1) > H_2 (3×10^{-3}). However, this activity pattern does not apply in general for other conditions and for catalyzed reactions (1). Nevertheless, the order of decreasing reaction rate of $O_2 > H_2O > H_2$ can be generalized.

Rates of gasification of coke or carbon are greatly accelerated by the same metal or metal oxide catalysts upon which carbon or coke deposits.

Because catalyzed removal of carbon with oxygen is generally very rapid at moderate temperatures (eg, 400–600°C), industrial processes typically regenerate catalysts deactivated by carbon or coke in air. Indeed, air regeneration is used to remove coke from catalysts in catalytic cracking (64), hydrotreating processes (261), and catalytic reforming (262).

One of the key problems in air regeneration is avoiding hot spots or overtemperatures which could further deactivate the catalyst. The combustion process is typically controlled by initially feeding low concentrations of air and by increasing oxygen concentration with increasing carbon conversion (261,306); nitrogen gas can be used as a diluent in laboratory-scale tests while steam is used as a diluent in full-scale plant operations (306). For example, in the regeneration of hydrotreating catalysts McCulloch (261) recommends keeping the temperature at less than 450°C to avoid the γ- to α-alumina conversion, MoO_3 sublimation, and cobalt or nickel aluminate formation, which occur at 815, 700, and 500–600°C respectively.

Table 17. **Conventional Methods for and Representative Examples of Catalyst Regeneration from Scientific and Patent Literatures**

Deactivation mechanism/ reaction/catalyst	Problem/cause	Method(s) of regeneration/phenomena studied/conclusions	Refs.
Deactivation by coke, carbon			
alkene aromatization oligomerization/zeolites, esp. ZSM-5, -22, -23, beta-zeolite, ferrierite	catalyst fouling by condensation of heavy oligomers to coke	(*1*) ZSM-5 catalyst for light olefin oligomerization containing 2–3% coke is treated in 8–10% steam/air mixture (1300 kPa, 93°C inlet) in a fluidized bed (*2*) a coked crystalline alumogallosilicate is contacted with oxygen at a concentration of 0.05–10 vol%, 420–580°C, and 300–4000 h^{-1}	264,265
alkylation of isoparaffins on solid catalysts/sulfated zirconia, USY[a], Nafion, silicalite, ZSM-5	rapid catalyst deactivation due to coke formation; unacceptable product quality, and thermal degradation of catalyst during regeneration	(*1*) coked zeolite is regenerated in liquid phase ($P > 3500$ kPa) fluid bed with H_2 in two steps: (a)at reaction temperature (20–50°C) and (b)at 25°C above reaction temperature (*2*) coked Pd- and Pt/Y-zeolite catalysts containing 10–13% coke are regenerated in either air or H_2; H_2 treatment enables removal of most of the coke at low-moderate temperatures; higher temperatures are required for air	266,267
catalytic reforming of naphtha/ Pt/Al_2O_3 promoted with Re, Sn, Ge, or Ir	poisoning and fouling by coke produced by condensation of aromatics and olefins	(*1*) coke on Pt bimetallic reforming catalyst is removed off-stream in a moving bed at 300–600°C, followed by oxychlorination (350–550°C) (*2*) coke on Pt/zeolite is removed in halogen-free oxygen-containing gas at $T < 415$°C (*3*) sintering during oxidation of coke on $Pt–Ir/Al_2O_3$ catalyst can be minimized at low regeneration temperature (*4*) study of influence of heating rate, temperature, and time on structural properties of regenerated $Pt–Sn/Al_2O_3$ (*5*) study of effects of Cl, Sn content, and regeneration sequence on dispersion and selectivity of $Pt–Sn/Al_2O_3$ (*6*) regenerated $Pt–Re/Al_2O_3$ is more stable that the fresh catalyst in *n*-heptane conversion and more selective for toluene	268–273
dehydrogenation of propane and butane/ Cr_2O_3/Al_2O_3, Cr_2O_3/ZrO_2, FeO/K/MgO, Pt/Al_2O_3, $Pt–Sn/Al_2O_3$, Pt–Sn/KL-zeolite	catalyst activity is low owing to equilibrium limitations and build-up of product H_2; rapid loss of activity occurs owing to coke formation	(*1*) temperatures gradients were measured during burn off of coke formed on a chromia–alumina catalyst during butene dehydrogenation; data were used in developing a mathematical model for predicting temperatures and coke profiles (*2*) coked supported palladium catalyst used in the dehydrogenation of dimethyltertrahydronaphthalenes to dimethylnaphthalenes is reactivated with an organic polar solvent at a temperature below 200°C	275,275

Table 17 (*Continued*)

Deactivation mechanism/ reaction/catalyst	Problem/cause	Method(s) of regeneration/phenomena studied/conclusions	Refs.
Fischer–Tropsch synthesis/ Co/Al_2O_3	loss of activity due to blocking of sites by carbon overlayers and heavy hydrocarbons	(*1*) carbidic surface carbon deposited on cobalt can be largely removed in hydrogen at 170–200°C and in steam at 300–400°C (*2*) slurry-phase cobalt catalysts may lose 50% activity during synthesis over a period of a few days; the activity can be rejuvenated *in situ* by injecting H_2 gas into vertical draft tubes inside the reactor	276,277
fluid catalytic cracking (FCC) of heavy hydrocarbons/USY or REO-Y^b in silica matrix	rapid loss of activity due to poisoning of acid sites and blocking of small zeolite pores by coke	(*1*) process and apparatus for increasing the coke burning capacity of FCC regenerators; auxiliary regenerator partially burns off the coke at turbulent or fast fluidized-bed conditions (*2*) multistage fluidized-bed regeneration of spent FCC catalyst in a single vessel by incorporating two relatively dense phase fluidized beds beneath a common dilute phase region	278,279
hydrocracking of heavy naphtha/CoMo, NiW, MoW on Al_2O_3 or SiO_2–Al_2O_3; Pt or Pd on Y-zeolite, mordenite, or ZSM-5	loss of activity due to poisoning of acid sites and blocking of small zeolite pores by coke	(*1*) regeneration of noble metal/zeolite via progressive partial removal of carbonaceous deposits under controlled oxidizing conditions to maximize sorption of a probe molecule while minimizing metal sintering (*2*) regeneration of noble metal/zeolite in air at about 600°C, followed by a mild treatment in aqueous ammonia to improve catalytic activity	280,281
hydrotreating of gas oil	loss of activity due to formation of types I, II, and III coke on metal sulfide and alumina surfaces and in pores	(*1*) TPO studies of oxidative regeneration of CoMo and NiW HDS catalysts; sulfur is removed at 225–325°C, carbon at 375–575°C. Redispersion of NiW was observed by EXAFS (*2*) physicochemical changes in CoMo and NiCoMo HDS catalysts during oxidative regeneration, including redispersion of Co, Ni, and Mo oxides and surface area loss, were examined (*3*) changes in NiMo catalyst structure and coke composition during reaction and regeneration were examined and correlated (*4*) properties of NiMo catalyst deactivated during shale oil hydrogenation and regenerated in O_2 or H_2 were examined. regeneration in 1.6% O_2 was more effective than that in 5% H_2. Ni aluminate spinel was observed after burn off (*5*) hard and soft cokes formed on CoMo catalysts during HDS of gas oil were characterized. At low coke levels, hard coke was more easily removed in H_2 than in O_2 (*6*) spent catalysts are washed with solvent and contacted with steam at about 600°C	282,283, 297–300

methanol to olefins or gasoline/ silica–alumina, Y-zeolite, ZSM-5, other zeolites, and aluminophosphate molecular sieves	severe coking and deactivation of silica–alumina and Y-zeolite catalysts observed during high conversions of methanol, also substantial coking of ZSM-5, other zeolites, and aluminophosphate molecular sieves	(*1*) kinetics of coke burnoff from a SAPO-34 used in converting methanol to olefins were studied; kinetics are strongly dependent on the nature of the coke. Kinetics are slowed by strong binding of coke to acid sites (*2*) ZSM-34 catalyst used in conversion of methanol to light olefins is effectively regenerated in H_2-containing gas; this approach avoids the formation of catalyst-damaging products such as steam that would be formed during burn off in air	284,285
Poisoning			
FCC of residues/USY or REO-Y in silica matrix	(*1*) poisoning of acid sites by N- containing compounds. (*2*) deposition of Ni and V metals on acid sites which change selectivity and decrease activity	(*1*) organometallic solutions of Sb and Bi are added to process steam to passivate Ni by forming inactive Ni–Sb and Ni–Bi species (*2*) V metal deposits are trapped by reaction with magnesium orthosilicate to form an unreactive magnesium vanadium silicate (*3*) spent metal-contaminated catalyst is demetallized by chlorinating and washing followed by contacting with NH_4F and one antimony compound (*4*) metal-contaminated catalyst is contacted with an aqueous solution of a carboxylic acid (eg, formic, acetic, citric, or lactic acid) (*5*) metal-contaminated catalyst is contacted with HCl, HNO_3, or H_2SO_4 (*6*) metal contaminated catalyst is contacted with reducing CO gas to form gaseous metal carbonyls that separated from the catalyst	284,285, 301–304
hydrogenation or dechlorination	poisoning of metal sites by arsenic, sulfur, and other poisons	(*1*) regeneration of Ni/SiO_2 catalyst poisoned by thiophene using a sequence of oxidation–reduction treatments at low PO_2 and 1 atm H_2 respectively (*2*) regeneration in dilute hypochlorite solution of a Pd/Al_2O_3 catalyst deactivated during the aqueous-phase dechlorination of trichloroethylene in the presence of sulfite or HS^- ions present in ground water	288,289
hydrotreating of residues/ Al_2O_3-supported Mo and CoMo	pore-mouth poisoning and blockage by Ni, V, and Fe sulfides present in feed as organometallics	(*1*) regeneration of catalysts containing V, Ni, or Fe by contacting with H_2O_2 solution and organic acid (*2*) following removal of coke by air or solvent wash, catalyst is acid leached to remove undesired metals	290,291

Table 17 (*Continued*)

Deactivation mechanism/ reaction/catalyst	Problem/cause	Method(s) of regeneration/phenomena studied/conclusions	Refs.
Thermal degradation			
Catalytic reforming of naphtha/Pt/Al_2O_3 promoted with Re, Sn, Ge, or Ir; Pt/ KL-zeolite	sintering of Pt causing formation of large metal crystallites crystals and loss of active surface area	(*1*) redispersion of Pt–Ir bimetallic catalysts using a wet HCl/air treatment, since the conventional oxychlorination is not effective (*2*) redispersion of Pt/KL-zeolite using wet HCl/air treatment followed by brief calcination and reduction (*3*) redispersion of Pt–Re/ Al_2O_3 in Cl_2 and O_2 (*4*) redispersion of supported Pt, other noble metals, and Ni in Cl_2 and O_2	270,273, 292,293
hydrocracking of heavy naphtha/CoMo, NiW, MoW on Al_2O_3 or SiO_2–Al_2O_3; Pt or Pd on Y-zeolite, mordenite, or ZSM-5	sintering of noble metal causing formation of large metal crystallites crystals and loss of active surface area	redispersion of noble metals on molecular sieves including silica-aluminates, ALPOS, SAPOS	294
hydrotreating of gas oil and residues/Al_2O_3-supported Mo and CoMo	sintering of Mo and Co sulfides causing formation of large sulfide crystals and loss of active surface area	(*1*) oxidative regeneration of hydroprocessing catalyst at 600°C optimizes surface area and Mo dispersion (*2*) oxidative regeneration in several steps with a final oxidation at 500–600°C to restore residual catalyst activity	295,296

[a]USY: ultrastable Y-zeolite.[b]REO-Y: rare-earth exchanged Y-zeolite.

Because coke burn-off is a rapid, exothermic process, the reaction rate is controlled to a large extent by film heat and mass transfer. Accordingly, burn-off occurs initially at the exterior surface and then progresses inward with the reaction occurring mainly in a shrinking shell consistent with a "shell-progressive" or "shrinking-core" model (307); as part of this same work, Richardson (307) showed how experimental burn-off rate data can be fitted to various coking transport models, eg, parallel or series fouling. Burn-off rates for coke deposited on SiO_2/Al_2O_3 catalysts were reported by Weisz and Goodwin (308); burning rate was found to be independent of initial coke level, coke type, and source of catalyst.

5.2. Regeneration of Poisoned Catalysts. Much of the previous literature has focused on regeneration of sulfur-poisoned catalysts used in hydrogenations and steam reforming. Studies of regeneration of sulfur-poisoned Ni, Cu, Pt, and Mo with oxygen/air, steam, hydrogen, and inorganic oxidizing agents have been reported (27). Rostrup-Nielsen (309) indicates that up to 80% removal of surface sulfur from Mg- and Ca-promoted Ni, steam reforming catalysts occurs at 700°C in steam. The presence of both SO_2 and H_2S in the gaseous effluent suggests that the following reactions occur:

$$Ni - S + H_2O \rightarrow NiO + H_2S \quad (5)$$

$$H_2S + 2\ H_2O \rightarrow SO_2 + 3\ H_2 \quad (6)$$

Although this treatment is partially successful in the case of low-surface-area steam reforming catalysts, the high temperatures required for these reactions would cause sintering of most high-surface-area nickel catalysts.

Regeneration of sulfur-poisoned catalysts, particularly base metal catalysts, in air or oxygen has been largely unsuccessful. For example, the treatment of nickel steam-reforming catalysts in steam and air results in the formation of sulfates, which are subsequently reduced back to nickel sulfide upon contact with hydrogen. Nevertheless, sulfur can be removed as SO_2 at very low oxygen partial pressures, suggesting that regeneration is possible under carefully controlled oxygen or species such as CO_2 or NO that dissociate to oxygen. Apparently, at low oxygen pressures the oxidation of sulfur to SO_2 occurs more rapidly than the formation of nickel oxide while at atmospheric pressure the converse is true, ie, the sulfur or sulfate layer is rapidly buried in a nickel oxide layer. In the latter circumstance, the sulfur atoms diffuse to the nickel surface during reduction, thereby restoring the poisoned surface. Regeneration of sulfur-poisoned noble metals in air is more easily accomplished than with steam, although it is frequently attended by sintering. Regeneration of sulfur-poisoned nickel catalysts using hydrogen is impractical because (*1*) adsorption of sulfur is reversible only at high temperatures at which sintering rates are also high, and (*2*) rates of removal of sulfur in H_2 as H_2S are slow even at high temperature.

Inorganic oxidizing agents such as $KMnO_4$ can be used to oxidize liquid phase or adsorbed sulfur to sulfites or sulfates (16). These electronically shielded structures are less toxic than the unshielded sulfides. This approach has somewhat limited application, ie, in partial regeneration of metal catalysts used in low temperature liquid-phase hydrogenation reactions or in liquid-phase destruction of chlorinated organic compounds. For example, Lowrey and

Table 18. **Typical Regeneration Procedure for Reforming Catalysts**[a]

1. *Preliminary operations:*
   cool the catalyst to about 200°C and strip hydrocarbons and H_2 with N_2
2. *Elimination of coke by combustion:*
   inject dilute air (0.5% O_2) at 380°C and gradually increase oxygen content to about 2% by volume while maintaining temperature below 450–500°C to prevent further sintering of the catalyst. To prevent excessive leaching of Cl_2, HCl or CCl_4 may be injected during the combustion step
3. *Restoration of catalyst acidity:*
   Restoration of acidity occurs at 500°C by injection of a chlorinated compound in the presence of 100–200 ppm water in air
4. *Redispersion of the metallic phase:*
   expose the catalyst to a few Torr of HCl or CCl_4 in 2–10% O_2 in N_2 at 510–530°C for a period of about 4 h. After redispersion, O_2 is purged from the unit and the catalyst is reduced in H_2

[a]Ref. 261 and 262.

Reinhard (289) reported successful regeneration in dilute hypochlorite solution of a Pd/Al_2O_3 catalyst deactivated during the aqueous-phase dechlorination of trichloroethylene (TCE) in the presence of sulfite or HS^- ions. These poisons are formed by sulfate-reducing bacteria present in natural groundwater and are apparently adsorbed on the alumina or Pd surfaces more strongly than sulfate ions.

5.3. Redispersion of Sintered Catalysts. During catalytic reforming of hydrocarbons on platinum-containing catalysts, growth of 1-nm platinum metal clusters to 5–20-nm crystallites occurs. An important part of the catalyst regeneration procedure is the redispersion of the platinum phase by a high temperature treatment in oxygen and chlorine, generally referred to as "oxychlorination." A typical oxychlorination treatment involves exposure of the catalyst to HCl or CCl_4 at 450–550°C in 2–10% oxygen for a period of 1–4 h (see details in Table 18). During coke burning some redispersion occurs, eg, D increases from 0.25 to 0.51, while during oxychlorination the dispersion is further increased, eg, from 0.51 to 0.81 (262).

Some guidelines and principles regarding the redispersion process are worth enumerating:

1. In cases involving a high degree of Pt sintering or poisoning, special regeneration procedures may be required. If large crystallites have been formed, several successive oxychlorinations are performed (262).
2. Introducing oxygen into reactors in parallel rather than in series results in a significant decrease in regeneration time (84).
3. Introduction of hydrocarbons present in the reactor recycle after regeneration is said to stabilize the catalyst; solvents such as ammonium acetate, dilute nitric acid containing lead nitrate, EDTA and its diammonium salt are reported to dissolve out metal aggregates without leaching out the dispersed metal (84).
4. The procedures for redispersion of Pt/alumina are not necessarily applicable to Pt on other supports or to other metals. For example, Pt/silica is redispersed at lower temperature and higher Cl_2 concentration (150–200°C

and 25% Cl_2). Pd/alumina can be redispersed in pure O_2 at 500°C. While Pt–Re/alumina is readily redispersed by oxychlorination at 500°C, Pt–Ir/alumina is not redispersed in the presence of O_2 unless the catalyst is pretreated with HCl (270).

An extensive scientific and patent literature of redisperson describes the use of chlorine, oxygen, nitric oxide, and hydrogen as agents for redispersion of sintered catalysts. Most of the early literature shows positive effects for chlorine compounds in the presence of oxygen in redispersing alumina-supported platinum and other noble metals. Recent literature demonstrates the need for understanding the detailed surface chemistry in order to successfully develop and improve redispersion processes, especially in more complex catalyst systems such as alumina-supported bimetallics. For example, on the basis of a fundamental study of the redispersion surface chemistry, Fung (270) developed a redispersion procedure for Pt–Ir bimetallic catalysts using a wet HCl/air treatment, since the conventional oxychlorination is not effective for this catalyst.

Redispersion of alumina-supported platinum and iridium crystallites is also possible in a chlorine-free oxygen atmosphere if chlorine is present on the catalyst. The extent of redispersion depends on the properties of the Pt/Al_2O_3 catalyst and temperature. The question whether redispersion of platinum occurs only in oxygen without chlorine present on the catalyst remains controversial.

Two models, "the thermodynamic redispersion model" and "the crystallite splitting model," have been advanced to explain the redispersion in oxygen (84,85,310). The "thermodynamic" redispersion model hypothesizes the formation of metal oxide molecules that detach from the crystallite, migrate to active sites on the support, and form surface complexes with the support. Upon subsequent reduction, the metal oxide complexes form monodisperse metal clusters. In the "crystallite splitting" model, exposure of a platinum crystallite to oxygen at 500°C leads to formation of a platinum oxide scale on the outer surface of the crystallite, which stresses and ultimately leads to splitting of the particle (310). Dadyburjor hypothesizes that the crystallite splitting model is most applicable to the behavior of large crystallites and to all particles at relatively small regeneration times while the thermodynamic migration model is useful for small particles and most particles after longer regeneration times.

6. Summary and Perspective

6.1. Summary

1. The causes of deactivation are basically of three kinds: chemical, mechanical, and thermal. The five intrinsic mechanisms of catalyst decay, (a) poisoning, (b) fouling, (c) thermal degradation, (d) chemical degradation, and (e) mechanical failure, vary in their reversibility and rates of occurrence. Poisoning and thermal degradation are generally slow, irreversible processes while fouling with coke and carbon is generally rapid and reversible by regeneration with O_2 or H_2.

2. Catalyst deactivation is more easily prevented than cured. Poisoning by impurities can be prevented through careful purification of reactants. Carbon deposition and coking can be prevented by minimizing the formation of carbon or coke precursors through gasification, careful design of catalysts and process conditions, and by controlling reaction rate regimes, eg, mass transfer regimes, to minimize effects of carbon and coke formation on activity. Sintering is best avoided by minimizing and controlling the temperature of reaction.
3. Prevention and monitoring are important engineering principles in "standard of care" practice. The prevention of catalyst decay is important in every aspect of a process including design, construction, operation, and regeneration. Careful monitoring of process variables is a necessity in understanding and preventing catalyst decay problems of either a slow or a catastrophic nature.
4. The optimization of a catalytic process considers optimum operation and regeneration policies subject to constraints of catalyst cost, operation cost, regeneration cost, and product value. The optimum operating policy maximizes the rate of formation of product during the operating period.
5. Catalyst deactivation kinetics for reactions involving relatively slow deactivation can be experimentally determined using a laboratory fixed-bed, mixed-fluid (CSTR) reactor. Reactors and processes involving a slowly deactivating catalyst can be designed using relatively simple numerical analysis of the design equations and a pseudo-steady-state approximation for the main reaction.
6. Modeling and experimental assessment of deactivation processes are useful in providing (a) accelerated simulations of industrial processes, (b) predictive insights into effects of changing process variables on activity, selectivity, and life, (c) estimates of kinetic parameters needed for design and modeling, (d) estimates of size and cost for scale-up of a process, and (e) a better understanding of the basic decay mechanisms. It is now possible to develop realistic mathematical models of most catalytic processes, which can be used in conjunction with short-term experimental tests to accurately predict catalyst life in a commercial unit. Proper application of this approach could save companies millions of dollars by alleviating the need for long-term deactivation tests and/or premature shutdown. For details on this aspect of assessment, refer to the expanded version of this article published in the *Encyclopedia of Catalysis* (78,311).

6.2. Perspectives and Trends. Research and development activities in the area of catalyst deactivation have grown steadily in the past three decades. Catalyst deactivation symposia are held annually as part of national meetings of chemical engineering and chemical societies in the United States and Europe. The rising quality of work presented at the international symposium on catalyst deactivation, held every four years, is evident. In view of the importance of deactivation problems in industrial processes, this trend will most probably continue.

Several other trends are evident:

1. The increasing use of more sophisticated analytical tools to investigate the chemistry and mechanisms of deactivation. Surface science tools such as AES, quantitative HRTEM, XPS, and STM are now routinely applied to investigate deactivation mechanisms at very fundamental levels.
2. The increasing development of more sophisticated models of deactivation processes.

These trends are also likely to continue. Moreover, the combination of more sophisticated methods and models will hasten the practical application of models for predicting catalyst/process life. This is already happening in selected companies. For example, for more than a decade now operators at Phillips Petroleum Co. have been using deactivation models (developed at their corporate research) in their refineries to predict when shutdown will be necessary. One of these models enables them to predict accurately the lifetime of hydrotreating catalysts on the basis of catalyst and feedstock properties.

6.3. Future Needs. *Collection of Data.* It is evident from careful examination of the literature that *few deactivation rate data are available* for even the most important large-scale catalytic systems. Accordingly, there is a *critical need for collection of such data at the laboratory, bench, and plant scale*. There is much that could be done with good data. Sophisticated analytical tools and well-designed reactors are available at most companies for collecting and analyzing such data. The field is ripe and ready to harvest. The wise will seize these opportunities.

Data Analysis and Model Development. Much of the previously collected data were analyzed using outdated methods. There is much that could be learned by reanalyzing some of these data using new approaches such as the GPLE and microkinetic modeling. Critical reviews that include collections of carefully selected rate and kinetic data would constitute important contributions to scientific knowledge and technological development. The incorporation of these data into models would enable more sophisticated design of catalysts, reactors, and processes.

BIBLIOGRAPHY

"Catalyst Regeneration, Metal Catalysts" in *ECT* (online), posting date: December 4, 2000, by D. W. Robinson, UOP.

1. J. L. Figuerido, in J. L. Figuerido, ed., *Carbon Formation and Gasification on Nickel*, M. Nijhoff Publishers, Boston, 1982.
2. R. Hughes, *Deactivation of Catalysts*, Academic Press, London, 1984.
3. J. Oudar and H. Wise, eds., *Deactivation and Poisoning of Catalysts*, Marcel Dekker, New York, 1985.
4. J. B. Butt and E. E. Petersen, *Activation, Deactivation, and Poisoning of Catalysts*, Academic Press, San Diego, 1988.

5. P. J. Denny and M. V. Twigg, in Ref. 9, p. 577.
6. C. H. Bartholomew, *Chem. Eng.* **91**, 96 (1984).
7. J. B. Butt, in J. R. Anderson and M. Boudart, eds., *Catalysis—Science and Technology*, Vol. 6, Springer-Verlag, New York, 1984, p. 1.
8. R. J. Farrauto, C. H. Bartholomew, *Fundamentals of Industrial Catalytic Processes*, Kluwer Academic Publishers, London, 1997.
9. B. Delmon and G. F. Froment, eds., *Catalyst Deactivation 1980* (Studies in Surface Science and Catalysis, Vol. 6), Elsevier, Amsterdam, 1980.
10. B. Delmon and G. F. Froment, eds., *Catalyst Deactivation 1987* (Studies in Surface Science and Catalysis, Vol. 34), Elsevier, Amsterdam, 1987.
11. C. H. Bartholomew and J. B. Butt, eds., *Catalyst Deactivation 1991* (Studies in Surface Science and Catalysis, Vol. 68), Elsevier, Amsterdam, 1991.
12. B. Delmon and G. F. Froment, eds., *Catalyst Deactivation 1994* (Studies in Surface Science and Catalysis, Vol. 88), Elsevier, Amsterdam, 1994.
13. C. H. Bartholomew and G. A. Fuentes, eds., *Catalyst Deactivation 1997* (Studies in Surface Science and Catalysis, Vol. 111), Elsevier, Amsterdam, 1997.
14. B. Delmon and G. F. Froment, eds., *Catalyst Deactivation 1999* (Studies in Surface Science and Catalysis, Vol. 126), Elsevier, Amsterdam, 1999.
15. J. A. Moulijn, ed., A series of papers on Catalyst Deactivation, *Appl. Catal., A: Gen.* **212**, 1–255 (2001).
16. E. B. Maxted, *Adv. Catal.* **3**, 129 (1951).
17. L. L. Hegedus and R. W. McCabe, in Ref. 9, p. 47.
18. L. L. Hegedus and R. W. McCabe, *Catalyst Poisoning*, Marcel Dekker, New York, 1984.
19. J. B. Butt, in J. L. Figuerido, ed., *Progress in Catalyst Deactivation* (NATO Advanced Study Institute Series E, No. 54), M. Nijhoff Publishers, Boston, 1982, p. 153.
20. J. Barbier, in Ref. 3, p. 109.
21. C. H. Bartholomew, in Ref. 10, p. 81.
22. J. R. Rostrup-Nielsen, in Ref. 11, p. 85.
23. V. J. Volter and M. Hermann, *Z. Anorg. Allg. Chem.* **405**, 315 (1974).
24. K. Baron, *Thin Solid Films* **55**, 449 (1978).
25. R. D. Clay and E. E. Petersen, *J. Catal.* **16**, 32 (1970).
26. R. J. Madon and H. Shaw, *Catal. Rev. Sci. Eng.* **15**, 69 (1977).
27. C. H. Bartholomew, P. K. Agrawal, and J. R. Katzer, *Adv. Catal.* **31**, 135 (1982).
28. J. R. Rostrup-Nielsen, in J. L. Figuerido, ed., *Progress in Catalyst Deactivation* (NATO Advanced Study Institute Series E, No. 54), M. Nijhoff Publishers, Boston, 1982, p. 209.
29. H. Wise, J. McCarty, and J. Oudar, in Ref. 3, p. 1.
30. J. R. Rostrup-Nielsen and P. E. Nielsen, in Ref. 3, p. 259.
31. M. Perdereau and J. Oudar, *Surf. Sci.* **20**, 80 (1970).
32. J. Oudar, *Catal. Rev. Sci. Eng.* **22**, 171 (1980).
33. J. J. McCarroll, T. Edmonds, and R. C. Pitkethly, *Nature* **223**, 1260 (1969).
34. T. Edmonds, J. J. McCarroll, and R. C. Pitkethly, *J. Cat. Sci. Technol.* **8**, 68 (1971).
35. L. Ruan, F. Besenbacher, I. Stensgaard, and E. Laegsgaard, *Phys. Rev.* **69**, 3523 (1992).
36. J. Hepola, J. McCarty, G. Krishnan, and V. Wong, *Appl. Catal. B* **20**, 191 (1999).
37. W. Erley and H. Wagner, *J. Catal.* **53**, 287 (1978).
38. K. D. Rendulic and A. Winkler, *Surf. Sci.* **74**, 318 (1978).
39. D. W. Goodman and M. Kiskinova, *Surf. Sci.* **105**, L265 (1981).
40. M. Kiskinova and D. W. Goodman, *Surf. Sci.* **108**, 64 (1981).
41. S. Johnson and R. S. Madix, *Surf. Sci.* **108**, 77 (1981).
42. R. J. Madix, M. Thornberg, and S. B. Lee, *Surf. Sci.* **133**, L447 (1983).

43. E. L. Hardegree, P. Ho, and J. M. White, *Surf. Sci.* **165**, 488 (1986).
44. E. J. Erekson and C. H. Bartholomew, *Appl. Catal.* **5**, 323 (1983).
45. J. R. Rostrup-Nielsen and D. L. Trimm, *J. Catal.* **48**, 155 (1977).
46. D. L. Trimm, *Catal. Rev. Sci. Eng.* **16**, 155 (1977).
47. D. L. Trimm, *Appl. Catal.* **5**, 263 (1983).
48. C. H. Bartholomew, *Catal. Rev. Sci. Eng.* **24**, 67 (1982).
49. L. F. Albright and R. T. K. Baker, eds., *Coke Formation on Metal Surfaces* (ACS Symposium Series 202), American Chemical Society, Washington, D.C., 1982.
50. P. G. Menon, *J. Mol. Catal.* **59**, 207 (1990).
51. J. D. Deken, P. G. Menon, G. F. Froment, and G. Haemers, *J. Catal.* **70**, 225 (1981).
52. W. G. Durer, J. H. Craig, Jr., and J. Lozano, *Appl. Surf. Sci.* **45**, 275 (1990).
53. A. D. Moeller and C. H. Bartholomew, *Prepr.—Am. Chem. Soc., Div. Fuel Chem.* **25**, 54 (1980).
54. K. J. Marschall and L. Mleczko, *Ind. Eng. Chem. Res.* **38**, 1813 (1999).
55. J. R. Rostrup-Nielsen, in J. R. Anderson and M. Boudart, eds., *Catalysis—Science and Technology*, Vol. 5, Springer-Verlag, New York, 1984, p. 1.
56. F. Besenbacher, I. Chorkendorff, B. S. Clausen, B. Hammer, A. M. Molenbroek, J. K. Norscov, and I. Stensgaard, *Science* **279**, 1913 (1998).
57. T. Nemes, A. Chambers, and R. T. K. Baker, *J. Phys. Chem.* **102**, 6323 (1998).
58. C. H. Bartholomew, M. V. Strasburg, and H. Hsieh, *Appl. Catal.* **36**, 147 (1988).
59. C. K. Vance and C. H. Bartholomew, *Appl. Catal.* **7**, 169 (1983).
60. R. T. K. Baker and J. J. Chludzinski, *J. Catal.* **64**, 464 (1980).
61. D. E. Brown, J. T. K. Clark, A. I. Foster, J. J. McCarroll, and M. L. Sims, in Ref. 49, p. 23.
62. J. H. Bitter, K. Seshan, and J. A. Lercher, *J. Catal.* **183**, 336 (1999).
63. J. R. Rostrup-Nielsen, *J. Catal.* **33**, 184 (1974).
64. B. C. Gates, J. R. Katzer, and G. C. A. Schuit, *Chemistry of Catalytic Processes*, McGraw-Hill, New York, 1979.
65. C. Naccache, in C. Naccache, ed., *Deactivation of Acid Catalysts*, Marcel Dekker, New York, 1985.
66. W. G. Appleby, J. W. Gibson, and G. M. Good, *Ind. Eng. Chem. Process Des. Dev.* **1**, 102 (1962).
67. H. Beuther, O. H. Larson, and A. J. Perrotta, in Ref. 9, p. 271.
68. A. G. Gayubo, J. M. Arandes, A. T. Aguayo, M. Olazar, and J. Bilbao, *Ind. Eng. Chem. Res.* **32**, 588 (1993).
69. S. M. Augustine, G. N. Alameddin, and W. M. H. Sachtler, *J. Catal.* **155**, 217 (1989).
70. M. Guisnet and P. Magnoux, *Appl. Catal.* **54**, 1 (1989).
71. F. Bauer, V. Karazirev, C. Vlaev, R. Hanisch, and W. Weiss, *Chem. Techn.* **41**, 297 (1989).
72. W. A. Grotten, B. W. Wojciechowski, and B. K. Hunter, *J. Catal.* **138**, 343 (1992).
73. A. Bellare and D. B. Dadyburjor, *J. Catal.* **140**, 510 (1993).
74. M. A. Uguina, D. P. Serrano, R. V. Grieken, and S. Venes, *Appl. Catal.* **99**, 97 (1993).
75. C. Li, Y. Chen, S. Yang, and R. Yen, *Appl. Surf. Sci.* **81**, 465 (1994).
76. J. G. Buglass, K. P. d. Jong, and H. H. Mooiweer, in *Proc. 120th National Meeting of the American Chemical Society*, Aug. 20–24, 1995, p. 631.
77. D. Chen, H. P. Rebo, K. Moljord, and A. Holmen, in *Proc. 14th International Symposium on Chemical Reaction Engineering, Part B*, May 5–9, 1996, p. 2687.
78. M. Gusinet, P. Magnoux, and D. Martin, in Ref. 13, p. 1.
79. T. Masuda, P. Tomita, Y. Fujikata, and K. Hashimoto, in Ref. 14, p. 89.
80. H. S. Cerqueira, P. Magnoux, D. Martin, and M. Gusinet, in Ref. 14, p. 105.
81. S. E. Wanke and P. C. Flynn, *Catal. Rev. Sci. Eng.* **12**, 93 (1975).
82. P. Wynblatt and N. A. Gjostein, *Prog. Solid State Chem.* **9**, 21 (1975).

83. E. Ruckenstein and B. Pulvermacher, *AIChE J.* **19**, 356 (1973).
84. E. Ruckenstein and D. B. Dadyburjor, *Rev. Chem. Eng.* **1**, 251 (1983).
85. S. E. Wanke, in J. L. Figueiredo, ed., *Progress in Catalyst Deactivation* (NATO Advanced Study Institute Series E, No. 54), M. Nijhoff Publishers, Boston, 1982, p. 315.
86. R. T. Baker, C. H. Bartholomew, and D. B. Dadyburjor, *Stability of Supported Catalysts: Sintering and Redispersion, Catalytic Studies Division, 1991.*
87. C. H. Bartholomew, *Catalysis (Spec. Period. Rept.).* **10** (1992).
88. C. H. Bartholomew, *Appl. Catal., A: Gen.* **107**, 1 (1993).
89. C. H. Bartholomew, in Ref. 12, p. 1.
90. C. H. Bartholomew, in Ref. 13, p. 585.
91. C. H. Bartholomew and W. Sorenson, *J. Catal.* **81**, 131 (1983).
92. J. A. Moulijn, A. E. van Diepen, and F. Kapteijn, *Appl. Catal., A: Gen.* **212**, 13–16 (2001).
93. G. W. Bridger, and M. S. Spencer, in M. V. Twigg ed., *Catalyst Handbook*, 2nd ed., Manson Publishing, London, 1996, p. 441.
94. G. A. Fuentes, *Appl. Catal.* **15**, 33 (1985); G. A. Fuentes and F. A. Ruiz-Trevino, in Ref. 11, pp. 637–644.
95. J. P. Bournonville and G. Martino, in Ref. 9, p. 159.
96. G. A. Somorjai, *X-ray and Electron Methods of Analysis*, Plenum Press, New York, 1968.
97. S. R. Seyedmonir, D. E. Strohmayer, G. J. Guskey, G. L. Geoffroy, and M. A. Vannice, *J. Catal.* **93**, 288 (1985).
98. D. L. Trimm, in Ref. 11, p. 29.
99. A. G. Shastri, A. K. Datye, and J. Schwank, *Appl. Catal.* **14**, 119 (1985).
100. L. L. Hegedus and K. Baron, *J. Catal.* **54**, 115 (1978).
101. J. Summers and L. L. Hegedus, *Ind. Eng. Chem. Prod. Res. Dev.* **18**, 318 (1979).
102. U.S. Pat. 6,003,303 (Dec. 21, 1999), J. D. Peter-Hoblyn, J. M. Valentine, B. N. Sprague, and W. R. Epperly (to Clean Diesel Technologies, Inc.).
103. U.S. Pat. 6,013,599 (Jan. 11, 2000), I. Manson (to Redem Corp.).
104. U.S. Pat. 6,093,378 (July 25, 2000), M. Deeba, Y. K. Lui, and J. C. Dettling (to Engelhard Corp.).
105. M. E. Dry, in J. Anderson and M. Boudart, eds., *Catalysis—Science and Technology*, Springer-Verlag, New York, 1981, p. 159.
106. G. W. Huber, C. G. Guymon, B. C. Stephenson, and C. H. Bartholomew, *Catalyst Deactivation 2001* (Studies in Surface Science and Catalysis, Vol. 139), Elsevier, Amsterdam, 2001, p. 423.
107. G. Busca, L. Lietti, G. Ramis, and F. Berti, *Appl. Catal., B: Environ.* **18**, 1–36 (1998).
108. T. P. Kobylinski, B. W. Taylor, and J. E. Yong, in *Proc. SAE*, Detroit, 1974.
109. M. Shelef and H. S. Gandhi, *Platinum Met. Rev.* **18**, 1 (1974).
110. H. S. Gandhi, H. K. Stepien, and M. Shelef, *Mat. Res. Bull.* **10**, 837 (1975).
111. C. H. Bartholomew, *Ind. Eng. Chem. Prod. Res. Dev.* **14**, 29 (1975).
112. R. W. Clark, J. K. Tien, and P. Wynblatt, *J. Catal.* **61**, 15 (1980).
113. W. M. Shen, J. A. Dumesic, and C. G. Hill, *J. Catal.* **68**, 152 (1981).
114. R. B. Pannell, K. S. Chung, and C. H. Bartholomew, *J. Catal.* **46**, 340 (1977).
115. G. Lohrengel and M. Baerns, *Appl. Catal.* **1**, 3 (1981).
116. I. Qamar and J. G. Goodwin, in *Proc. 8th Am. Meeting Catal. Soc.*, Philadelphia, 1983 (Paper C-22).
117. J. G. Goodwin, D. O. Goa, S. Erdal, and F. H. Rogan, *Appl. Catal.* **24**, 199 (1986).
118. O. Watzenberger, T. Haeberle, D. T. Lynch, and G. Emig, in Ref. 11, p. 441.
119. M. Agnelli, M. Kolb, and C. Mirodatos, *J. Catal.* **148**, 9 (1994).
120. H. C. Lee and R. J. Farrauto, *Ind. Eng. Chem. Res.* **18**, 1 (1989).
121. R. J. Farrauto and H. C. Lee, *Ind. Eng. Chem. Res.* **29**, 1125 (1990).

122. F. Sperner and W. Hohmann, *Platinum Met. Rev.* **20**, 12 (1976).
123. J. M. Hess and J. Phillips, *J. Catal.* **136**, 149 (1992).
124. C. H. Bartholomew, *Catalysis Lett.* **7** (1990).
125. N. L. Wu and J. Phillips, *J. Phys. Chem.* **89**, 591 (1985).
126. N. L. Wu and J. Phillips, *Appl. Phys.* **59**, 769 (1986).
127. N. L. Wu and J. Phillips, *J. Catal.* **113**, 129 (1988).
128. A. Bielanski and M. Najbar, in Ref. 9, p. 127.
129. N. Burriesci, F. Garbassi, M. Petrera, and G. Petrini, in Ref. 9, p. 115.
130. Y. L. Xiong, R. Castillo, C. Papadopoulou, L. Dada, J. Ladriere, P. Ruiz, and B. Delmon, in Ref. 11, p. 425.
131. R. J. Farrauto, M. Hobson, T. Kennelly, and E. Waterman, *Appl. Catal.* **81**, 227 (1992).
132. P. L. Gai-Boyes, *Catal. Rev. Sci. Eng.* **34**, 1 (1992).
133. B. Delmon, in Ref. 12, p. 113.
134. K. M. Erickson, D. A. Karydis, S. Boghosian, and R. Fehrmann, *J. Catal.* **155**, 32 (1995).
135. B. Delmon, in Ref. 13, p. 39.
136. N. B. Jackson, A. K. Datye, L. Mansker, R. J. O'Brien, and B. H. Davis, in Ref. 13, p. 501.
137. S. A. Eliason and C. H. Bartholomew, in Ref. 13, p. 517.
138. A. Baranski, R. Dziembaj, A. Kotarba, A. Golebiowski, Z. Janecki, and J. B. C. Pettersson, in Ref. 14, p. 229.
139. C. A. Querini, F. Ravelli, M. Ulla, L. Cornaglia, and E. Miro, in Ref. 14, p. 257.
140. H. N. Pham, J. Reardon, and A. K. Datye, *Powder Technol.* **103**, 95 (1999).
141. D. S. Kalakkad, M. D. Shroff, S. Kohler, N. Jackson, and A. K. Datye, *Appl. Catal.* **133**, 335 (1995).
142. W. D. Callister, *Materials Science and Engineering: An Introduction*, John Wiley & Sons, Inc., New York, 2000.
143. R. L. Coble and W. D. Kingery, *J. Am. Ceram. Soc.* **39**, 381 (1956).
144. S. G. Deng and Y. S. Lin, *AIChE J.* **43**, 505 (1997).
145. S. G. Thoma, M. Ciftcioglu, and D. M. Smith, *Powder Technol.* **68**, 53 (1991).
146. M. Bankmann, R. Brand, B. H. Engler, and J. Ohmer, *Catal. Today* **14**, 225 (1992).
147. V. M. Kenkre and M. R. Endicott, *J. Am. Ceram. Soc.* **79**, 3045 (1996).
148. H. Song and J. R. G. Evans, *J. Am. Ceram. Soc.* **77**, 806 (1994).
149. J. Werther and W. Xi, *Powder Technol.* **76**, 39 (1993).
150. B. L. Bhatt, E. S. Schaub, E. C. Hedorn, D. M. Herron, D. W. Studer, and D. M. Brown, in G. J. Stiegel and R. D. Srivastava, eds. *Proc. of Liquefaction Contractors Review Conference*, U.S. Department of Energy, Pittsburgh, Pa., 1992, p. 403.
151. H. N. Pham and A. K. Datye, *Catal. Today* **58**, 233 (2000).
152. C. R. Bemrose and J. Bridgewater, *Powder Technol.* **49**, 97 (1987).
153. M. Ghadiri, J. A. S. Cleaver, V. G. Tuponogov, and J. Werther, *Powder Technol.* **80**, 175 (1994).
154. S. A. Weeks, P. Dumbill, *Oil Gas J.* **88**, 38 (Apr. 16, 1990).
155. R. Zhao, J. G. Goodwin, K. Jothimurugesan, J. J. Spivey, and S. K. Gangwal, *Ind. Eng. Chem. Res.* **39**, 1155 (2000).
156. P. K. Doolin, D. M. Gainer, and J. F. Hoffman, *J. Testing Evaluation* **21**, 481 (1993).
157. R. Oukaci, A. H. Singleton, D. Wei, and J. G. Goodwin, *Preprints, 217th National Meeting, ACS Division of Petroleum Chemistry*, Anaheim, Calif., 1999, p. 91.
158. M. J. Adams, M. A. Mullier, and J. P. K. Seville, *Powder Technol.* **78**, 5 (1994).
159. G. Emig and F. G. Martin, *Ind. Eng. Chem. Res.* **30**, 1110 (1991).
160. P. W. N. M. van Leeuwen, *Appl. Catal., A: Gen.* **212**, 61 (2001).
161. P. E. Garrou, *Chem. Rev.* **85**, 171 (1985).

162. B. C. Gates, *Catalytic Chemistry*, John Wiley & Sons, Inc., New York, 1992.
163. J. L. Latham and A. E. Burgess, *Elementary Reaction Kinetics*, 3rd ed., Butterworths, London, 1977.
164. W. Hartmeier (translated by J. Wiesner), *Immobilized Biocatalysts*, Springer-Verlag, Berlin, 1988; J. A. Hurlbut and co-workers, *J. Chem. Educ.* **50**, 149 (1973).
165. O. R. Zaborsky, in J. Burton and L. Garten, eds., *Advanced Materials in Catalysis*, Academic press, New York, 1977.
166. S. L. Neidleman, *Catalysis of Organic Reactions*, Marcel Dekker, New York, 1984.
167. S. Kindel, *Technology* **1**, 62 (1981).
168. M. N. Gupta, *Biotechnol. Appl. Biochem.* **14**, 1 (1991).
169. A. W. H. Fersht, *Enzyme Structure and Mechanism*, W. H. Freeman & Co., New York, 1984.
170. J. R. Whitaker, *Principles of Enzymology for the Food Sciences*, 2nd ed., Marcel Dekker, New York, 1994.
171. M. Matsumoto, K. Kida, and K. Kondo, *J. Chem. Technol. Biotechnol.* **70**, 188 (1997).
172. A. M. Azevedo, D. M. F. Prazeres, J. M. S. Cabral, and L. P. Fonseca, *J. Mol. Catal., B: Enzymatic* **15**, 147 (2001).
173. A. M. Klibanov, *Tibtech* **15**, 97 (1997).
174. D. Li, Z. Guo, and H. Liu, *J. Am. Chem. Soc.* **188**, 275 (1996).
175. S. Colombie, A. Gaunand, and B. Lindet, *J. Mol. Catal., B: Enzymatic* **11**, 559 (2001).
176. Z. Zhang, Z. He, and M. He, *J. Mol. Catal., B: Enzymatic* **14**, 85 (2001).
177. G. Toscano, D. Pirozzi, M. Maremonti, and G. Greco, Jr., *Biotechnol. Bioeng.* **44**, 682 (1994).
178. M. Mohanty, R. S. Ghadge, N. S. Patil, S. B. Sawant, J. B. Joshi, and A. V. Deshpande, *Chem. Eng. Sci.* **56**, 3401 (2001).
179. A. Ginsberg and W. R. Carroll, *Biochemistry* **4**, 2159 (1965).
180. T. J. Ahern and A. M. Klibanov, *Meth. Biochem. Anal.* **33**, 91 (1988).
181. K. A. Dill, D. O. V. Alonso, and K. Hutchinson, *Biochemistry* **28**, 5439 (1989).
182. T. J. Hancock and J. T. Hsu, *Biotechnol. Progr.* **12**, 494 (1996).
183. M. Longo and D. Combes, *J. Chem. Technol. Biotechnol.* **74**, 25 (1999).
184. L. M. M. Tijskens, R. Greiner, E. S. A. Biekman, and U. Konietzny, *Biotechnol. Bioeng.* **72**, 323 (2001).
185. V. V. Mozhaev and K. Martinek, *Enzyme Microb. Technol.* **6**, 50 (1984).
186. V. V. Mozhaev, N. S. Melik-Nubarov, V. Siksnis, and K. Martinek, *Biocatalysis* **3**, 189 (1990).
187. M. G. Roig and J. F. Kennedy, *Crit. Rev. Biotechnol.* **12**, 391 (1992).
188. A. M. Klibanov, *Anal. Biochem.* **93**, 1 (1979).
189. P. Monsan and D. Combes, *Methods Enzymol.* **137**, 584 (1988).
190. J. M. Guisan, P. Sabuquillo, R. Fernandez-Lafuent, G. Fernandez-Lorente, C. Mateo, P. J. Halling, D. Kennedy, E. Miyata, and D. Re., *J. Mol. Catal., B: Enzymatic* **11**, 817 (2001).
191. P. Wang, S. Dai, S. D. Waezsada, A. Y. Tsao, and B. H. Davison, *Biotechnol. Bioeng.* **74**, 249 (2001).
192. R. G. Silver, J. C. Summers, and W. B. Williamson, *Catalysis and Automotive Pollution Control II*, Elsevier, Amsterdam, 1991, p. 167.
193. G. B. Fisher, M. G. Zammit, and J. LaBarge, SAE Report 920846, 1992.
194. R. J. Farrauto and R. M. Heck, *Catal. Today* **51**, 351 (1999).
195. G. W. Huber, C. G. Guymon, B. C. Stephenson, and C. H. Bartholomew, *Catalyst Deactivation 2001* (Studies in Surface Science and Catalysis, Vol. 139), Elsevier, Amsterdam, 2001, p. 423.
196. U.S. Pat. 6,169,120 (Jan. 2, 2001), G. L. Beer (to Syntroleum Corp.).
197. C. H. Bartholomew, M. W. Stoker, L. Mansker, and A. Datye, in Ref. 14, p. 265.

198. U.S. Pat. 5,728,894 (Mar. 17, 1998), O. Nagano and T. Watanabe (to Ashahi Kasei Kogyo Kabushiki Kaisha).
199. T. Maillet, J. Barbier, and D. Duprez, *Appl. Catal., B* **9**, 251 (1996).
200. WIPO Pat. 93/16020A3 (Sept. 16, 1993), G. Mathys, L. Martens, M. Baes, J. Verduijn, D. Huybrechts, and C. Renata (to Exxon Chem.).
201. U.S. Pat. 5,672,800 (Sept. 30, 1997), G. Mathys, L. Martens, M. Baes, J. Verduijn, and D. Huybrechts (to Exxon Chem.).
202. U.S. Pat. 6,080,903 (June 26, 2000), L. Stine, B. Muldoon, S. Gimre, and R. Frame (to UOP).
203. B. Subramaniam, V. Arunajatesan, and C. J. Lyon, in Ref. 14, p. 63.
204. WIPO Pat. 99/33769 (July 8, 1999), D. Ginosar, R. Fox, and P. Kong (to Lockheed Martin).
205. F. H. Ribeiro, A. L. Bonivardi, and C. Kim, *J. Catal.* **150**, 186 (1994).
206. D. Ginosar and B. Subramaniam, in Ref. 12, p. 327.
207. E. E. Petersen, in Ref. 13, p. 87.
208. J. W. Gosselink and J. A. R. V. Veen, in Ref. 14, p. 3.
209. L. Lin, T. Zao, J. Zang, and Z. Xu, *Appl. Catal.* **67**, 11 (1990).
210. D. E. Resasco and G. L. Haller, *Catalysis (Spec. Period. Rept.)* **11**, 379 (1994).
211. R. D. Cortright and J. A. Dumesic, *J. Catal.* **148**, 771 (1994).
212. H. Weyten, K. Keizer, A. Kinoo, J. Luyten, and R. Leysen, *AIChE J.* **43**, 1819 (1997).
213. P. Praserthdam, T. Mongkhonsi, S. Kunatippapong, B. Jaikaew, and N. Lim, in Ref. 13, p. 153.
214. WIPO Pat. 00/69993 (May 12, 2000), B. Rose and T. Kiliany (to Mobil Oil Corp.).
215. A. Guerrero-Ruiz, A. Sepulveda-Escribano, and I. Rodriguez-Ramos, *Catal. Today* **21**, 545 (1994).
216. D. Qin and J. Lapszewicz, *Catal. Today* **21**, 551 (1994).
217. S. Stagg and D. Resasco, in Ref. 13, p. 543.
218. K. Fujimoto, K. Tomishige, O. Yamazaki, Y. Chen, and X. Li, *Res. Chem. Intermed.* **24**, 259 (1998).
219. U.S. Pat. 5,191,142 (Mar. 2, 1993), C. Marshall and J. Miller (to Amoco Corp.).
220. A. G. Gayubo, A. T. Aguayo, A. E. S. D. Campo, P. L. Benito, and J. Bilbao, in Ref. 14, p. 129.
221. U.S. Pat. 5,248,647 (Sept. 28, 1993), P. T. Barger (to UOP).
222. WIPO Pat. 99/42202 (Feb. 20, 1998), J. Cox and J. Evans (to Johnson Matthey).
223. WIPO Pat. 98/50487 (May 2, 1997), S. Leviness, C. Mart, W. Behrmann, S. Hsia, and D. Neskora (to Exxon Research and Engineering Co.).
224. C. H. Bartholomew, in M. Oballa and S. Shih, eds., *Catalytic Hydroprocessing of Petroleum and Distillates*, Marcel Dekker, New York, 1993, p. 1.
225. J. Summers and W. B. Williamson, in J. Armor, ed., *Environmental Catalysis 1993*, Vol. 552, American Chemical Society, Washington, D.C., 1993, p. 94.
226. J. Dettling, Z. Hu, Y. K. Lui, R. Smaling, C. Z. Wan, and A. Punke, in *Studies in Surface Science and Catalysis*, Vol. 96, Elsevier, Amsterdam, 1995, p. 461.
227. U.S. Pat. 4,910,180 (Mar. 20, 1990), M. Berndt and D. Ksinsik (to Doduco).
228. U.S. Pat. 4,985,387 (Jan. 15, 1991), M. Prigent, G. Blanchard, and P. Phillippe (to ProCatalyse).
229. U.S. Pat. 5,041,407 (Aug. 20, 1991), W. Williamson, D. Linden, and J. Summers (to Allied-Signal Inc.).
230. U.S. Pat. 5,116,800 (May 26, 1992), W. Williamson, D. Linden, and J. Summers (to Allied-Signal Inc.).
231. U.S. Pat. 5,234,881 (Aug. 10, 1993), C. Narula, W. Watkins, and M. Chattha (to Ford Motor Co.).

232. U.S. Pat. 5,254,519 (Oct. 19, 1993), C. Wan, S. Tauster, and H. Rabinowitz (to Engelhard Corp.).
233. T. Furuya, S. Yamanaka, T. Hayata, J. Koezuka, T. Yoshine, and A. Ohkoshi, in *Proc. Gas Turbine Conference and Exhibition*, Anaheim, Calif., 1987.
234. T. Kawakami, T. Furuya, Y. Sasaki, T. Yoshine, Y. Furuse, and M. Hoshino, in *Proc. Gas Turbine and Aeroengine Congress and Exposition*, Toronto, Ont., June 4–8, 1989.
235. U.S. Pat. 5,250,489 (1993), R. D. Betta, F. Ribeiro, T. Shoji, K. Tsurumi, N. Ezawa, and S. Nickolas (to Catalytica, Inc.).
236. T. Fujii, Y. Ozawa, and S. Kikumoto, *J. Eng. Gas Turbines Power* **120**, 509 (1998).
237. D. O. Borio and N. S. Schbib, *Comput. Chem. Eng.* **19**, S345 (1995).
238. U.S. Pat. 5,028,634 (July 2, 1991), R. Fiato (to Exxon Research and Engineering Co.).
239. R. Zhao and J. G. Goodwin, Jr., K. Jothimurugesan, S. K. Gangwal, and J. J. Spivey, *Ind. Eng. Chem. Res.* **40**, 1065–1075 (2001).
240. R. Zhao, J. G. Goodwin, Jr., K. Jothimurugesan, S. K. Gangwal, and J. J. Spivey, *Ind. Eng. Chem. Res.* **40**, 1076 (2001).
241. U.S. Pat. 5,939,350 (Aug. 17, 1999), A. H. Singleton, R. Oukaci, and J. G. Goodwin (to Energy International Corp.).
242. U.S. Pat. 6,087,405 (July 11, 2000), S. Plecha, C. H. Mauldin, and L. E. Pedrick (to Exxon Research and Engineering Co.).
243. U.S. Pat. 6,124,367 (Sept. 26, 2000), S. Plecha, C. H. Mauldin, and L. E. Pedrick (to Exxon Research and Engineering Co.).
244. W.O. Pat. 00/71253 (Nov. 30, 2000), A. H. Singleton, R. Oukaci, and J. G. Goodwin (to Energy International Corp.).
245. M. Seitz, E. Klemm and G. Emig, in Ref. 14, p. 211.
246. S. Masamune and J. M. Smith, *AIChE J.* **12**, 384 (1966).
247. Y. Murakami, T. Kobayashi, T. Hattori, and M. Masuda, *Ind. Eng. Chem. Fundam.* **7**, 599–605 (1968).
248. W. H. J. Stork, in G. F. Froment, B. Delmon, and P. Grange, eds., *Hydrotreatment and Hydrocracking of Oil Fractions*, (Studies in Surface Science and Catalysis, Vol. 106), Elsevier, New York, 1997, pp. 41–67.
249. G. D. Parks, A. M. Schaffer, M. J. Dreiling, and C. B. Shiblom, *Prepr.—Am. Chem. Soc., Div. Petr. Chem.* **25**, 335 (1980).
250. D. L. Trimm, in J. L. Figueiredo, ed., *Progress in Catalyst Deactivation* (NATO Advanced Study Institute Series E, No. 54), M. Nijhoff Publishers, Boston, 1982, pp. 3–18.
251. E. R. Becker and J. J. Wei, *J. Catal.* **46**, 365–381 (1977).
252. U.S. Pat. 5,498,638 (Mar. 12, 1996), D. C. Long (to Exxon Research and Engineering Co.).
253. C. H. Bartholomew, *Appl. Catal., A: Gen.* **107**, 1–57 (1993).
254. B. R. Powell, *Presented at the Materials Research Society Annual Meeting*, Boston, Nov. 16–21, 1980 (Paper H9).
255. R. Heck and R. Farrauto, *Catalytic Air Pollution Control: Commercial Technology*, Van Nostrand Reinhold, New York, 1995.
256. D. L. Trimm, *Appl. Catal., A: Gen.* **212**, 153 (2001).
257. G. Berrebi, P. Dufresne, and Y. Jacquier, *Environ. Prog.* **12**, 97 (1993).
258. R. L. D'Aquino, *Chem. Eng.* **107**, 32 (2000).
259. T. Chang, *Oil Gas J.* **96**(41), 49 (1998).
260. S. R. Blashka and W. Duhon, *Int. J. Hydrocarbon Eng.* **4**(1), 60 (1998).
261. D. C. McCulloch, in B. E. Leach, ed., *Applied Industrial Catalysis*, Academic Press, New York, 1983, pp. 103–110.

262. J. P. Franck and G. Martino, in J. L. Figueiredo, ed., *Progress in Catalyst Deactivation* (NATO Advanced Study Institute Series E., No. 54), M. Nijhoff Publishers, Boston, 1982, pp. 355–398.
263. J. J. Spivey, G. W. Roberts, and B. H. Davis, eds., *Catalyst Deactivation 2001* (Studies in Surface Science and Catalysis, Vol. 139), Elsevier, Amsterdam, 2001.
264. U.S. Pat. 5,043,517 (Aug. 27, 1991), J. H. Haddad, N. Mohsen, and H. Owen (to Mobil Oil Corp.).
265. U.S. Pat. 5,306,682 (Apr. 26, 1994), M. Ueda, T. Murakami, S. Shibata, K. Hirabayashi, T. Kondoh, K. Adachi, N. Hoshino, and S. Inoue (to Research Association for the Utilization of Light Oil JP).
266. U.S. Pat. 5,675,048 (Oct. 7, 1997), S. Y.-F. Zhang, C. D. Gosling, P. A. Sechrist, and G. A. Funk (to UOP).
267. G. Panattoni and C. A. Querini, in Ref. 263, p. 181.
268. U.S. Pat. 5,854,162 (Dec. 29, 1998), P. Dufresne and N. Brahma (to Eurecat).
269. U.S. Pat. 5,883,031 (Mar. 16, 1999), R. A. Innes, D. L. Holtermann, and B. F. Mulaskey (to Chevron).
270. S. C. Fung, *Chemtech* **24**, 40 (1994).
271. J. C. Alfonso, D. A. G. Aranda, M. Schmal, and R. Frety, *Fuel Proc. Technol.* **50**, 35 (1997).
272. G. J. Arteaga, J. A. Anderson, and C. H. Rochester, *J. Catal.* **187**, 219 (1999).
273. C. L. Pieck, C. R. Vera, and J. M. Parera, in Ref. 263, p. 279.
274. D. R. Acharya, R. Hughes, M. A. Kennard, and Y. P. Liu, *Chem. Eng. Sci.* **47**, 1687 (1992).
275. U.S. Pat. 4,999,326 (Mar. 12, 1991), D. L. Sikkenga, I. C. Zaenger, and G. S. Williams (to Amoco).
276. A. Ekstrom and J. Lapszewicz, *J. Phys. Chem.* **88**, 4577 (1984); *J. Phys. Chem.* **91**, 4514 (1987).
277. U.S. Pat. 5,268,344 (Dec. 7, 1993), L. E. Pedrick, C. H. Mauldin, and W. C. Behrmann (to Exxon Research and Engineering Co.).
278. U.S. Pat. 5,338,439 (Aug. 16, 1994), H. Owen and P. H. Schipper (to Mobil Oil Corp.).
279. U.S. Pat. 5,198,397 (Mar. 30, 1993), M. F. Raterman (to Mobil Oil Corp.).
280. U.S. Pat. 5,393,717 (Feb. 28, 1995), M. R. Apelian, A. S. Fung, G. H. Hatzikos, C. R. Kennedy, C.-H. Lee, T. R. Kiliany, P. K. Ng, and D. A. Pappal (to Mobil Oil Corp.).
281. U.S. Pat. 5,340,957 (Aug. 23, 1994), D. E. Clark (to Union Oil Co.).
282. Y. Yoshimura, T. Sato, H. Shimada, N. Matsubayashi, M. Imamura, A. Nishijima, S. Yoshitomi, T. Kameoka, and H. Yanase, *Energy Fuels* **8**, 435 (1994).
283. E. S. Oh, Y. C. Park, and I. C. Lee, *J. Catal.* **172**, 314 (1997).
284. A. T. Aquavo, A. G. Gayubo, A. Atutxa, M. Olazar, and J. Bilbao, *J. Chem. Tech. Biotech.* **74**, 1082 (1999).
285. U.S. Pat. 4,777,156 (Oct. 11, 1988), N. P. Forbus, M. May-Som Wu (to Mobil Oil Corp.).
286. A. Krishna, C. Hsieh, A. E. English, T. Pecoraro, and C. Kuehler, *Hydrocarbon Process.* 59–66 (Nov. 1991).
287. C. Altomare, G. Koermer, P. Schubert, S. Suib, and W. Willis, *Chem. Mater.* **1**, 459–463 (1989).
288. A. Aguinaga and M. Montes, *Appl. Catal., A: Gen.* **90**, 131 (1992).
289. G. V. Lowry and M. Reinhard, *Environ. Sci. Technol.* **34**, 3217 (2000).
290. U.S. Pat. 4,830,997 (May 16, 1989), D. C. Trinh and A. Desvard (to Institut Français du Petrole).
291. U.S. Pat. 5,230,791 (July 27, 1993), D. E. Sherwood (to Texaco Inc.).
292. S. C. Fung, in Ref. 263, p. 399.
293. U.S. Pat. 5,672,801 (Sept. 30, 1997), B. Didillon (to Institut Français Du Petrole).

294. U.S. Pat. 4,929,576 (May 29k 1990), Y.-Y. P. Tsao and R. von Ballmoos (to Mobil Oil Corp.).
295. P. Dufresne, N. Brahma, and F. Girardier, *Revue de I'Institut Français due Petrole* **50**, 283 (1995).
296. U.S. Pat. 5,275,990 (Jan. 4, 1994), F. T. Clark and A. L. Hensley, Jr. (to Amoco Corp.).
297. A. Brito, R. Arvelo, and A. R. Gonzalez, *Ind. Eng. Chem. Res.* **37**, 374 (1998).
298. V. L. S. Teixeira-da-Silva, F. P. Lima, and L. C. Dieguez, *Ind. Eng. Chem. Res.* **37**, 882 (1998).
299. C. E. Snape, M. C. Diaz, Y. R. Tyagi, S. C. Martin, and R. Hughes, in Ref. 263, p. 359.
300. U.S. Pat. 5,445,728 (Aug. 29, 1995), D. E. Sherwood, Jr., and J. R. Hardee, Jr. (to Texaco Inc.).
301. U.S. Pat. 5,021,377 (June 4, 1991), M. K. Maholland, C.-M. Fu, R. E. Lowery, D. H. Kubicek, and B. J. Bertus (to Phillips Petroleum Co.).
302. U.S. Pat. 5,141,904 (Aug. 25, 1992), D. H. Kubicek, C.-M. Fu, R. E. Lowery, and M. K. Maholland (to Phillips Petroleum Co.).
303. U.S. Pat. 5,151,391 (Sept. 29, 1992), C.-M. Fu, M. Maholland, and R. E. Lowery (to Phillips Petroleum Co.).
304. U.S. Pat. 6,063,721 (May 16, 2000), Y. Hu, B. Luo, K. Sun, Q. Yang, M. Gong, J. Hu, G. Fang, and Y. Li (to China Petro-Chemical Corp.).
305. P. L. Walker, Jr., F. Rusinko, Jr., and L. G. Austin, *Adv. Catal.* **11**, 133–221 (1959).
306. J. W. Fulton, *Chem. Eng.* **96**, 111–114 (1988).
307. J. T. Richardson, *Ind. Eng. Chem. Process Des. Dev.* **11**, 8 (1972).
308. P. B. Weisz and R. B. Goodwin, *J. Catal.* **6**, 227 (1966).
309. J. R. Rostrup-Nielsen, *J. Catal.* **21**, 171–178 (1971).
310. D. B. Dadyburjor, in B. Delmon and G. F. Froment, eds., *Catalyst Deactivation*, Elsevier, Amsterdam, 1980, pp. 341–351.
311. C. Bartholomew in I. I. Harvath, eds., *Encyclopedia of Catalysis*, Vol. 2, John Wiley & Sons, New York, 2003, pp. 182–315.

CALVIN BARTHOLOMEW
Brigham Young University